

Aus dem Adolf Butenandt-Institut für Physiologische Chemie der
Ludwig-Maximilians-Universität, München
Direktor: Prof. Dr.med. Dr. rer. nat. W. Neupert

Conformational Dynamics of the Mitochondrial TIM23 Preprotein Translocase

Dissertation
zum Erwerb des Doktorgrades der Medizin
an der Medizinischen Fakultät der
Ludwig-Maximilians-Universität zu München

vorgelegt von
Koyeli Mapa
aus
Chinsurah, West Bengal, India

München
2009

**Mit Genehmigung der Medizinischen Fakultät
der Universität München**

- | | |
|-------------------------|-------------------------------|
| 1. Berichterstatter: | Prof. Dr. Dr. Walter Neupert |
| 2. Berichterstatter: | Priv. Doz. Dr. Andreas Bender |
| 1. Mitberichterstatter: | Prof. Dr. Josef Müller-Höcker |
| 2. Mitberichterstatter: | Priv. Doz. Dr. Kai Hell |

Dekan: Prof. Dr. Dr. h.c. M. Reiser, FACR, FRCR

Tag der mündlichen Prüfung: 23.07.2009.

“The dream is not what you see in sleep, dream is the thing which does not let you sleep”

- Dr. A P J Abdul Kalam, XIth President of India

Contents

1	Introduction	1
1.1	Intracellular protein trafficking.....	1
1.2	Overview on protein translocation into mitochondria.....	1
1.3	Translocases of the outer mitochondrial membrane	4
1.3.1	Translocase of the outer membrane (TOM Complex).....	4
1.3.2	The TOB Complex.....	5
1.4	Protein translocation machinery in the intermembrane space (IMS) of mitochondria	6
1.4.1	The Mia40-Erv1 disulfide relay system.....	6
1.5	Translocases of inner mitochondrial membrane	7
1.5.1	The TIM22 Complex	7
1.5.2	The OXA1 Complex.....	8
1.5.3	The TIM23 complex	9
1.5.3.1	The membrane embedded part of the TIM23 complex	11
1.5.3.2	Import motor part of the TIM23 complex	12
1.6	Mitochondrial Hsp70: A chaperone with two functions	14
1.6.1	Mitochondrial Hsp70 in preprotein translocation	15
1.6.2	Protein folding by mtHsp70 and its cochaperones in the mitochondrial matrix	18
1.7	Aims of the present study.....	19
2	Materials and Methods	20
2.1	Molecular biology methods.....	20
2.1.1	Isolation of DNA.....	20
2.1.1.1	Isolation of yeast genomic DNA	20
2.1.1.2	Isolation of plasmid DNA from <i>Escherichia coli</i>	20
2.1.2	Amplification of DNA sequences by Polymerase Chain Reaction (PCR) ..	21
2.1.3	DNA analysis and purification.....	22
2.1.3.1	Agarose gel electrophoresis of DNA.....	22
2.1.3.2	Isolation of DNA from agarose gels.....	23
2.1.3.3	Measurement of DNA concentration.....	23
2.1.4	Enzymatic manipulation of DNA	23
2.1.4.1	Digestion of DNA with restriction endonucleases	23
2.1.4.2	Ligation of DNA fragments.....	23
2.1.5	Transformation of electrocompetent <i>E. coli</i> cells	24

2.1.5.1	Overview of E. coli strains used.....	24
2.1.5.2	Preparation of electrocompetent cells.....	24
2.1.5.3	Transformation of E. coli cells by electroporation.....	25
2.1.6	Overview of yeast strains used.....	25
2.1.7	Cloning strategies for generation of yeast strains by homologous recombination.....	26
2.1.7.1	Deletions of PAM17 gene and double deletion of PAM17/TIM21	26
2.1.7.2	Disruption of TIM44 in the haploid strain YPH499.....	26
2.1.8	Overview of different plasmids used.....	27
2.1.9	Cloning strategies for plasmids used for the transformation of yeast.....	28
2.1.9.1	pRS314[His6Pam17].....	28
2.1.9.2	pVT-102U[Tim21].....	28
2.1.9.3	pVT-W[Pam17].....	29
2.1.10	Cloning strategies for plasmids used for recombinant proteins expressions	29
2.1.10.1	Cloning of mature Tim44 in bacterial expression vector.....	29
2.1.10.2	Cloning of N-terminal domain of Tim44 (Tim44-NTD) in bacterial expression vector.....	30
2.1.10.3	Cloning of C-terminal domain of Tim44 (Tim44-CTD) in bacterial expression vector.....	30
2.1.10.4	Cloning of Nucleotide binding domain of Ssc1(Ssc1-NBD) in bacterial expression vector.....	30
2.1.10.5	Cloning of Peptide binding domain of Ssc1(Ssc1-PBD) in bacterial expression vector.....	31
2.1.10.6	Cloning of mature Mdj1 in bacterial expression vector.....	31
2.1.10.7	Point mutations of Tim44, Ssc1 and Mdj1.....	31
2.1.10.8	List of Primers used for site directed mutagenesis.....	32
2.1.11	Cloning strategies for plasmids used for the transformation of yeast for checking the <i>in vivo</i> functionality.....	33
2.1.11.1	Cloning of full length Tim44 and domains of Tim44 in pRS314.....	33
2.1.11.2	Making of point mutants of Tim44 in yeast vector.....	34

2.1.11.3	Making of point mutants of Ssc1 in yeast vector	34
2.1.12	Checking the <i>in vivo</i> functionality of mutant Tim44	35
2.1.13	Checking the <i>in vivo</i> functionality of mutant Ssc1	35
2.2	Methods in cell biology	35
2.2.1	<i>E. coli</i> – media and growth	35
2.2.1.1	Media for <i>E. coli</i>	35
2.2.1.2	Cultivation of <i>E. coli</i>	36
2.2.2	<i>S. cerevisiae</i> – media and growth	36
2.2.2.1	Media for <i>S. cerevisiae</i>	36
2.2.2.2	Cultivation of <i>S. cerevisiae</i>	37
2.2.2.3	Transformation of <i>S. cerevisiae</i> by the lithium acetate method	37
2.2.3	Isolation of mitochondria from <i>S. cerevisiae</i>	38
2.2.4	Isolation of crude mitochondria from <i>S. cerevisiae</i>	39
2.3	Immunology methods	39
2.3.1	Generation of antibodies	39
2.3.1.1	Generation of polyclonal antisera against Pam17 protein	39
2.3.1.2	Affinity purification of antibodies against different components of the TIM23 complex	40
2.3.2	Immunodecoration	41
2.4	Protein biochemistry methods	42
2.4.1	Purification of different recombinant proteins	42
2.4.1.1	Purification of His ₆ Tim44 and other His-tagged proteins	42
2.4.1.2	Purification of recombinant Ssc1	42
2.4.2	Protein analysis	43
2.4.2.1	SDS-Polyacrylamide gel electrophoresis (SDS-PAGE)	43
2.4.2.2	CBB staining of SDS-PAGE gels	44
2.4.2.3	Transfer of proteins onto nitrocellulose/PVDF membrane (Western- Blot)	44
2.4.2.4	Determination of protein concentration	45
2.4.3	Protein experiments <i>in organello</i>	45
2.4.3.1	Co-immuno precipitation experiments	45

2.4.3.2	Ni-NTA Pull down experiments with tagged proteins expressed in mitochondria	45
2.4.3.3	Crosslinking of mitochondrial proteins	46
2.4.4	Protein experiments <i>in vitro</i>	47
2.4.4.1	Ni-NTA pull-down experiments.....	47
2.4.4.2	Cross-linking experiments.....	47
2.5	Methods for Fluorescence spectroscopy	47
2.5.1	Labelling of Cystine mutants of Tim44 and Ssc1 with sulfhydryl-specific fluorophores	47
2.5.2	Steady-state and Kinetic Ensemble FRET Measurements.....	48
2.5.3	Steady-state Ensemble FRET Efficiencies of Tim44:Ssc1, and P5:Ssc1 complexes	48
2.5.4	Semi-quantitative intramolecular FRET measurement.....	48
2.5.5	Single Molecule FRET Experiments	49
2.5.6	Determination of the Equilibrium Dissociation Constant of Tim44:Ssc1 Complexes.....	49
2.6	Far-UV CD spectroscopy	50
2.7	Screening of cellulose-bound peptides (Peptide scans)	50
2.8	Methods for enzymatic activity of purified proteins.....	51
2.8.1	Coupled assay for ATPase activity of Ssc1	51
3	Results.....	52
3.1	Characterization of Pam17 and Tim21, the two non-essential subunits of the TIM23 complex	52
3.1.1	Both Tim21 and Pam17 bind to the Tim17-Tim23 core of the TIM23 complex.....	52
3.1.2	The major cross-linked adduct of Tim23 is to Pam17.....	55
3.1.3	Deletion of Pam17 affects the conformation of both motor and membrane part of the TIM23 complex	56
3.1.4	Binding of Tim21 and of Pam17 to the TIM23 complex is mutually exclusive	59
3.2	Reconstitution of the Tim44:Ssc1 interaction cycle of the mitochondrial import motor using the purified components	62
3.2.1	Recombinant Ssc1 and Tim44 are functional and can associate to form Tim44:Ssc1 complex <i>in vitro</i>	63

3.2.2	Development of a FRET based assay system to monitor Tim44-Ssc1 interaction cycle in real time.....	65
3.2.2.1	Generation of cysteine mutants of Tim44 and Ssc1 for maleimide specific fluorophore labeling	65
3.2.3	Interaction of Tim44 and Ssc1 can be monitored in real time by Fluorescence Resonance Energy Transfer	68
3.2.4	Mapping of interaction sites in Tim44:Ssc1 complex	69
3.2.5	Interaction of isolated domains of Ssc1 and Tim44.....	70
3.2.5.1	The solubility of Ssc1-NBD in E.coli strictly depends on its co-expression along with Hep1 and addition of the linker sequence.....	71
3.2.5.2	Isolated Ssc1-PBD can form a complex with Tim44 while the NBD does not interact	71
3.2.5.3	The N-terminal domain (NTD) of Tim44 is the major interacting domain with Ssc1	73
3.2.5.4	Isolated domains of Tim44 cannot replace the full-length protein in vivo even when expressed together in trans	75
3.2.6	Substrate induced dissociation of Tim44:Ssc1	76
3.2.7	Nucleotide induced dissociation drives Tim44:Ssc1 reaction cycle.....	78
3.2.8	The dissociation of Tim44:Ssc1 complex is a single-step reaction.....	81
3.2.9	Ssc1 and Tim44 share complementary binding sites on matrix targeted pre-proteins	82
3.3	Conformational dynamics of mtHsp70 (Ssc1) and the effects of co-chaperones and substrates on it.....	85
3.3.1	Development of double cysteine substitution mutants of Ssc1 for fluorophore labelling.....	85
3.3.2	Development of a FRET-based Ssc1 conformation sensor	88
3.3.3	Effect of nucleotides on the conformation of Ssc1 from ensemble FRET measurements.....	89
3.3.4	Effect of nucleotides on the conformation of Ssc1 from Single-molecule FRET measurements.....	90
3.3.5	Effect of J-domain co-chaperone and peptide substrate on the conformation of Ssc1	94

3.3.5.1	Binding of substrate and Mdj1 to Ssc1	94
3.3.5.2	Binding of Mge1 to the substrate captured complex of Ssc1	102
4	Discussion	105
4.1	Characterization of Pam17 and Tim21, the non-essential components of the TIM23 complex	105
4.2	<i>In vitro</i> reconstitution of the Tim44:Ssc1 interaction cycle	107
4.3	The chaperone cycle of Ssc1 in the mitochondrial matrix	109
5	Summary.....	113
6	Zusammenfassung.....	115
7	References:.....	118
	ABBREVIATIONS.....	133
	Publications resulting from this thesis	136
	ACKNOWLEDGEMENTS.....	137
	Curriculum Vitae	139

1 Introduction

1.1 Intracellular protein trafficking

The eukaryotic cell is structurally and functionally divided in a number of membrane bound sub-compartments or organelles. In the crowded cellular environment, this enables physical separation of various biochemical reactions accomplished by different sets of proteins present in different organelles. With the exception of those few proteins encoded by the mitochondrial and chloroplast genomes, most of the cellular proteins are synthesized by the cytosolic ribosomes and have to be transported to the specific organelles, the final place of their biochemical functions (Neupert and Herrmann, 2007; Soll and Schleiff, 2004). The correct sorting of all proteins to the right compartment is therefore crucial for the proper functioning of the cell and as a whole for the continuation of life. The fundamental concept of intracellular protein trafficking is that proteins have targeting signals which are recognized by receptors, usually present on the surface of the organelles. Each organelle has developed its own translocases (or translocons) which are complex molecular machines specialised for recognition and translocation of preproteins (Blobel, 1980; Schnell and Hebert, 2003). Extensive studies in the protein translocation field have started to elucidate the dynamic and versatile nature of different translocases in the cell.

1.2 Overview on protein translocation into mitochondria

All mitochondrial proteins, with the exception of those few encoded by the mitochondrial genome, must be transported into the organelle and correctly sorted into one of its various sub-compartments, the outer and inner mitochondrial membranes, intermembrane space and mitochondrial matrix. For recognition, translocation and subsequent sorting, mitochondria have developed a complex network of translocases.

Mitochondrial precursors are mainly transported into the organelle in a post-translational manner, though certain evidence in support of co-translational translocation also exists (Fujiki and Verner, 1991, 1993). The precursors have to be largely unfolded to be

accommodated by the channels of mitochondrial translocases and after their synthesis they are kept in a translocation competent forms by the help of cytosolic chaperones: Hsp70, Hsp90 and other factors, e.g. mitochondrial import stimulation factor (MSF) (Deshaies et al., 1988; Hachiya et al., 1994; Murakami et al., 1988; Young et al., 2003). The mitochondrial precursors are targeted to the organelle by virtue of their targeting signals. The typical mitochondrial targeting signal is a cleavable N-terminal sequence called a presequence or a matrix targeting sequence (MTS). In the absence of any other targeting information, MTSs direct preproteins to the mitochondrial matrix. Presequences are usually ca. 10-80 amino acid residues long with no apparent primary sequence conservation. What is conserved is the ability to form amphipathic helices with a positively charged and a hydrophobic surface (Mokranjac and Neupert, 2008; Neupert and Herrmann, 2007). N-terminal targeting signals are usually cleaved off by the mitochondrial processing peptidase (MPP) as soon as precursors enter the mitochondrial matrix. N-terminal positioning of the presequence leads to N to C terminal translocation of preproteins but artificial implantation of the MTS at the C terminus leads to translocation in the reverse direction. So far, only one example is known, that of the DNA helicase Hmi1, where the MTS is naturally present at the C terminus of the protein (Lee et al., 1999).

All mitochondrial preproteins enter the organelle through the translocase of outer mitochondrial membrane (TOM). From the TOM complex, β -barrel precursors are transferred to another complex in the outer membrane called TOB complex (topogenesis of mitochondrial outer membrane β -barrel proteins) or SAM complex (sorting and assembly machinery). The TOB complex mediates the insertion of the β -barrel precursors into the outer membrane (Kozjak et al., 2003; Paschen et al., 2003; Wiedemann et al., 2003). For import of preproteins across or into the inner membrane, the TOM complex cooperates with the TIM23 and TIM22 complexes in the inner membrane. The TIM22 complex mediates the insertion of proteins with four or six transmembrane segments into the inner membrane. The TIM23 complex mediates translocation of preproteins with presequences into the mitochondrial matrix or inserts single transmembrane proteins into the inner membrane (Mokranjac and Neupert, 2008; Neupert and Herrmann, 2007). The OXA1 complex mediates export of proteins from the matrix into the inner membrane and

also inserts proteins synthesized by the mitochondrial ribosome into the inner mitochondrial membrane. In the IMS of mitochondria, Mia40 and Erv1 constitute a disulfide relay system which drives the import of a specific class of cysteine containing proteins by an oxidative folding mechanism (Figure 1.1)(Hell, 2008; Herrmann et al., 2008).

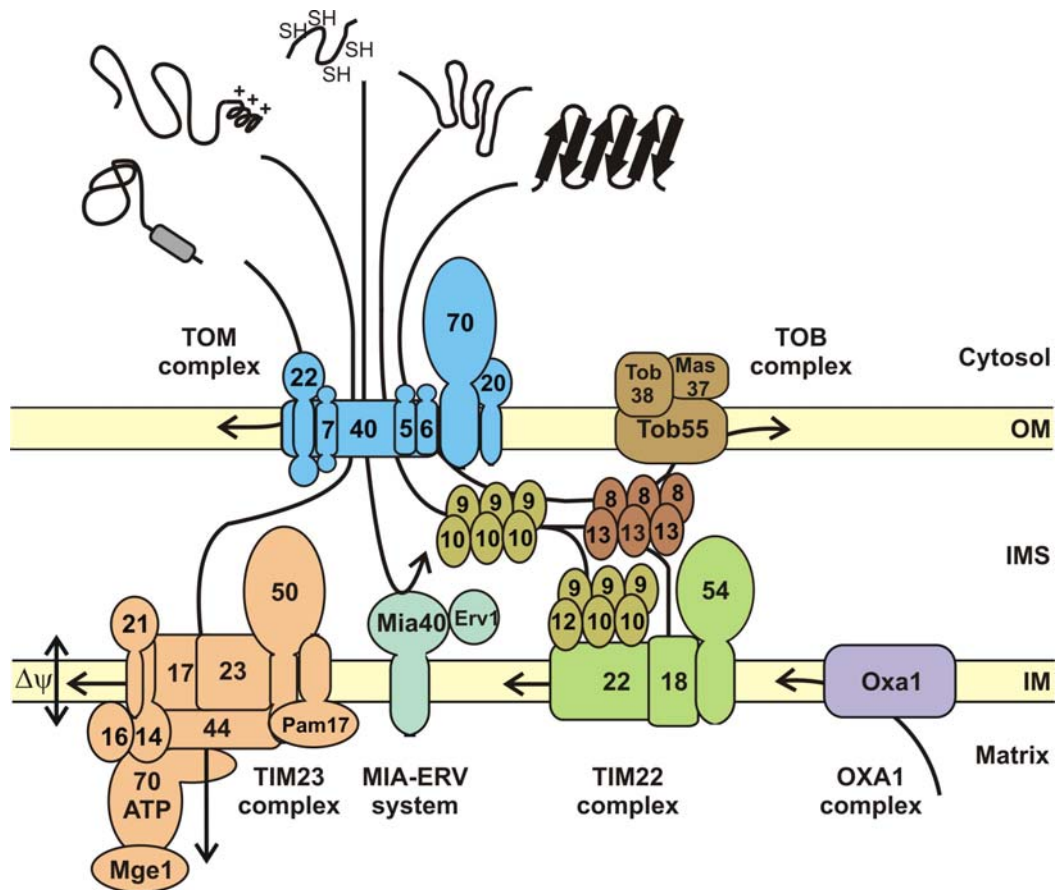


Figure 1.1. Translocation machineries in mitochondria. The TOM complex acts as the common entry gate for all kinds of mitochondrial preproteins. The β -barrel proteins are assembled in the outer membrane through the concerted action of the TOM complex, small Tim proteins and the TOB complex. After crossing the outer membrane (OM), presequence containing preproteins are either translocated into the matrix or inserted in the inner membrane (IM) by the TIM23 complex, whereas polytopic membrane proteins lacking presequences are inserted in the inner membrane via the TIM22 complex. After crossing the TOM complex small cysteine containing proteins of intermembrane space (IMS) are trapped by the MIA-ERV disulfide relay system.

1.3 Translocases of the outer mitochondrial membrane

1.3.1 Translocase of the outer membrane (TOM Complex)

The TOM complex is the major translocase of the outer mitochondrial membrane and is the common entry gate for all preproteins destined for various mitochondrial sub-compartments. The general import pore (GIP) or the TOM 'core complex' is formed by the pore forming subunit Tom40, receptor protein Tom22 and three small Tom proteins Tom5, Tom6 and Tom7. Two receptor proteins Tom70 and Tom20 are loosely associated with the TOM core complex to form the 'holo complex' (Becker et al., 2008b; Neupert and Herrmann, 2007; Rapaport, 2002).

The TOM complex contains two broadly defined binding sites for preproteins. The so called *cis* site is on the cytosolic surface and the *trans* site is on the IMS side of the TOM complex. Presumably, an increase in the binding affinity to the passenger protein from the *cis* to the *trans* binding site drives the vectorial translocation across the outer membrane (Komiya et al., 1998). The TOM complex, purified with the mild detergent digitonin is about 490-600 kDa in size (Ahting et al., 2001; Kunkele et al., 1998a; Model et al., 2002). Negative staining of the purified TOM complex showed a structure with two or three pores. The complex purified under harsher conditions is a complex with two pores (Ahting et al., 1999).

The receptors Tom20 and Tom70 are anchored to the outer mitochondrial membrane with their N-terminal transmembrane domains while exposing their C-terminal domains in the cytosol by which they recognize the preproteins. Tom20 mainly recognize preproteins with N-terminal cleavable presequences while Tom70 recognizes proteins with internal targeting signals (Chan et al., 2006; Lithgow et al., 1995; Wu and Sha, 2006). However, the substrate recognition properties overlap partially for these two receptors. They can partly substitute each other but deletion of both receptors lead to cell death (Ramage et al., 1993).

Tom22 spans the outer membrane once and exposes its negatively charged N-terminal domain to the cytosol and C-terminal domain to the IMS. Tom22 connects Tom20 to the central translocation pore and may have a role in binding and unfolding of precursor proteins together with Tom20. Tom22 is also critical for the integrity of the TOM

complex (Mayer et al., 1995; van Wilpe et al., 1999). Tom40, the major pore forming unit, is a membrane-embedded protein that presumably forms a β -barrel structure. Purified Tom40 forms pores in artificial membranes even in the absence of other subunits of the TOM complex (Becker et al., 2005; Hill et al., 1998; Kunkele et al., 1998b). It is not clear whether the pore is formed by single or multiple Tom40 molecules. The small TOM proteins, Tom5, Tom6 and Tom7, consist of ca. 50-70 amino acid residues and all are tail-anchored with only a few residues exposed on the IMS. The exact function of small Tom proteins is still not clear though there is indication that they have a role in the dynamics of the TOM complex. Individually they are dispensable for cell viability but simultaneous deletion of all three leads to cell death (Dekker et al., 1998; Dietmeier et al., 1997; Sherman et al., 2005).

1.3.2 The TOB Complex

Mitochondrial outer membrane contains a number of β -barrel proteins (Rapaport, 2003). The translocation and assembly mechanisms of these proteins were enigmatic until the TOB (SAM) complex was discovered (Paschen et al., 2003; Wiedemann et al., 2003). Like other mitochondrial precursor proteins, β -barrel precursors cross the outer membrane through the TOM complex. They are then handed over to small Tim proteins in the IMS which guide them to the TOB complex. So far three components of the TOB complex are known: two essential components, an integral membrane protein Tob55 (Sam50) (Kozjak et al., 2003; Paschen et al., 2003) and peripheral membrane protein Tob38 (Tom38/Sam35) (Ishikawa et al., 2004; Milenkovic et al., 2004; Waizenegger et al., 2004) and one non-essential protein Mas37 (Wiedemann et al., 2003). The central component Tob55 is a β -barrel protein that has homologues in the entire eukaryotic kingdom and also in Gram-negative bacteria (Omp85/YaeT) (Gentle et al., 2004; Voulhoux et al., 2003). Tob55 spans the outer membrane with its C-terminal domain which is predicted to contain 14-16 transmembrane β -sheets. In addition, it has a hydrophilic N-terminal domain which is exposed to the IMS forming a characteristic polypeptide translocation associated (POTRA) domain (Sanchez-Pulido et al., 2003). The POTRA domain was proposed to have a receptor-like function in the biogenesis of β -barrel proteins (Habib et al., 2007). Very recently, a receptor function in the TOB

complex has also been ascribed to Tob38. The recognition of the signal in precursors of β -barrel proteins by Tob38 led to changes in gating properties of the TOB channel which was proposed to facilitate membrane insertion of β -barrel precursors into the outer membrane (Kutik et al., 2008). Tob38 is an essential peripheral outer membrane protein largely exposed to the cytosol (Waizenegger et al., 2004). If the proposed receptor function is correct, then Tob38 should have domains exposed to IMS as well, an issue that is unclear so far. Like Tob38, Mas37 is a peripheral outer membrane protein exposed to the cytosol. In contrast, its deletion is not deleterious for cell growth in yeast although it results in defective import of β -barrel precursors (Habib et al., 2005; Waizenegger et al., 2004).

Recently a protein named Mim1 or Tom13 was identified and was shown to selectively affect the assembly of Tom40, but not of other β -barrel proteins. Mim1 is the component of neither the TOM nor the TOB complex, but it forms a separate high molecular weight complex of 180 kDa and acts in the later stages of the assembly of the TOM complex (Ishikawa et al., 2004; Popov-Celeketic et al., 2008b; Waizenegger et al., 2005). Recently, Mim1 was also shown to promote the membrane insertion and assembly of signal anchored receptors of the TOM complex (Becker et al., 2008a).

1.4 Protein translocation machinery in the intermembrane space (IMS) of mitochondria

1.4.1 The Mia40-Erv1 disulfide relay system

The intermembrane space (IMS) of mitochondria harbours a number of proteins containing conserved cysteine residues. They are involved in several functions like chaperoning the hydrophobic mitochondrial preproteins in the aqueous environment of IMS to reach the correct destination and biogenesis of respiratory chain complexes (Hell, 2008; Herrmann et al., 2008). These proteins possess a conserved twin C_x3C or C_x9C motif involved in the formation of intramolecular disulfide bonds or metal binding. Recently the import pathway for these proteins into the IMS was identified. The essential components of this pathway are Mia40 (Tim40) and Erv1. Mia40 is conserved among eukaryotes from yeast to human. It contains a highly conserved C-terminal domain ca. 60

amino acid residues with six cysteines that are involved in the formation of three intramolecular disulfide bonds (Chacinska et al., 2004; Hofmann et al., 2005; Terziyska et al., 2005). Erv1 is a sulfhydryl oxidase with a CxxC motif in its N-terminus and a FAD-binding region and another CxxC motif in the C-terminus (Coppock and Thorpe, 2006; Hofhaus et al., 2003).

The precursors of the cysteine-rich IMS proteins cross the outer membrane in a reduced and extended form through the TOM complex and are recognized by the redox-activated receptor Mia40. Mixed disulfide bonds are formed between Mia40 and cysteine-rich proteins and subsequently substrates are released in oxidized and folded form leaving Mia40 in a reduced and inactive form (Grumbt et al., 2007; Muller et al., 2008). These oxidized and folded precursors cannot move back to the cytosol through the TOM complex and thereby get trapped in the IMS. In order to regenerate the oxidized, substrate acceptor state of Mia40, Erv1 oxidizes Mia40 in a disulfide transfer reaction. Finally, Erv1 transfers the electrons to molecular oxygen through cytochrome c, and complex IV of respiratory chain and gets re-oxidized to start a new cycle of substrate import (Hell, 2008; Herrmann et al., 2008). Thus Mia40 and Erv1 constitute a disulfide relay system that drives the import of cysteine-containing proteins into the IMS of mitochondria by an oxidative folding mechanism.

1.5 Translocases of inner mitochondrial membrane

1.5.1 The TIM22 Complex

Precursors of proteins belonging to the solute carrier family and components of the TIM translocases with multiple transmembrane segments (Tim17, Tim23 and Tim22), are sorted into inner mitochondrial membrane by the TIM22 complex. The TIM22 complex is ca. 300kDa in size and consists of three membrane proteins, Tim22, Tim54 and Tim18 and three small Tim proteins Tim9, Tim10 and Tim12 (Mokranjac and Neupert, 2008; Neupert and Herrmann, 2007). The precursors cross the TOM complex in a specific hairpin loop conformation and are handed over to the soluble small Tim complex. This complex acts as a chaperone to escort the hydrophobic segments through the aqueous

environment of the IMS to the TIM22 complex. There are two homologous small TIM complexes in the IMS, the essential Tim9-Tim10 complex and the nonessential Tim8-Tim13 complex. Small TIM complexes are hexameric and contain three copies of each subunit. The small Tim proteins contain ‘twin C_xC motif’ in which cysteine residues are forming intramolecular disulfide bonds. Structural analysis revealed that the Tim9–Tim10 and Tim8-Tim13 complexes have a six-blade α -helical propeller structure that resembles a flattened jellyfish with 12 flexible tentacles. These were proposed to shield hydrophobic regions of carrier proteins on their way from the *trans* side of the TOM complex to the TIM22 complex (Lu et al., 2004; Vergnolle et al., 2005; Webb et al., 2006). The core component of the TIM22 complex is Tim22 which by itself can mediate the insertion of carrier proteins in the absence of Tim54 and Tim18 though only with very low efficiency (Kovermann et al., 2002). The exact mechanism of membrane insertion by the TIM22 translocase is still not clear. It has been shown that precursors are tethered to the translocase in a membrane potential independent manner. After initial tethering, actual membrane insertion occurs in two steps with the help of energy from membrane potential (Rehling et al., 2003). Tim54 is important for the functionality of the translocase but not essential for cell viability. Tim54 might help in tethering of the Tim9.Tim10.Tim12 to the IMS side of the TIM22 complex because the association of the small Tims was destabilized in *TIM54* deletion strain (Kovermann et al., 2002). In addition to its role in protein translocation via TIM22 translocase, the function of Tim54 in the assembly of Yme1p into proteolytically active complex was described (Hwang et al., 2007). Tim18 has been found only in fungal mitochondria so far. The exact roles of Tim54 and Tim18 are still under investigation.

1.5.2 The OXA1 Complex

The OXA1 complex is involved in the membrane potential dependent insertion of inner membrane proteins from the matrix side. OXA1 substrates are of two origins. One class of substrates are nuclear encoded and are first translocated to the matrix with the aid of TOM and TIM23 translocase and subsequently into the inner membrane with the help of OXA1 complex. The second class of substrates is encoded by mtDNA and is inserted into the inner membrane in a co-translational manner (Hell et al., 1997; Hell et al., 1998; Hell

et al., 2001). The matrix exposed C-terminal domain of Oxa1 is involved in ribosome recruitment to the inner mitochondrial membrane (Jia et al., 2003; Szyrach et al., 2003). This function is shared by Mba1, a peripheral membrane protein that binds to a large ribosomal subunit (Ott et al., 2006). Although Mba1 and Oxa1 together are involved in ribosome recruitment, they do not seem to belong to the same complex (Preuss et al., 2001).

1.5.3 The TIM23 complex

The TIM23 complex is the major translocase of inner mitochondrial membrane. All matrix targeted preproteins are translocated to mitochondrial matrix and some inner membrane proteins are inserted into the membrane by the TIM23 complex. Translocation across the TIM23 complex is an energy driven process. The energy sources are membrane potential across the inner mitochondrial membrane ($\Delta\psi$) and ATP in the mitochondrial matrix. For simplicity reasons, the translocase is conventionally divided into membrane embedded translocation channel and channel associated import motor. The membrane embedded part is formed by channel forming subunits Tim23 and Tim17 along with receptor protein Tim50. Import motor is constituted of mtHsp70 along with its co-chaperones: J-protein Tim14 (Pam18), J-like protein Tim16 (Pam16), the membrane-anchor for Hsp70 Tim44 and the nucleotide exchange factor Mge1 (Figure 1.2). All these components of the TIM23 complex are essential for cell viability. Recently, two additional components were identified, Tim21 and Pam17. They are both dispensable for cell growth (Chacinska et al., 2005; Mokranjac et al., 2005; van der Laan et al., 2005). Mmp37 (Tam41) was recently found to affect transport via the translocase but its direct association with the translocase is still unclear (Gallas et al., 2006; Tamura et al., 2006).

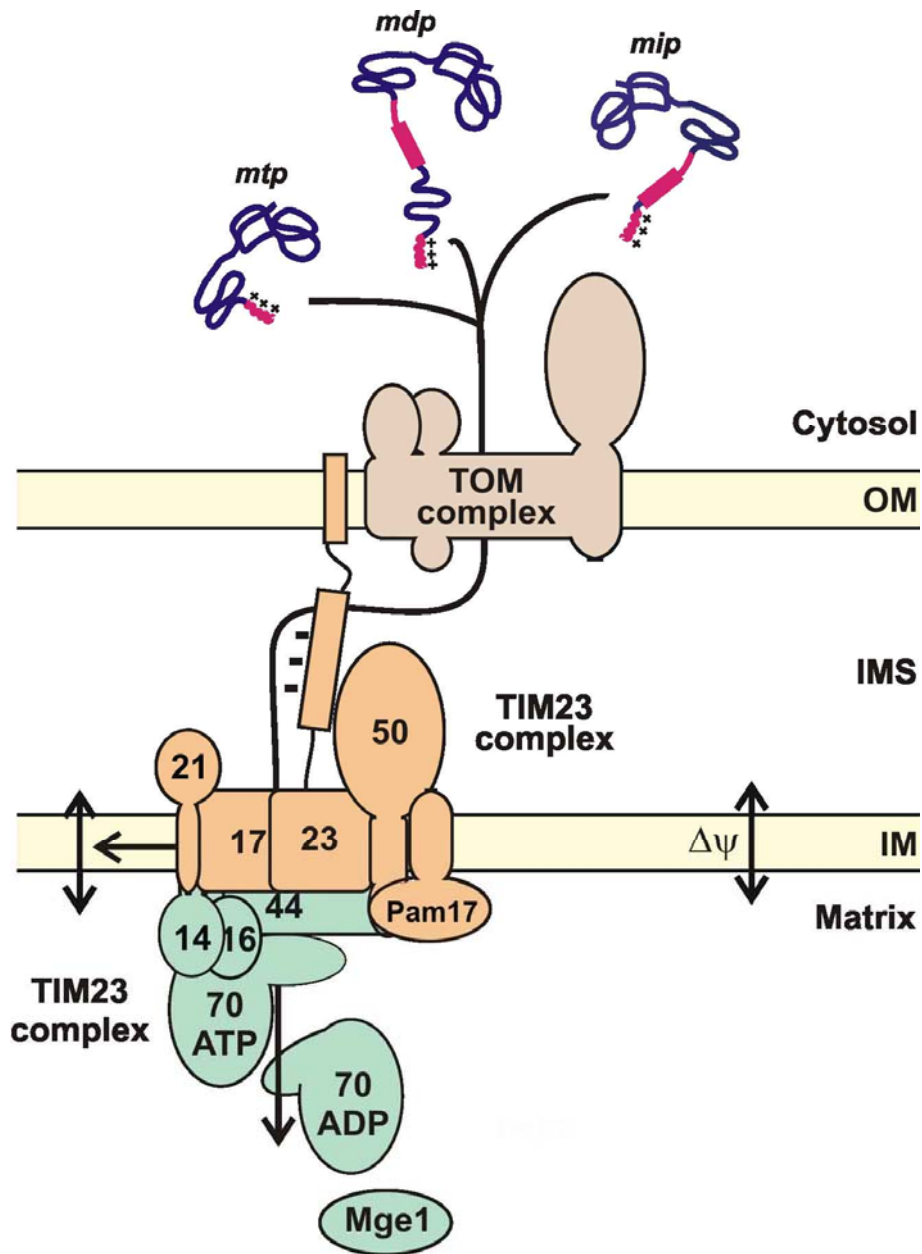


Figure 1.2. The TIM23 complex. Preproteins with positively charged N-terminal presequence (magenta) synthesized in cytosol are imported into mitochondria through the concerted action of the TOM complex in the outer membrane (OM) and the TIM23 complex in the inner membrane (IM) in a membrane-potential ($\Delta\psi$) and ATP-dependent manner. The membrane embedded part (shown in light orange) of the TIM23 complex contains receptor Tim50, the translocon channel formed by Tim23 and Tim17 and Tim21. The import motor (shown in light green) formed by Tim44, mtHsp70, J-protein Tim14, J-like protein Tim16 and nucleotide exchange factor Mge1 is responsible for translocation of all matrix targeted preproteins (*mtp*) through ATP-driven cycles. The TIM23 complex also mediates the lateral insertion of preproteins containing additional hydrophobic stop-transfer signal (magenta). Some of these preproteins require the presence of ATP in the matrix for their import (motor dependent preproteins – *mdp*) and some are inserted with no apparent activity of the import motor (motor independent preproteins – *mip*).

1.5.3.1 The membrane embedded part of the TIM23 complex

Tim50 serves as the receptor to accept precursor proteins from the TOM complex. Precursors stalled at the level of TOM complex can be cross-linked to Tim50 (Mokranjac et al., 2003a; Yamamoto et al., 2002). Tim50 is anchored to the inner membrane by a single transmembrane domain and exposes a large hydrophilic domain in the IMS of mitochondria. The latter domain was recently implicated in maintenance of permeability barrier of inner membrane (Meinecke et al., 2006).

Tim23 is the central component of the translocase. It is embedded in the inner membrane with four transmembrane helices at its C-terminal domain, which form the translocation channel. Recombinant Tim23 forms a hydrophilic, cation selective channel which gets activated by membrane potential and presequences (Truscott et al., 2001). Using environment specific fluorescent probes, the trans-membrane helix 2 of Tim23 was found to face an amphipathic environment. Its hydrophilic side also contacts the preprotein in transit, in a fully functional, membrane-embedded TIM23 channel (Alder et al., 2008).

The N-terminal, IMS exposed domain of Tim23 can be divided in two segments. The first half of the N-terminal domain is dispensable whereas the second half of the N-terminal is necessary for the function of Tim23 (Bauer et al., 1996). The first ca.20 amino acids of yeast Tim23 are inserted into the outer membrane independent of the TOM complex (Donzeau et al., 2000). The second half of the N-terminal domain interacts with Tim50 and serves as a presequence receptor of the TIM23 complex (Yamamoto et al., 2002). This segment of Tim23 can dimerise in a membrane potential dependent manner (Bauer et al., 1996).

Tim17 has been identified over 15 years ago; however, its function in the translocase is still enigmatic. Like Tim23, Tim17 is anchored to the inner membrane by four transmembrane helices, which are homologous to those of Tim23. They are however not interchangeable pointing towards their different functions (Emtage and Jensen, 1993; Ryan et al., 1998; Ryan et al., 1994). Patch clamping of reconstituted inner membranes have shown that Tim17 is important in making 'twin pores' of the TIM23 complex and depletion of it leads to the collapse of twin pores into single ones (Martinez-Caballero et al., 2007). Interestingly, the N-terminal segment of the protein harbours several negative

charges which are critical for protein import and gating of the translocation channel (Martinez-Caballero et al., 2007; Meier et al., 2005).

Recently, Tim21 was identified as a component of the TIM23 complex dispensable for the cell growth (Chacinska et al., 2005; Mokranjac et al., 2005). Tim21 is anchored to the inner membrane by single transmembrane domain and exposes a C-terminal domain to the IMS. The recombinant IMS domain of Tim21 has been found to interact with Tom22 of the TOM complex *in vitro*. This interaction of TOM complex and IMS domain of Tim21 might play a role in TOM-TIM23 tethering during preprotein translocation. Tim21 was also suggested to promote the dissociation of the motor part of the TIM23 complex from the membrane embedded part. This second role of Tim21 led to the hypothesis of 'Two states' of the TIM23 complex. The first state would be sorting competent and would consist of the membrane embedded part containing Tim21 but free of the import motor. The second modular state of the TIM23 complex is capable of targeting proteins to the matrix which is free of Tim21 but has the motor part bound to the rest of the translocase (Chacinska et al., 2005). The 'Two translocase' theory was one of the inceptive hypothesis explaining differential sorting of precursors by the TIM23 complex.

1.5.3.2 Import motor part of the TIM23 complex

The import motor of TIM23 complex is comprised of mitochondrial Hsp70 (mtHsp70) and its co-chaperones.

The central component of the import motor is mtHsp70 (Ssc1 in *S. cerevisiae*). In ATP-dependent cycles of binding to and release from the incoming precursor protein, mtHsp70 leads to vectorial movement of precursors into the matrix assisted by a number of co-chaperones.

For a long time Tim44 was assigned as the J co-chaperone for mtHsp70 though it lacked the typical HPD motif in the active site of J proteins (Merlin et al., 1999). Recently works from different groups have identified Tim14 (Pam18), the J protein of mtHsp70 in the import motor of TIM23 complex (D'Silva et al., 2003; Mokranjac et al., 2003b; Truscott et al., 2003). Tim14 has been found to accelerate the ATP hydrolysis activity of mtHsp70 *in vitro* (D'Silva et al., 2003; Truscott et al., 2003) typical of J co-chaperones. Tim16, a J-like protein was recently identified. It forms a stable sub-complex with Tim14 (Frazier et

al., 2004; Kozany et al., 2004). Though the function of Tim16 is elusive still today, there are some indications that Tim16 can suppress the unwanted acceleration of ATP hydrolysis by Tim14 thereby preventing unnecessary energy consumption (Li et al., 2004; Mokranjac et al., 2006). The crystal structure of Tim14-Tim16 subcomplex could uncover the logics of the repressing behavior of Tim16 on Tim14. When bound to Tim16, Tim14 is in a conformation apparently not suitable for accelerating the ATP hydrolysis by mtHsp70 (Mokranjac et al., 2006).

Tim44 is a peripheral membrane protein which interacts with Tim23-Tim17 core on one side and with mtHsp70 and Tim14-Tim16 subcomplex on the other side. Tim44 recruits the chaperone and the co-chaperones to the translocation channel. Tim44 has two domains. The apparently highly folded C-terminal domain has been shown to bind to cardiolipin containing vesicles indicating its role in membrane binding (Weiss et al., 1999). Recently, the crystal structure of Tim44 C-terminal domain has been solved providing hints but no real evidences for lipid binding nature of this domain (Josyula et al., 2006). The property of Tim44 to recruit mtHsp70 is a key element of the import motor of the TIM23 complex. This recruitment of the chaperone near the translocation channel where the matrix targeted precursors emerge is critical in effective translocation into mitochondrial matrix. In mitochondria, Tim44 and Ssc1 form nucleotide dependent complexes (Rassow et al., 1994; Schneider et al., 1994; von Ahsen et al., 1995; Voos et al., 1996) which can be faithfully recapitulated *in vitro* from purified proteins (D'Silva et al., 2004; Liu et al., 2003; Slutsky-Leiderman et al., 2007).

Very recently, Pam17, another non-essential component of the TIM23 complex was discovered as a component of the import motor. Pam17 was specifically found to be co-isolated with the matrix translocating form of the TIM23 complex. Pam17 was shown to affect the correct organization of Tim14-Tim16 subcomplex of the motor part of the TIM23 complex suggesting its role in matrix translocation of preproteins by the TIM23 complex (van der Laan et al., 2005).

1.6 Mitochondrial Hsp70: A chaperone with two functions

There are three species of Hsp70s in the matrix of *S. cerevisiae* namely Ssc1, Ssq1 and Ecm10 as soluble proteins (Voos and Rottgers, 2002). All three Hsp70s have significant sequence homology to the bacterial Hsp70, DnaK. The most abundant and most vital among these three is Ssc1. *SSC1* is an essential gene and the protein plays vital roles in the biogenesis of mitochondria (Craig et al., 1987). In addition to protein import into the mitochondrial matrix, the chaperone plays crucial role in folding of newly imported proteins in the mitochondrial matrix. Being a member of the highly conserved Hsp70 group of chaperones, mtHsp70 possesses an N-terminal nucleotide binding domain (NBD) and a C-terminal peptide binding domain (PBD). The NBD influences the properties of the PBD by an as yet unclear mechanism of interdomain communication. The nucleotide bound to the NBD induces certain conformational changes of Hsp70s which in turn dictates the substrate binding affinity of the PBD. In the ATP-bound state, the PBD is in an open conformation with high on and off rates of substrate binding. On the other hand in the ADP-bound state, the PBD is in closed conformation and has a high binding affinity for substrates (Genevaux et al., 2007; Hartl and Hayer-Hartl, 2002). Specific partner proteins, also known as cochaperones, regulate the functions of Hsp70s. Based on extensive research on bacterial DnaK, two major types of cochaperones for Hsp70s have been identified. The efficient chaperone function goes on with the participation of co-chaperones of DnaJ family which stimulates the process of ATP hydrolysis by the Hsp70s and assist in efficient substrate binding. Cochaperones of the GrpE family catalyze the exchange of nucleotides on Hsp70 and are therefore also called nucleotide exchange factors (NEF). A schematic picture of a functional chaperone cycle of Hsp70s is presented in Figure 1.3.

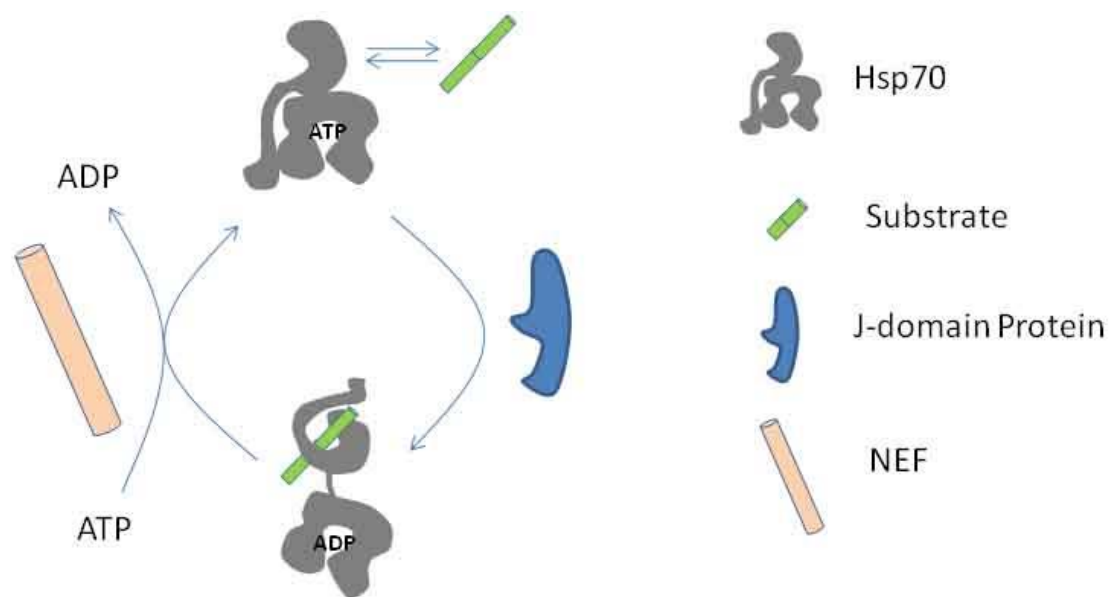


Figure.1.3: Model of the Hsp70 chaperone cycle. Hsp70 in the ATP-bound state interacts with the substrate via its PBD in an open conformation with low affinity. Subsequently, ATP hydrolysis stimulated by a J-domain protein and the substrate closes the PBD leading to high affinity binding of the substrate. Binding of the NEF catalyses the release of ADP and subsequent binding of ATP opens the PBD releasing the substrate.

1.6.1 Mitochondrial Hsp70 in preprotein translocation

Protein import into mitochondrial matrix is mediated by motor protein mtHsp70 (Ssc1 in *S. cerevisiae*), the key component of import motor which is situated in the *trans*-side of the inner mitochondrial membrane.

Both the protein folding and preprotein translocation activities of Hsp70s rely on its two basic properties: affinity to unfolded proteins and ATPase activity. Precursor proteins in transit represent ideal substrates for mtHsp70 and the interaction of mtHsp70 with the precursors is absolutely necessary for the translocation. Two energy sources have been found for the translocation of mitochondrial matrix targeted proteins, one of them is membrane potential across inner membrane ($\Delta\psi$) which mainly drives the positively charged presequence into the matrix (Geissler et al., 2000; Martin et al., 1991). For the translocation of the rest of the precursor ATP hydrolysis by mtHsp70 is required (Cyr et al., 1993; Wachter et al., 1994). Mutants of Ssc1 that are defective in ATP hydrolysis

show similar translocation defects as depletion of matrix ATP (Gambill et al., 1993; Stuart et al., 1994).

Ssc1 is recruited to the translocation channel of the TIM23 complex via peripheral membrane protein Tim44. It thereby helps the chaperone to be placed in the vicinity of the incoming preprotein (Blom et al., 1993; Maarse et al., 1992). Genetic interactions in yeast and physical interaction of these two proteins suggest that reversible interaction of membrane associated Tim44 and a fraction of soluble mtHsp70 forms the basis of precursor translocation into the matrix (Kronidou et al., 1994; Rassow et al., 1994; Schneider et al., 1994). This interaction is very specific but sensitive to the presence of nucleotides. It was shown that a stable complex is formed in presence of ADP whereas the complex becomes unstable in presence of ATP (Rassow et al., 1994; Schneider et al., 1994; von Ahsen et al., 1995; Voos et al., 1996). This nucleotide dependent sensitivity of Tim44-mtHsp70 interaction resembles the properties of substrate-mtHsp70 interaction raising the possibility that mtHsp70 binds Tim44 just like a substrate. However, this possibility has been excluded by several experiments. The temperature sensitive mutant of mtHsp70 from yeast Ssc1 (Ssc1-2) has been shown to interact significantly in increased amount with the newly imported proteins whereas interactions with Tim44 is destabilized under similar conditions (Rassow et al., 1994; Schneider et al., 1994; Voos et al., 1996). These results clearly demonstrated the distinct properties of Tim44 and substrates in binding mtHsp70. The major function of Tim44 in import motor is ascribed to its role in complex formation with mtHsp70. It is still not clear whether Tim44 serves only as a membrane anchor to Hsp70 to place the chaperone in the vicinity of the precursor or it serves as a fulcrum for the generation of an active force by the mtHsp70.

As in the case of other motor proteins, two models: power-stroke and Brownian ratchet, exist explaining how import motor drives unidirectional protein translocation (Neupert and Brunner, 2002). According to Brownian ratchet model the preproteins are in spontaneous sliding movements in the import channel (Ungermann et al., 1994). Binding of mtHsp70 traps the translocated segments in the matrix as it prevents the retrograde movement (Neupert and Brunner, 2002; Schneider et al., 1994). Subsequently, mtHsp70 bound to the preprotein diffuses further into the matrix and a new molecule of mtHsp70 binds to Tim44 waiting for the next segment to catch. Thus, step-wise inward movement

of preprotein is achieved towards the matrix without any active force exerted on the preprotein. Different evidences for Brownian ratchet mechanism of the import motor have been presented in the past years. There are several evidences in favor of oscillations of unfolded precursors which could be vectorially moved by trapping on the matrix side by mtHsp70 (Liu et al., 2003; Okamoto et al., 2002). In addition, the capacity of a domain to be imported did not depend on the global unfolding but was correlated with the extent of local unfolding following the MTS. Also forces required to unfold domains, as measured by atomic force microscopy, was not related to their capacity to be imported (Ainavarapu et al., 2005; Junker et al., 2005; Sato et al., 2005). Introduction of polyglycine or polyglutamine stretches in the preproteins, which disfavor Hsp70 binding, did not affect the import of these proteins once it is initiated by the $\Delta\psi$ (Okamoto et al., 2002). All these results are in agreement with the ratchet mechanism of import motor.

According to the alternative 'power stroke' or the 'active pulling' model, Hsp70 acts as a lever arm, which mechanically pulls on the incoming polypeptide chain by a conformational change resulting from ATP hydrolysis (Glick, 1995; Matouschek et al., 2000). Tim44 recruits the mtHsp70 near the translocation channel. A mutant form of Ssc1 (Ssc1-2) which was shown to be defective in interaction with Tim44, was inefficient in translocating tightly folded proteins but unfolded proteins were translocated at low $\Delta\psi$ (Voisine et al., 1999; Voos et al., 1996). Furthermore, loosely folded proteins are translocated more efficiently by Ssc1-2 than the wild type protein (Geissler et al., 2001). All these data pointed towards the idea that different mechanisms may exist for mtHsp70 for different preproteins. Translocation of tightly folded domains may require a large force, while trapping could be sufficient for loosely folded precursors. It remains to be established whether interaction of mtHsp70 with Tim44 or Tim14 can indeed serve as the fulcrum to provide a large force needed for active pulling or the interaction just increases the local concentration of Hsp70 near the translocation channel to increase the probability of binding to incoming polypeptide chain.

1.6.2 Protein folding by mtHsp70 and its cochaperones in the mitochondrial matrix

In addition to its essential function in translocation of preproteins into mitochondria, mtHsp70 is also involved in folding of proteins in the mitochondrial matrix. Direct evidence in support of a role of mtHsp70 in protein folding was provided by the identification of mitochondrial homologue of bacterial DnaJ protein, Mdj1 in yeast (Rowley et al., 1994). Deletion of MDJ1 is not lethal for yeast but leads to respiratory defects. There was no evidence of association of Mdj1 with the arrested preproteins speaking against its role in protein translocation. However, newly imported proteins tend to misfold and aggregate in a *MDJ1* mutant strain indicating its role in protein folding (Prip-Buus et al., 1996). Apart from protein folding, Mdj1 is also involved in the inheritance of mitochondrial DNA (Duchniewicz et al., 1999). It was shown that the activity of the mitochondrial DNA polymerase is influenced by Mdj1 (Duchniewicz et al., 1999).

The chaperone function of mtHsp70 is also regulated by Mge1, a homologue of bacterial GrpE protein. Mge1 forms a very stable but ATP sensitive complex with mtHsp70 (Bolliger et al., 1994; Nakai et al., 1994). The interaction leads to release of ADP and Pi in exchange of ATP from the mtHsp70. Interestingly, compared to other cochaperone Mdj1, Mge1 plays more crucial role, since *MGE1* is essential for cell viability. Prominent roles of Mge1 in protein translocation has been shown. On the other hand defects in Mge1 function lead to an insufficient interaction of mtHsp70 with the substrates making it a crucial component in the folding machinery as well.

The chaperone activity of the mitochondrial Hsp70 system have been demonstrated by *in vitro* refolding assays. A reconstituted system comprising of Ssc1, Mdj1 and Mge1 was able to prevent the aggregation of heat-denatured luciferase and could increase the efficiency of refolding of luciferase significantly (Kubo et al., 1999; Westermann and Neupert, 1997).

1.7 Aims of the present study

The objective of the present work was to gain new insights into the structure and function of the TIM23 complex, in particular the import motor. A major aim was to reconstitute the mtHsp70 cycle using recombinant and purified components of the import motor *in vitro*. In addition, detailed characterization of the role of Pam17, a recently discovered component of the complex postulated as subunit of the import motor, was to be addressed.

2 Materials and Methods

2.1 Molecular biology methods

2.1.1 Isolation of DNA

2.1.1.1 Isolation of yeast genomic DNA

Genomic DNA from yeast strains was isolated using the ‘Wizard Genomic DNA purification kit (Promega)’. Yeast strains were inoculated in 5 ml YPD medium and incubated overnight (ON) at 30°C while shaking at 130 revolutions per min (rpm). Cells were harvested from 1ml of ON cultures by centrifugation [13,000-16,000 x g, 2 min, at room temperature (RT)], resuspended in 293µl of 50 mM EDTA, pH 8.0. To the resuspended cells 7.5µl of zymolyase solution (10mg/ml) was added, mixed gently and incubated for 30-60 min at 30° C. After incubation with zymolyase, cells were centrifuged at 13,000-16,000× g, 2 min, RT and the supernatant was discarded. To the cell pellet, 300µl of nuclei lysis solution followed by 100µl of protein precipitation solution were added and incubated on ice for 5 min. Cells were centrifuged at 13,000-16,000× g, 3 min, RT. The supernatant was transferred to fresh Eppendorf tubes containing RT 300µl isopropanol and mixed by inversion of the tube and was centrifuged at 13,000-16,000× g, 2 min, RT. After the centrifugation, the supernatant was decanted and the DNA pellet was washed with 300µl of RT 70% ethanol and was centrifuged at 13,000-16,000× g, 2 min at RT. To the DNA pellet, 50µl of DNA rehydration solution containing RNase was added and incubated at 37° C for 15 min. Finally the DNA was rehydrated at 65° C for 1h and stored at -20° C for further use.

2.1.1.2 Isolation of plasmid DNA from Escherichia coli

Plasmid DNA from *E. coli* was isolated using a “PureYieldPlasmid Midiprep System (Promega)”. Single bacterial colonies carrying plasmids of interest were inoculated in 50 ml LB-Amp medium and incubated overnight at 37°C while shaking at 140 rpm. The next day cells were harvested by centrifugation (10,000 x g, 10 min, RT) and resuspended in 6

ml of 'Cell Resuspension Solution'. Cells were lysed by addition of 6 ml of 'Cell Lysis Solution'. Tubes were inverted 5 times and left for 3 min at RT. After neutralization with 10 ml of 'Neutralization Solution', tubes were again inverted 5 times and incubated for 3 min at RT to ensure thorough clearing. Samples were centrifuged (10,000 x g, 10 min, RT), and the supernatants immediately applied onto clarifying columns fixed on top of anion-exchange columns placed onto a vacuum manifold. After the entire volume of the sample passed under vacuum through the column stacks, the clarifying columns were removed and the anion-exchange column was washed first with 5 ml of 'Endotoxin Removal Wash Solution' and then with 20 ml of the 'Column Wash Solution'. The column was left to dry for 30 sec under vacuum and DNA was then eluted from the column with 600 µl of sterile deionized water (ddH₂O). Plasmid DNA isolated this way was stored at -20°C.

2.1.2 Amplification of DNA sequences by Polymerase Chain Reaction (PCR)

DNA sequences were amplified by PCR as described previously (Sambrook. J., 1989). The DNA templates for PCR were: (i) isolated DNAs from yeast or bacteria (when the PCR product was used for subsequent cloning), (ii) commercial cassettes for deletion of specific open reading frames (ORFs) (when the PCR product was used for homologous recombination in yeast cells) and (iii) whole cell extracts from yeast or bacteria (to check the successfulness of cloning). Thermostable DNA polymerases used were *Taq* (isolated from *Thermus aquaticus*) and *Pfu* (isolated from *Pyrococcus furiosus*). As *Taq* DNA polymerase has no proofreading ability, *Pfu* DNA polymerase was added in the PCR mix when the PCR product was used for cloning of some genes.

PCR mix (total volume of 50 µl) contained: 1 U DNA polymerase (*Taq* DNA polymerase and/or *Pfu* DNA polymerase), 5 µl 10 x PCR-buffer (1% Triton X-100, 500 mM KCl, 15 mM MgCl₂, 100 mM Tris·HCl, pH 8.8), 2 µl dNTPs (10 mM each), 1.25 µl primers (20 pmol/µl each) and 20 ng plasmid DNA or 200 ng genomic DNA as templates. When the successfulness of cloning was checked by PCR, single *E.coli* colonies were resuspended in 15 µl sterile H₂O or single *S. cerevisiae* colonies were resuspended in 15 µl sterile H₂O containing 100 µg/ml zymolyase, and 1 µl of cell suspensions was used as a template for

test PCR. The following PCR program, with small variations depending on the DNA sequence, was used:

1) 95°C, 3 min	Nuclease inactivation and complete DNA denaturation;	
2) 30-35 cycles	DNA amplification:	
	95°C, 30 s	DNA denaturation
	52°C, 45 s	Annealing of primers
	72°C, 1 min per 1 kb	Extension of primers (DNA synthesis)
3) 72°C, 10 min	Completion of the final extension reaction	

To avoid occurrence of possible non-specific PCR products in few cases, several values of annealing temperature were tested ($52 \pm 5^\circ\text{C}$) in temperature gradient PCR machine (Mastercycler gradient – Eppendorf). The PCR products were subsequently analyzed by agarose gel electrophoresis.

2.1.3 DNA analysis and purification

2.1.3.1 Agarose gel electrophoresis of DNA

DNA fragments were separated by horizontal agarose gel electrophoresis according to their molecular weights. Agarose was dissolved in TAE buffer (40 mM Tris-acetate, pH 7.5, 20 mM Na-acetate, 1 mM EDTA) at the boiling temperature in the microwave oven. When it cooled down to 65°C, ethidium-bromide was added (0.5 µg/ml) and, while still hot, agarose was poured in a cuboid mould to cool down to RT and solidify. DNA in solution (either isolated DNA or PCR product) was mixed in 4:1 ratio with 5 x loading dye (30% (v/v) glycerol, 0.25% (w/v) bromphenol-blue, 0.25% (w/v) xylencyanol) and loaded on a 0.8-3% (w/v) agarose gel, depending on the size of DNA fragments to be separated. Gels were run in TAE buffer at $U = 80\text{-}140\text{ V}$ depending on the size of the gel. Separated DNA fragments were visualized under UV light (366 nm). Commercially available molecular weight markers were used in each run.

2.1.3.2 Isolation of DNA from agarose gels

DNA bands were excised from the gel with a sterile scalpel under UV light. DNA was extracted from the gel using the “Wizard SV Gel and PCR Clean-Up System” (Promega). 10µl of membrane binding solution was added per 10mg of gel slice with DNA and was incubated for ~ 10min at 60°C till the gel piece completely dissolve. The dissolved mixture was loaded to SV mini column inserted into collection tube and was centrifuged at 16,000x g for 1 min and the flow-through was discarded. After passing the whole gel-mix through the SV mini column, column was washed two times, each with 700µl of membrane wash buffer (containing ethanol). After washing, the column was dried by centrifuging the column for 2 min at 16,000x g. DNA was eluted with 30 µl sterile ddH₂O and 1 µl of the eluted DNA was loaded on an analytical agarose gel to check the efficiency of purification. Extracted DNA was routinely stored at –20°C.

2.1.3.3 Measurement of DNA concentration

To determine DNA concentration the absorption of DNA solutions was measured at 260 nm. One optical unit (OD = 1.0) corresponds to a concentration of 50 µg/ml of double stranded DNA, 33 µg/ml single stranded DNA, 40 µg/ml RNA or 20 µg/ml oligonucleotides.

2.1.4 Enzymatic manipulation of DNA

2.1.4.1 Digestion of DNA with restriction endonucleases

DNA was digested with 2-5 U of specific restriction endonucleases per 1 µg of DNA. For analytical purposes, up to 100 ng of DNA was digested in a 10 µl reaction volume. For preparative purposes up to 3 µg of DNA was digested in a 60 µl reaction volume. DNA was usually digested for 3 h at 37°C in the buffer specific for the restriction enzyme, according to the manufacturer’s recommendations. Digested DNA fragments were analyzed by agarose gel electrophoresis and used for ligation reactions.

2.1.4.2 Ligation of DNA fragments

One DNA fragment (after digestion with restriction endonucleases) and a cloning vector or another DNA fragment (digested with the same or compatible enzymes) were ligated

together in a buffer containing DNA ligase from bacteriophage T4. Linearized vector (100-200 ng) and 5-10 fold molar excess of DNA fragment were incubated in a 10 μ l reaction with 1 μ l of 10 x ligation buffer (50 mM Tris·HCl, 10 mM MgCl₂, 1 mM DTT, 1 mM ATP, 5% (w/v) PEG-8000, pH 7.6) and 0.5 μ l (1 U) T4 DNA ligase (NEB). Ligation reaction was performed at 14°C for 16 h and 0.5-1 μ l of the ligation mixture was transformed into electrocompetent *E. coli* cells.

2.1.5 Transformation of electrocompetent *E. coli* cells

2.1.5.1 Overview of *E. coli* strains used

Strain	Genotype	Reference
MH1	MC1061 derivative; <i>araD139</i> , <i>lacX74</i> , <i>galU</i> , <i>galK</i> , <i>hsr</i> , <i>hsm+</i> , <i>strA</i>	(Casadaban and Cohen, 1980)
XL1-Blue	<i>supE44</i> , <i>hsdR17</i> , <i>recA1</i> , <i>endA1</i> , <i>gyrA96</i> , <i>thi-1</i> , <i>relA1</i> , <i>lac</i> ⁻ , F' <i>[proAB</i> ⁺ , <i>lacI</i> ^d <i>lacZ</i> Δ M15, Tn10(<i>tet</i> ^r)]	commercially available from Stratagene
BL21(DE3)	F ⁻ <i>ompT gal dcm lon hsdS_B(r_B⁻ m_B⁻)</i> λ (DE3 [<i>lacI lacUV5-T7 gene 1 ind1 sam7 nin5</i>])	Commercially available from Novagen

2.1.5.2 Preparation of electrocompetent cells

The electro-competent *E. coli* cells (MH1 or XL1-Blue or BL21-DE3) were prepared as described in (Dower et al., 1988). 50 ml of LB medium was inoculated with a single colony of the corresponding bacterial strain and grown overnight at 37°C while shaking at 140 rpm. Next morning 1 l of LB medium, preheated to 37°C, was inoculated with 2 ml of the overnight culture and the cells were grown until they reached OD₅₇₈ \approx 0.5. The culture was then incubated on ice for 30 min and the cells were subsequently harvested by centrifugation for 5 min at 4,400 x g and at 4°C and washed sequentially with 400 ml, 200 ml and 50 ml of sterile 10% (v/v) glycerol. The competent cells were finally resuspended in 1 ml of LB medium with 10% (v/v) glycerol and stored at -80°C in 40 μ l aliquots.

2.1.5.3 Transformation of *E. coli* cells by electroporation

The ligation mixture or isolated plasmid DNA (0.5-1 μ l) was added on ice to 40 μ l of electrocompetent cells and this transformation mixture was then transferred to ice-cold 0.2 cm electroporation cuvette. High electric voltage pulse was delivered to the cells in the cuvette through the electroporation Gene Pulser apparatus (BioRad) (settings: U = 2.5 kV, R = 400 Ω , C = 25 μ F; time constant obtained (τ) was 7.2-8.8 ms); cell suspension treated in this way was diluted with 1 ml of LB-medium and incubated for 45 min at 37°C while shaking at 140 rpm to allow cell recovery. Cells were briefly centrifuged, most of the medium was poured off, cell pellet resuspended in the ca. 150 μ l remaining medium and plated on LB-Amp plates (LB with 2% (w/v) agar supplemented with 100 μ g/ml ampicillin). Plates were incubated overnight at 37°C and the successfulness of transformation was usually checked by test PCR.

2.1.6 Overview of yeast strains used

Yeast strain	Reference
<hr/>	
Wild type strain	
<hr/>	
YPH499	(Sikorski and Hieter, 1989)
<hr/>	
Strains generated by homologous recombination	
<hr/>	
TIM21::HIS3	(Mokranjac et al., 2005)
PAM17::HIS3	This thesis
Tim21::HIS3/Pam17::kanMX4	This thesis
GAL-Tim17	(Popov-Celeketic et al., 2008a)
GAL-Tim23	(Popov-Celeketic et al., 2008a)
GAL-Tim50	(Mokranjac et al., 2003a)
GAL-Tim44	(Popov-Celeketic et al., 2008a)
GAL-Tim14	(Mokranjac et al., 2003b)
GAL-Tim16	(Kozany et al., 2004)
<hr/>	
Strains generated by transformations with yeast vectors	
<hr/>	
<i>PAM17::HIS3</i> + pRS314[His ₆ Pam17]	This thesis
YPH499 + pVT-102U[Tim21]	This thesis

YPH499 + pVT-W[Pam17] This thesis
 YPH499 + pVT-102U[Tim21] + pVT- This thesis
 W[Pam17]

2.1.7 Cloning strategies for generation of yeast strains by homologous recombination

2.1.7.1 Deletions of *PAM17* gene and double deletion of *PAM17/TIM21*

PAM17 gene was deleted by homologous recombination of the PCR product obtained, in the haploid yeast strain YPH499. PCR products contained an auxotrophic-marker-cassette *HIS3* and short sequences homologous to the flanking regions of *PAM17* locus. Primers Pam17deltafor and Pam17deltarev were used for amplification of *PAM17* deletion cassette using pFA6HIS3MX6 (Wach et al., 1997) as the template. The obtained PCR product was transformed in yeast and integrated into the corresponding chromosome via the regions homologous to *PAM17*. To isolate positive clones, yeast transformants were grown on selective medium lacking histidine and homologous recombination was checked by PCR and fast mito prep. For generation of the strain where both *PAM17* and *TIM21* were deleted, PCR product was amplified from pFA6KANMX4 (Wach et al., 1997) using Pam17deltafor and Pam17deltarev primers and transformed in *TIM21::HIS3* strain (Mokranjac et al., 2005). To isolate positive clones, yeast transformants were grown on selective medium lacking histidine and containing kanamycin. Homologous recombination was checked by PCR and fast mito prep.

Pam17deltafor	5'– AAG AAG TGT TAA AAA CAT TCA GAA AAC ATT GTC CGC CTC TTC AAA CGT ACG CTG CAG GTC GAC – 3'
Pam17deltarev	5'– GTA TAT ATA CAG AGT CTG AGA AGA AGG AAA AGA TCA CAC GTT CAA ATC GAT GAA TTC GAG CTC – 3'

2.1.7.2 Disruption of *TIM44* in the haploid strain YPH499

First YPH499 strain was transformed with pVT-102U [Tim44] plasmid and selected on SD-URA medium to make the strain YPH + pVT-102U[Tim44]. pVT-102U [Tim44] was

made by amplifying the sequence of *TIM44* from yeast genomic DNA using the primers BamTim44 and Tim44Xho and cloning it into pVT-102U [Tim44] vector in between BamHI and XhoI restriction sites.

BamTim44	5'–CCC GGA TCC ATG CAC AGA TCC ACT TTT ATC – 3'
Tim44Xho	5'– GGG CTC GAG TCA GGT GAA TTG TCT AGA ACC – 3'

TIM44 gene was disrupted by homologous recombination of the PCR product obtained, in the haploid yeast strain YPH499 + pVT-102U [Tim44]. PCR products contained an auxotrophic-marker-cassette *HIS3* and short sequences homologous to the flanking regions of *TIM44* locus. Primers Tim44deltafor and Tim44deltarev were used for deletion of *TIM44* gene using pFA6HIS3MX6 (Wach et al., 1997) as the template and these PCR products were transformed in yeast and stably integrated into the corresponding chromosome via the regions homologous to the *TIM44* gene. To isolate positive clones, yeast transformants were grown on selective medium lacking histidine and uracil and homologous recombination was checked by PCR.

Tim44deltafor	5'–TTA TTC CTG AAT TTT TCA CTA CCG CAG CAA TTG CTA TTT CAG TTC CGT ACG CTG CAG GTC GAC – 3'
Tim44deltarev	5'– TAG GAA GGA AAA GGA AAA GAA AAC AAA AGA GTA CAT CGA AAC CAA ATC GAT–3'

2.1.8 Overview of different plasmids used

Plasmids	Reference
Wild type strain	
pRS314[His ₆ Pam17]	This thesis
pVT-102U[Tim21]	This thesis
pVT-W[Pam17]	This thesis
pETDuet-1[His ₆ Tim44(44-431)]	This thesis
pETDuet-1[His ₆ Tim44(44-233)]	This thesis
pETDuet-1[His ₆ Tim44(234-431)]	This thesis

pETDuet-1-Hep1[Ssc1(24-654)]	(Sichting et al., 2005)
pETDuet-1-Hep1[Ssc1(24-415)]	This thesis
pETDuet-1 [Ssc1(410-654)]	This thesis
pETDuet-1[Mdj1(56-511)]	This thesis
pRS314[promoter-Tim44(1-431)-3'UTR]	This thesis
pRS314[promoter-Tim44(1-233)-3'UTR]	This thesis
pRS314[promoter-Tim44(210-431)-3'UTR]	This thesis

2.1.9 Cloning strategies for plasmids used for the transformation of yeast

2.1.9.1 pRS314[His6Pam17]

Promoter region 400 bp upstream of *PAM17* gene containing sequence coding for its mitochondrial targeting signal followed by hexahistidine tag at its 3' end was amplified from yeast genomic DNA using primers BamPam17p and Pam17preHis6Pst. Coding sequence of *PAM17* gene lacking the sequence coding for mitochondrial targeting signal was amplified from yeast genomic DNA using primers PstPam17m and Pam17fXho. These two PCR products were cloned in pRS314 vector that was transformed in *PAM17::HIS3* yeast strain. Yeast transformants were subsequently grown on selective medium lacking tryptophan and checked by fast mito prep.

BamPam17p	5' – CCC GGA TCC ATG TTT ACC AGT GCC ATT AGA TTG – 3'
Pam17preHis ₆ Pst	5' – TTT CTG CAG GTG ATG GTG ATG GTG ATG ATA TGA TCT TAA GGG TAA GGT TG – 3'
PstPam17m	5' – AAA CTG CAG TCT CAG CCC GCA TCC CTT CAA G – 3'
Pam17fXho	5' – GGG CTC GAG CAA ATG CGC ATA AAG GAA ATG C – 3'

2.1.9.2 pVT-102U[Tim21]

Coding sequence of *TIM21* gene was subcloned from pGEM4 [Tim21] (Mokranjac et al., 2005) to pVT-102U vector using *Bam*HI and *Hind*III restriction sites. The obtained

plasmid was transformed in YPH499 yeast strain. Yeast transformants were subsequently grown on selective medium lacking uracil and the levels of overexpression of Tim21 in the transformants were checked by fast mito prep.

2.1.9.3 *pVT-W[Pam17]*

Coding sequence of *PAM17* gene was amplified from yeast genomic DNA using primers BamPam17 and Pam17Hind. The construct was cloned in pVT-W vector using *BamHI* and *HindIII* restriction sites. The obtained plasmid was transformed in YPH499 yeast strains with and without pVT-102U[Tim21] plasmid. Yeast transformants were subsequently grown on selective medium lacking tryptophan or tryptophan and uracil and the levels of overexpression of Pam17 in the transformants were checked by fast mito prep.

BamPam17	5'– CCC GGA TCC ATG TTT ACC AGT GCC ATT AGA TTG – 3'
Pam17Hind	5'– CCC AAG CTT TCA CAA AAA TTC TTT GGC TTT C – 3'

2.1.10 Cloning strategies for plasmids used for recombinant proteins expressions

2.1.10.1 Cloning of mature *Tim44* in bacterial expression vector

The nucleotide sequence coding for mature Tim44 (aa.44-431) was cloned into the 1st MCS of pETDuet-1 vector (Novagen) in between BamHI and EcoRI restriction sites. A TEV cleavage site was introduced between the His₆ tag and the sequence of Tim44 to get rid of the tag subsequently by treating with TEV protease. Yeast genomic DNA was used as the template DNA and the primers used for the PCR amplification are

BamTEVTim44_43	5'-CCC GGA TCC GTC AGA GAA TCT TTA TCA GGG ACA AGG TGG AAA CCC TCG ATC-3'
Tim44Eco	5'-CCC GAA TTC TCA GGT GAA TTG TCT AGA ACC-3'

2.1.10.2 Cloning of N-terminal domain of Tim44 (Tim44-NTD) in bacterial expression vector

The nucleotide sequence coding for N-terminal domain of Tim44 (aa.44-233) was cloned into the 1st MCS of pETDuet-1 vector (Novagen) in between BamHI and EcoRI restriction sites. A TEV cleavage site was introduced between the His₆ tag and the sequence of Tim44-NTD, to get rid of the tag subsequently by treating with TEV protease. Yeast genomic DNA was used as the template DNA and the primers used for the PCR amplification are

BamTEVTim44_43	(sequence mentioned with cloning of mature Tim44)
Tim44_233stopEco	5'-TTT GAA TTC TCA ACG GCC AAC CAC GGT TTT CTC-3'

2.1.10.3 Cloning of C-terminal domain of Tim44 (Tim44-CTD) in bacterial expression vector

The nucleotide sequence coding for N-terminal domain of Tim44 (aa.234-431) was cloned into the 1st MCS of pETDuet-1 vector (Novagen) in between BamHI and EcoRI restriction sites. A TEV cleavage site was introduced between the His₆ tag and the sequence of Tim44-CTD to get rid of the tag subsequently by treating with TEV protease. Yeast genomic DNA was used as the template DNA and the primers used for the PCR amplification are

BamTEVTim44_234	5'-CCC GGA TCC GTC AGA GAA TCT TTA TTT TCA GGG ATC TAT ACA ATC TTT AAA GAA CAA ATT G-3'
Tim44Eco	(sequence mentioned with cloning of mature Tim44)

2.1.10.4 Cloning of Nucleotide binding domain of Ssc1(Ssc1-NBD) in bacterial expression vector

The nucleotide sequence coding for nucleotide binding domain of Ssc1 (Ssc1-NBD, aa.24-415) was cloned into the 2nd MCS of pETDuet-1 vector (Novagen) in between NdeI and XhoI restriction sites with and without *HEPI* in the 1st MCS of the same vector.

Yeast genomic DNA was used as the template DNA and the primers used for the PCR amplification are

NdeISsc1_24	5'- GGA ATT GCA TAT GCA GTC AAC CAA GGT TCA AAG -3'
Ssc1_415stopXho	5'-GGG CTC GAG TTA TAA TAA TAA GAC GTC AGT AAC CTC -3'

2.1.10.5 Cloning of Peptide binding domain of Ssc1(Ssc1-PBD) in bacterial expression vector

The nucleotide sequence coding for peptide binding domain of Ssc1 (Ssc1-PBD, aa.410-654) was cloned into the 1st MCS of pETDuet-1 vector (Novagen) in between BamHI and PstI restriction sites. A TEV cleavage site was introduced between the His₆ tag and the sequence of Ssc1-PBD to get rid of the tag subsequently by treating with TEV protease. Yeast genomic DNA was used as the template DNA and the primers used for the PCR amplification are

BamTEVSsc1_410	5'-CCC GGA TCC GTC AGA GAA TCT TTA TTT TCA GGG AAC TGA CGT CTT ATT ATT AGA TG-3'
Ssc1Pst	5'-GGG CTG CAG TTA CTG CTT AGT TTC ACC AG-3'

2.1.10.6 Cloning of mature Mdj1 in bacterial expression vector

The nucleotide sequence coding for mature Mdj1 (aa.56-511) was cloned into the pETDuet-1 vector (Novagen) in between XbaI and HindIII restriction sites.

2.1.10.7 Point mutations of Tim44, Ssc1 and Mdj1

Two methods were used to generate point mutants. In the first one, 5'-phosphorylated primers harbouring desired mutation were used to amplify the whole plasmid, purified PCR product was ligated and subsequently transformed into suitable competent cells. In the second method point mutations were generated by the Stratagene's 'QuikChange mutagenesis kit' according to the manufacturer's protocol. The primers used for mutagenesis are listed below.

2.1.10.8 List of Primers used for site directed mutagenesis

Tim44K90Cf	5'-Pho-ACA AAT GTC CTA GGG AAG CAT ATT TGA AAG CTC-3'
Tim44K90Cr	5'- Pho-AGG CTT CAG ACT CGC CTA ACT TTC CCG AAG C-3'
Tim44D187Cf	5'- Pho-GAG ATG CCT GGC CTC TGC GAA AAG ACA CAG G-3'
Tim44D187Cr	5'- Pho-TCA CGC TTA AGT CTC CTT TGC TCT TTC GTG-3'
Tim44V252Cf	5'- Pho-AAA ATA ACC AAC AAA GTG GGC GGT TTC TTT GC-3'
Tim44V252Cr	5'- Pho-CCT CAT CAC ACA AAT TAA GGG GTT TTC ACT TTC-3'
Tim44R272Cf	5'- Pho-TCC TGT GTA TAC AGT CAA TTT AAG CTA ATG GAC-3'
Ssc1K72Cf	5'- Pho-AGA ACG ATT GGT TGG TAT TCC AGC CAA GCG-3'
Ssc1K72Cr	5'- Pho-CCC TCA CAA GTG AAA GCT ACT ACA GAA GG-3'
Ssc1K161Cf	5'- Pho-GGT TGT CCA GTT AAG AAT GCT GTT GTC ACT G-3
Ssc1K161Cr	5'- Pho-CAA GTA CGC CTC AGC TGT TTC CTT CAT CTT G-3'
Ssc1S212Cf	5'- Pho-AAA TGC GAC TCT AAA GTT GTT GCC GTT TTC-3'
Ssc1S212CrK	5'- Pho-TTC CAA ACC GTA AGC TAA GGC AGC GGC GG-3'
Ssc1S265Cf	5'- Pho-GAA ACT GGT ATT GAT TTG GAA AAT GAC CGT ATG-3'
Ssc1S265Cr	5'- Pho- GGT TTT AAA ACG ACA AAC AAT CTC TCT CAA C-3'
Ssc1D341Cf	5'- Pho-GTC TGC CCA GTC AAG AAG GCT TTG AAA GAC-3'
Ssc1D341Cr	5'- Pho-AGT TCT CTT AAC TAG TGG GGC TGT CAA AGT C-3'
Ssc1I448C FO	5'- Pho-AAA TCT CAA TGT TTC TCC ACT GCC GCT GCT GGT-3'

Ssc1I448C RE	5'- Pho-CTT TGT TGG AAT AGT AGT GTT TCT TGG ATT-3'
Ssc1T481C FO	5'- Pho-GGT AAC TTC TGT TTA GCC GGT ATC CCA CCT GCT-3'
Ssc1T481C RE	5'- Pho-AAT CAA TTT GTT GTC TCT AAC CAA TTC TCT-3'
Ssc1590Cf	5'- GCC CAA AAG GTT AGG TGT CAA ATC ACT TCC TTG-3'
Ssc1590Cr	5'- CAA GGA AGT GAT TTG ACA CCT AAC CTT TTG GGC-3'
DnaKC15Af	5'- GTA CTA CCA ACT CTG CCG TAG CGA TTA TGG ATG-3'
DnaKC15Ar	5'- CAT CCA TAA TCG CTA CGG CAG AGT TGG TAG TAC-3'
DnaKE318Cf	5'- GTA AAC CGT TCC ATT TGC CCG CTG AAA GTT GCA-3'
DnaKE318Cr	5'- TGC AAC TTT CAG CGG GCA AAT GGA ACG GTT TAC-3'
DnaKV425Cf	5'- ACC AAG CAC AGC CAG TGC TTC TCT ACC GCT GAA-3'
DnaKV425Cr	5'- TTC AGC GGT AGA GAA GCA CTG GCT GTG CTT GGT-3'
DnaKN458Cf	5'- TCT CTG GGT CAG TTC TGC CTA GAT GGT ATC AAC-3'
DnaKN458Cr	5'- GTT GAT ACC ATC TAG GCA GAA CTG ACC CAG AGA-3'
DnaKT563Cf	5'- CCG GCT GAC GAC AAA TGC GCT ATC GAG TCT GCG-3'
DnaKT563Cr	5'- CGC AGA CTC GAT AGC GCA TTT GTC GTC AGC CGG-3'
Mdj1H89Qf	5'- CTG GCA AAG AAG TAC CAA CCG GAT ATC AAC AAG- 3'
Mdj1H89Qr	5'- CTT GTT GAT ATC CGG TTG GTA CTT CTT TGC CAG-3'

2.1.11 Cloning strategies for plasmids used for the transformation of yeast for checking the *in vivo* functionality

2.1.11.1 Cloning of full length Tim44 and domains of Tim44 in pRS314

The nucleotide sequence coding for Tim44 including the promoter and 3'UTR was cloned into the pRS314 vector in between BamHI and XhoI restriction sites. The primers used for the PCR amplification are

BamTim44p	5'- CCC GGA TCC GAA CAC CAC GAC TAA TAA AAC-3'
Tim44fXho	5'- CCC CTC GAG GGT ACG AAG CCT TTG CAC CTG-3'

The full length Tim44 (with the promoter and 3'UTR) served as the template for amplifying the N-terminal domain (with the promoter and until aa.233) using the primers BamTim44p as the forward one and Tim44_233stopEco as the reverse one.

The 3'UTR was amplified separately using the primers

EcoTim44f	5'- CCC GAA TTC TTG GTT TCG ATG TAC TCT TTT G-3'
Tim44fXho	(sequence as mentioned before)

The C-terminal domain was amplified using the primers and

EcoTim44_210	5'- AAA GAA TTC AAT ATC GAG TCT AAA GAA TCG-3'
Tim44fXho	(sequence as mentioned before)

was cloned in frame with the promoter which was amplified separately by using the primers

BamTim44p	(sequence as mentioned before)
Tim44preEco	5'- TAA GAA TTC CGC ACG GGT CGT AGA GGT GG-3'

2.1.11.2 Making of point mutants of Tim44 in yeast vector

The full length Tim44 (including the promoter and the 3' UTR) was subcloned into pBleuescript(+) vector for mutagenesis as pRS314 vector was not suitable for mutagenesis, using the same primers as used for bacterial expression vector. The obtained mutants were subcloned back into pRS314 for checking the *in vivo* functionality of the mutant proteins.

2.1.11.3 Making of point mutants of Ssc1 in yeast vector

The mature Ssc1 containing the point mutation was amplified from the respective mutants in pETDuet-1 vector using the primers and cloned in frame with the Ssc1-promoter-presequence in pRS314.

BamSsc1m	5'-CCC GGA TCC CAG TCA ACC AAG GTT CAA GG-3'
Ssc1_Xho	5'- ATA TCT CGA GCT GCT TAG TTT CAC CAG ATT C -3'

2.1.12 Checking the *in vivo* functionality of mutant Tim44

Yeast strains expressing only the mutant versions of Tim44 were made by transforming the yeast strain *TIM44::HIS3+* pVT-102U [Tim44] (*URA3* containing plasmid) with the plasmids carrying mutant *TIM44* and chasing out the *URA3* containing plasmid carrying the wild type copy, by growth on 5-Fluoroorotic acid (5-FOA) containing media.

2.1.13 Checking the *in vivo* functionality of mutant Ssc1

Yeast strains expressing only the mutant versions of Ssc1 were made by transforming the yeast strain *Ssc1::LEU+* pVT-102U [Ssc1-his] (*URA3* containing plasmid) (Bolliger et al., 1994) with the plasmids carrying mutant *Ssc1* and chasing out the *URA3* containing plasmid carrying the wild type copy, by growth on 5-Fluoroorotic acid (5-FOA) containing media.

2.2 Methods in cell biology

2.2.1 *E. coli* – media and growth

2.2.1.1 Media for *E. coli*

LB-medium: 0.5% (w/v) yeast extract, 1% (w/v) bacto-tryptone, 1% (w/v) NaCl.

LB-Amp medium: LB-medium supplemented with 100 µg/ml of ampicillin.

Above mentioned composition of the media were used for preparing liquid cultures. For preparation of solid media (LB or LB-Amp plates) 2% (w/v) bacto-agar was added to the liquid media solutions and autoclaved (120°C, 20 min). The ampicillin was added after the media had been cooled down to 50°C.

2.2.1.2 Cultivation of *E. coli*

Liquid medium (usually 50 ml of LB-Amp) was inoculated with the single colony from the plate and grown overnight at 37°C while shaking at 140 rpm. If necessary, cells were grown for up to 24h at lower temperatures (30 or 24°C).

2.2.2 *S. cerevisiae* – media and growth

2.2.2.1 Media for *S.cerevisiae*

Non-selective media:

YP-medium: 10 g yeast extract, 20 g bacto-peptone, H₂O to 930 ml, pH 5.0 (adjusted with HCl).

YPD-medium: YP-medium supplemented with 2% glucose.

YPG-medium: YP-medium supplemented with 3% (v/v) glycerol.

YPGal-medium: YP-medium supplemented with 2% galactose.

Lactate medium: 3 g yeast extract, 1 g KH₂PO₄, 1 g NH₄Cl, 0.5 g CaCl₂ x 2H₂O, 0.5 g NaCl, 1.1 g MgSO₄ x 6H₂O, 0.3 ml 1% FeCl₃, 22 ml 90% lactic acid, H₂O to 1 l, pH 5.5 (adjusted with KOH) and supplemented with 0.1% glucose or 0.5% galactose.

Selective media:

SD medium: 1.7 g yeast nitrogen base, 5 g (NH₄)₂SO₄, 20 g glucose, H₂O to 1 l.

SLac medium: 1.7 g yeast nitrogen base, 5 g (NH₄)₂SO₄, 22 ml 90% lactic acid, H₂O to 1 l, pH 5.5 (adjusted with KOH).

For selective media, stock solutions: histidine (10 mg/ml, 500 x stock), leucine (10 mg/ml, 333 x stock), lysine (10 mg/ml, 333 x stock), uracil (2 mg/ml, 100 x stock) and adenine (2 mg/ml, 100 x stock) were separately autoclaved for 20 min at 120°C, whereas tryptophan (10 mg/ml, 500 x stock) was filter sterilized.

The above described media were used for preparing liquid cultures. For preparation of plates with solid media, 2% w/v bacto-agar was added. Bacto-agar, glucose, and media

were autoclaved separately. The amino acid solutions were added to the selective media just before pouring the plates.

2.2.2.2 Cultivation of *S.cerevisiae*

Liquid cultures were inoculated with yeast strains from the glycerol stocks or from the agar plates and were grown in the appropriate liquid medium at 30°C while shaking at 140 rpm. Prior to the isolation of mitochondria cells were passaged for approximately 60 h in the way that OD₅₇₈ never exceeded 1. Temperature-sensitive mutants were grown at 24°C for the same period of time. For the generation of mitochondria depleted of one its essential proteins a yeast strain having the corresponding gene under *GAL* promoter was grown for 48-60 h on galactose-containing media after which cells were collected, washed with water, resuspended in glucose-containing media and grown in the latter media for 8-18 h depending on the strain. For the generation of mitochondria with increased levels of one its proteins encoded on the gene under *ADH* promoter, the corresponding yeast strain was grown on selective lactate medium supplemented with 0.1% glucose.

2.2.2.3 Transformation of *S.cerivisiae* by the lithium acetate method

The corresponding yeast strain was grown overnight in YPD-medium and diluted the next morning to 50 ml medium with an OD₆₀₀ of 0.1-0.2. Cells were grown further, till they reached an OD₆₀₀ of 0.5-0.6. Then, cells were transferred to a sterile centrifuge tube, and harvested by centrifugation (1,000×g, 3 min, RT). After washing with 25 ml of sterile water, cells were recollected, resuspended in 1 ml 100 mM lithium acetate and transferred to an Eppendorf tube. Cells were centrifuged again (7,500×g, 15 sec, RT) and were resuspended in 400 µl 100 mM lithium acetate. For each transformation 50 µl of the cell suspension was centrifuged (7,500×g, 5 min, RT) and the supernatant was removed. Next, cells were overlaid in the following order with: 240 µl PEG 3350 (50% v/v), 36 µl 1 M lithium acetate, 5 µl single stranded salmon sperm DNA (10 mg/ml; previously incubated for 5 min at 95°C), 70 µl H₂O containing 0.1-10 µg of DNA to be transformed. The mixture was vortexed for 1 min and incubated for 30 min at 30°C, with moderate shaking, followed by another 20-25 min at 42°C. The cells were harvested by

centrifugation (7,000×g, 15 sec, RT), washed with sterile water, resuspended in a small volume of sterile water (150 µl), and spread on plates with the appropriate selective media. The plates were incubated for 2-4 days at 30°C to recover transformants.

2.2.3 Isolation of mitochondria from *S. cerevisiae*

Mitochondria were isolated from *S. cerevisiae* following the previously described method (Daum et al., 1982a; Daum et al., 1982b). Yeast cells were cultivated to OD₆₀₀ of 1-1.5 and collected by centrifugation (4,400×g, 5 min, RT). The pellets were washed with H₂O and resuspended to a final concentration of 0.5 g/ml in DTT buffer (100 mM Tris-SO₄, 10 mM dithiotreitol (DTT), pH 9.4). The cell suspension was incubated for 10 min at 30°C with gentle shaking, followed by another centrifugation step and resuspended in 100 ml of 1.2 M sorbitol buffer (1.2 M sorbitol, 20mM potassium phosphate-KOH, pH 7.4). The cell wall was digested by 2.5 mg Zymolyase per gram wet cells dissolved in Sorbitol buffer. Cells were incubated for 30-45 min at 30°C, under moderate shaking conditions. To test the cell wall digestion (obtaining of spheroplasts), 50 µl cell suspension was diluted with 2 ml H₂O or into a solution of 1.2 M sorbitol. Formation of spheroplasts was complete when the OD of the H₂O dilution was 10-20% of the OD of the sorbitol dilution. The solution of spheroplasts in pure H₂O becomes clear because spheroplasts burst under these conditions. All the subsequent steps were performed at 4°C. The spheroplasts were isolated by centrifugation (3,000×g, 5 min, 4°C), resuspended (0.15 g/ml) in homogenization buffer (0.6 M sorbitol, 10 mM Tris-HCl, 1 mM EDTA, 0.2% (w/v) BSA, 1 mM PMSF, pH 7.4) and homogenized 10 times in a Dounce-Homogeniser. The cell remnants and unopened cells were sedimented by double centrifugation (2,000×g, 5 min, 4°C). The supernatant was spun (17,400×g, 12 min, 4°C) and the sedimented mitochondria were resuspended in SH buffer (0.6M sorbitol, 20mM HEPES, pH 7.4) and separated again from cell's remnants (2,000×g, 5 min, 4°C). The mitochondria were sedimented again as above (17,400×g, 12 min, 4°C). Finally, mitochondria were resuspended in a small volume of SH buffer to a concentration of 10 mg/ml protein, aliquoted, frozen in liquid nitrogen, and stored at – 80°C till use.

2.2.4 Isolation of crude mitochondria from *S. cerevisiae*

Cells corresponding to 10-20 OD units were harvested by centrifugation (800 x g, 5 min, RT) and washed with water. The cells were resuspended in 300 µl SHK buffer (0.6M sorbitol, 20mM HEPES, pH 7.4, 80mM KCl) containing 1mM PMSF and to the resuspended cells 0.3 g glass beads (diameter 0.3 mm) were added. The samples were vortexed four times 30 sec each, with 30 sec breaks in between (during this break the samples were incubated on ice) and centrifuged (1,000 x g, 3 min, 4°C). After the centrifugation, the supernatant was transferred to a new tube and was centrifuged (10,000×g, 10 min, 4°C), resulting in crude mitochondrial pellets.

2.3 Immunology methods

2.3.1 Generation of antibodies

2.3.1.1 Generation of polyclonal antisera against Pam17 protein

Polyclonal antisera were generated in rabbits. Recombinant protein was expressed in bacteria, purified using a specific tag and used as antigens. After the purification on the column remaining contaminants were separated from the proteins of interest by SDS-PAGE. Upon Western blotting, the bands corresponding to the protein of interest were excised from nitrocellulose membranes. Up to 200 µg of proteins (10 bands) were dissolved in 300 µl DMSO by vortexing for 3 min. TiterMax adjuvant (300 µl) was added and the emulsion injected subcutaneously into rabbits. The antigen was injected twice within ten days before the first bleeding was taken. All subsequent injections took place every four weeks. Freund's incomplete adjuvant was used instead of TiterMax adjuvant for all the injections except the first one. The rabbits were bled 10-12 days after each injection cycle. Approximately 30-40 ml of blood was taken from the ear vein and left to coagulate at RT for 2 h. Coagulated blood was centrifuged twice (5 min at 3000 x g and 15 min at 20000 x g, RT), and the supernatant was incubated at 56°C for 20 min to inactivate complement system. The antisera prepared this way were then aliquoted and frozen at -20°C.

2.3.1.2 Affinity purification of antibodies against different components of the TIM23 complex

Affinity purification was performed in order to reduce the cross-reactivity of the antisera. Antibodies against Tim23, Tim44, Tim50, Tim16, Tim14, Tim17, Tim21 and Pam17 were purified on the affinity columns made by coupling the proteins that served as antigens to the CNBr-activated Sepharose 4B (Amersham) via their -NH₂ groups. To remove all other amino group containing substances from protein in the solution prior to coupling, the buffer was exchanged with a bicarbonate one on the PD-10 column (Amersham). The column was equilibrated with 30 ml 0.1 M NaHCO₃, 0.5 M NaCl, pH 8.3 and 2.5 ml of solution containing 4-8 mg protein was loaded on the column by the gravity flow. First 2.5 ml of the eluate was discarded and the protein was collected from the column in the following 3.5 ml. During equilibration of the PD-10 column, CNBr-Sepharose was prepared in a way that 0.4 g of the beads was placed in 5 ml 1 mM HCl to swell. After 45 min the beads gave rise to ca. 1.5 ml gel. Gel was washed on a sintered glass filter with 200 ml 1 mM HCl and transferred into a column (max. volume 10 ml). Remaining HCl solution was allowed to pass through and the column was closed at the bottom. Upon addition of 3.5 ml of protein solution column was closed at the top and gently mixed by slowly revolving around vertical axis for 1 h at RT. The column was put in the vertical position; buffer was allowed to pass through and it was quickly analyzed for protein content with Ponceau S staining to check the efficiency of coupling. Remaining active groups were blocked by loading 6 ml 0.1 M ethanolamine, pH 8.0; 2 ml were allowed to pass through before the column was closed and gently mixed by slow revolving for additional 2 h at RT. Subsequently, the column was put in the vertical position; ethanolamine was allowed to pass through and all nonspecifically bound proteins were removed by 3 washing cycles of alternating pH. Each cycle consisted of 6 ml 0.1 M Na-acetate, 0.5 M NaCl, pH 4.5 followed by 6 ml 0.1 M Tris·HCl, 0.5 M NaCl, pH 8.0. Column was finally washed with 10 ml 10 mM Tris·HCl, pH 7.5, and it was ready for affinity purification of antibodies. If the antibodies were not purified the same day, 3 ml 0.05% NaN₃ water solution was added and the column was stored at 4°C. Before purification, the column was left at RT for 45 min and then equilibrated with 10 ml of 10 mM Tris·HCl, pH 7.5. Antiserum (6 ml) was diluted with 24 ml 10 mM

Tris·HCl, pH 7.5 and loaded on the corresponding affinity column under gravity flow. The column was washed with 10 ml 10 mM Tris·HCl, pH 7.5 followed by 10 ml 10 mM Tris·HCl, 0.5 M NaCl, pH 7.5. For the elution, column was subjected to alternating pH through application of 10 ml of each of the following buffers in given order: 10 mM Na-citrate, pH 4.0, 100 mM glycine·HCl, pH 2.5 and 100 mM Na₂HPO₄, pH 11.5. Fractions of 1 ml were collected and neutralized immediately with 200 µl 1 M Tris·HCl, pH 8.8 in the case of the first two buffers, and with 100 µl glycine, pH 2.2 in the case of the phosphate one. Several fractions eluted with each of the elution buffers were checked for specificity by immunodecoration on nitrocellulose membrane carrying yeast mitochondrial proteins. The majority of the specific antibodies were eluted with the glycine buffer in fractions 2-6. These fractions were usually pooled and 150 µl aliquots were stored at -20°C.

2.3.2 Immunodecoration

Proteins blotted onto nitrocellulose or PVDF membranes were visualized by immunodecoration with specific antibodies. After Western blot, membranes were incubated for 30 min in 5% (w/v) milk powder in TBS (150 mM NaCl, 10 mM Tris·HCl, pH 7.5) to block all nonspecific binding sites. The membranes were then incubated with specific primary antibody (1:100 to 1:20000 dilutions in 5% milk in TBS) for 1-2.5 h at RT, or overnight at 4°C. The membranes were then washed for 5 min in TBS, 10 min in TBS containing 0.05% Triton X-100 and again 5 min in TBS and subsequently incubated with goat Anti-rabbit antibodies coupled to horseradish peroxidase (diluted 1:10.000 in 5% milk in TBS) for 1-2 h at RT. The membrane was then washed as already described, treated with the chemiluminescent substrate of peroxidase (ECL reagents 1 and 2) and the signals were detected on X-ray films (Fuji New RX).

ECL reagent 1: 3 ml Tris·HCl, pH 8.5 (1M stock), 300 µl luminol (440 mg/10 ml DMSO), 133 µl p-coumaric acid (150 mg/10 ml DMSO), H₂O to 30ml.

ECL reagent 2: 3 ml Tris·HCl, pH 8.5 (1M stock), 18 µl H₂O₂ (30%), H₂O to 30ml.

Solutions are stable for 7-10 days if kept in light-protected bottles at 4°C. Chemiluminescent substrate of peroxidase was made by mixing equal volumes of ECL reagents 1 and 2.

2.4 Protein biochemistry methods

2.4.1 Purification of different recombinant proteins

2.4.1.1 Purification of His₆Tim44 and other His-tagged proteins

The recombinant plasmid carrying the yeast Tim44 was transformed by electroporation into *E.coli* (BL21 DE3) cells and expressed in 1 l LB medium with 0.5mM isopropyl- β -D-thiogalactopyranoside at 37° C for 3 h. The cells were harvested, suspended in 50ml of buffer A (50mM Na-phosphate buffer pH 7.8 with 300mM NaCl) containing 10mM imidazole, 1mg/ml lysozyme, 1mM/ml PMSF and protease inhibitor cocktail tablet (Roche) and incubated at 4°C for 45 min followed by cell disruption by sonication. The lysed cells were centrifuged at 20,000 \times g and the clear supernatant was loaded into 1.5 ml of Ni-NTA column (QIAGEN) pre-equilibrated with buffer A containing 10mM imidazole. The column was washed with 10 column volume of buffer A containing 10mM imidazole and finally eluted with buffer A containing 300mM imidazole. The proteins were further purified by size-exclusion chromatography using Superdex 200 gel filtration column (GE healthcare) in buffer A.

Essentially the same procedure was used to purify other His-tagged proteins like N- and C-terminal domains of Tim44. Purification of Ssc1-PBD differed in the way that buffer B (50mM Tris-HCl pH 7.5 with 250mM KCl, 5mM MgCl₂ and 5% glycerol) was used for the purification steps.

2.4.1.2 Purification of recombinant Ssc1

The plasmid containing both Hep1 and Ssc1 genes (Sichting et al., 2005) was transformed by electroporation into *E.coli* (BL21 DE3) cells and expressed in 1lit LB medium with 0.5mM IPTG at 37° C for 3 h. The cells were harvested, suspended in 50ml of buffer B (50mM Tris-HCl pH 7.5 with 250mM KCl, 5mM MgCl₂ and 5% glycerol) containing 10mM imidazole, 1mg/ml lysozyme, 1mM/ml PMSF and incubated at 4°C for 45 min followed by cell disruption by sonication. The lysed cells were centrifuged at 20,000 \times g and the clear supernatant containing both recombinant His₆Hep1 and Ssc1

was loaded into 1.5 ml of Ni-NTA column (QIAGEN) pre-equilibrated with buffer B to remove His₆Hep1. The flow-through from the first Ni-NTA column containing Ssc1 was loaded into a 2nd column containing pre-bound His₆Mge1. The second column was washed with 10 column volume of buffer B and finally eluted with buffer B containing 2mM ATP.

Essentially the same procedure was used to purify the Ssc1-NBD.

2.4.2 Protein analysis

2.4.2.1 SDS-Polyacrylamide gel electrophoresis (SDS-PAGE)

The proteins were separated according to their molecular weights under denaturing conditions using one-dimensional vertical SDS-polyacrylamide gel electrophoresis (SDS-PAGE). The concentrations of acrylamide and bis-acrylamide in the separating gel were chosen according to the molecular sizes of proteins of interest. The volume of the protein solution loaded per lane was between 5 and 50 μ l, and the amount of loaded protein was between 25 and 150 μ g. The samples were resuspended in 5-50 μ l sample buffer and incubated at 95°C for 5 min before loading.

The electrophoresis was performed at 35 mA for 100 min for large gels of dimensions of approximately 14 cm x 9 cm x 0.1 cm and at 25 mA for 50 min for 1 h for small gels (Mini-PROTEAN II, Bio-Rad) of dimensions of approximately 10 cm x 5.5 cm x 0.075 cm. Protein molecular weight markers of 116, 66, 45, 35, 25, 18 and 14 kDa (PepLab) were usually used.

Buffers for SDS-PAGE:

Running gel: 8-16% (w/v) acrylamide, 0.16-0.33% (w/v) bis-acrylamide, 375 mM Tris·HCl (pH 8.8), 0.1% (w/v) SDS, 0.05% (w/v) APS, 0.05% (v/v) TEMED.

Stacking gel: 5% (w/v) acrylamide, 0.1% (w/v) bis-acrylamide, 60 mM Tris·HCl (pH 6.8), 0.1% (w/v) SDS, 0.05% (w/v) APS, 0.05% (v/v) TEMED.

Electrophoresis buffer: 50 mM Tris base, 384 mM glycine, 0.1% (w/v) SDS, pH 8.3 without adjustment.

1 x sample (Laemmli) buffer: 60 mM Tris·HCl, pH 6.8, 2% (w/v) SDS, 10% glycerol, 5% (v/v) β -mercaptoethanol, 0.05% (w/v) bromphenol-blue.

Separated proteins were either stained with Coomassie-Brilliant-blue (CBB) or transferred onto a nitrocellulose membrane.

2.4.2.2 CBB staining of SDS-PAGE gels

After SDS-PAGE separating gel was incubated in aqueous solution containing 30% (v/v) methanol, 10% (v/v) acetic acid, and 0.1 (w/v) CBB G-250 at RT for 30 min. The gel was then destained with aqueous solution containing 30% (v/v) methanol and 10% (v/v) acetic acid until the protein bands were clearly visible, which required several washing steps with fresh destaining solutions. The gel was dried overnight between two gel-drying films (Promega).

2.4.2.3 Transfer of proteins onto nitrocellulose/PVDF membrane (Western-Blot)

Proteins separated by SDS-PAGE were transferred onto nitrocellulose membranes using a modified semi-dry method. The nitrocellulose membrane was incubated for three minutes in water and subsequently in blotting buffer (20 mM Tris base, 150 mM glycine, 20% (v/v) methanol, 0.08% SDS) prior to the transfer procedure. A respective membrane was placed onto three pieces of Whatman 3MM filter paper that were previously soaked in the blotting buffer, lying on the graphite anode electrode. The gel was placed on the membrane and then covered with another three soaked filter papers. The cathode graphite electrode was placed on top creating the “blotting sandwich”. The electrotransfer was performed at 2 mA/cm² for 1 h for big and for 45 min for small gels (for big gels of dimensions of approximately 14 cm x 9 cm x 0.1 cm it translates to 250 mA for 1 h and for small gels of dimensions of approximately 10 cm x 5.5 cm x 0.075 cm it translates to 110 mA for 45min). Only in the case of the cross-linking experiments that were analyzed on big gels the time of transfer was increased to 75 min.

To verify transfer efficiency, and to visualize and label the marker proteins' bands, the nitrocellulose membranes were reversibly stained with Ponceau S solution [0.2% (w/v) Ponceau S in 3% (w/v) TCA]. The membranes were then immunodecorated, or the radioactive material visualized by autoradiography.

2.4.2.4 Determination of protein concentration

Protein concentration was determined according to Bradford assay. Protein solutions (1-10 μ l) were diluted with 1 ml of 1:5 dilution of commercially available “Bio-Rad Protein-assay” reagent and incubated for 10 min at RT. The absorbance was measured at 595 nm using a 1 cm path length micro-cuvette. Protein concentration was determined from a calibration curve obtained using the known amounts of the commercially available bovine IgG proteins (BioRad) as a standard.

2.4.3 Protein experiments *in organello*

2.4.3.1 Co-immuno precipitation experiments

Desired amount of Protein A Sepharose CL-4B (PAS) (GE healthcare) beads were washed first with water, followed by 3 x 5 min washing with TBS. Appropriate amounts of purified antibodies (enough antibodies to immunodeplete the corresponding antigen from the extract) were added and incubated for 2 h at 4°C, by slowly rotating the Eppendorf tubes overhead. The beads were then washed from the unbound antibodies and were ready for incubation with proteins from the mitochondrial extract. While the PAS beads were incubating with the desired antibodies, isolated mitochondria were centrifuged (17400 x g, 10 min, 4°C) and the mitochondrial pellet was resuspended at 2 mg/ml in 20 mM TrisHCl, 80 mM KCl, pH 7.5, containing 1% (w/v) digitonin and 1 mM PMSF for 20 min at 4°C. After a clarifying spin (90700 x g, 20 min, 2°C), mitochondrial extract was added to antibodies prebound to PAS and incubated for 2 h at 4°C. Beads were washed twice with 20 mM TrisHCl, 80 mM KCl, pH 7.5, containing 0.05% (w/v) digitonin and 1 mM PMSF. Specifically bound proteins were eluted with either reducing or nonreducing Laemmli buffer (5 min at 95°C). Samples were analyzed by SDS-PAGE and immunodecoration.

2.4.3.2 Ni-NTA Pull down experiments with tagged proteins expressed in mitochondria

Isolated mitochondria were centrifuged (17400 x g, 10 min, 4°C) and the mitochondrial pellet was solubilized at 2 mg/ml in 20 mM Tris·HCl, 80 mM KCl, pH 7.5 containing 1%

(w/v) digitonin and 1 mM PMSF for 20 min at 4°C. After a clarifying spin (90700 x g, 20 min, 2°C), mitochondrial extract was added to Ni-NTA beads (Qiagen). The beads (20-60 µl) were previously washed with 3 x 1 ml TBS (150 mM NaCl, 10 mM Tris·HCl, pH 7.5) and equilibrated with 200 µl solubilization buffer containing 0.05% . Mitochondrial extract was incubated with the beads for 1 h at 4°C. The beads were then washed three times with 200 µl solubilization buffer containing 0.05% digitonin, and the bound proteins were eluted with sample buffer containing 300 mM imidazole. Upon incubation at 95°C for 5 min, samples were analyzed by SDS-PAGE and immunodecoration.

2.4.3.3 Crosslinking of mitochondrial proteins

For the crosslinking analysis of interactions between mitochondrial proteins, isolated mitochondria were resuspended in the SI buffer (without BSA) and energized by addition of 2 mM NADH, 1 mM ATP, 10 mM creatine phosphate and 100 µg/ml creatine kinase. After incubation for 3 min at 25°C, the crosslinker was added from a 100-fold stock in DMSO. In this work two membrane permeable and lysine-specific chemical crosslinkers were used: DSG (disuccinimidylglutarate) and DSS (disuccinimidylsuberate). After 30 min incubation on ice, excess crosslinker was quenched for 10 min on ice with 100 mM glycine, pH 8.8. Mitochondria were reisolated and analyzed by SDS-PAGE and immunodecoration.

When crosslinking adducts were purified via His tag from one of the crosslinked proteins on the NiNTA-agarose beads, 250 µg of reisolated mitochondria were solubilized in buffer containing 1% SDS (v/v), 50 mM Na₂HPO₄, 100 mM NaCl, 10% glycerol, 10 mM imidazole, 1 mM PMSF, pH 8.0 for 15 min with vigorous shaking at 25°C. Samples were diluted 20 fold in the same buffer containing 0.2% Triton X-100 instead of SDS and, after a clarifying spin, added to 50 µl NiNTA-agarose beads. After 1 h of incubation at 4°C while slowly rolling, beads were washed and bound proteins eluted with 2 x sample buffer containing 300 mM imidazole during incubation for 5 min at 95°C.

2.4.4 Protein experiments *in vitro*

2.4.4.1 Ni-NTA pull-down experiments

His₆Tim44 (wild type or labeled cysteine mutants) were mixed with Ssc1 in a molar ratio of 1:4 in buffer C (20mM Tris-HCl pH7.5, 300mM NaCl, 100mM KCl, 5mM MgCl₂) containing 10mM imidazole, in a final reaction volume of 200μl at 25°C for 5min in absence or presence of 2mM nucleotides. After incubation the reaction mixture were incubated with 50μl of Ni-NTA beads pre-equilibrated with buffer C for 45min at 4°C. The beads were washed with 10 column volume of buffer C in batch and bound proteins were eluted from the beads with buffer C containing 300mM imidazole. The eluted proteins were used for SDS-PAGE followed by staining with CBB.

2.4.4.2 Cross-linking experiments

Tim44 was mixed with Ssc1 in a molar ratio of 1:4 in buffer D (20 mM HEPES/KOH pH7.4, 80mM KCl, 5mM MgCl₂, 1mM PMSF) in a final reaction volume of 200μl at 25°C for 5min, in absence or presence of 2mM nucleotides. After incubation for 5 min at 25°C, the crosslinker (DSS) was added from a 100-fold stock in DMSO. After 30 min incubation on ice, excess crosslinker was quenched for 10 min on ice with 100 mM glycine, pH 8.8. The cross-linked proteins were precipitated with TCA and washed with ice cold acetone and subsequently analyzed by SDS-PAGE and CBB staining.

2.5 Methods for Fluorescence spectroscopy

2.5.1 Labelling of Cystine mutants of Tim44 and Ssc1 with sulfhydryl-specific fluorophores

The single cysteine mutants of Tim44 and Ssc1(usually 50-75μM of protein) were labeled by incubating with 2 fold molar excess of Alexa-594 maleimide (INVITROGEN) for Tim44 and Atto-647N maleimide (ATTO-TEC) for Ssc1, in buffer A and buffer B respectively for 2 h at 4°C. Unreacted dyes were removed by size exclusion chromatography through a NAP5 column (GE healthcare) equilibrated with buffer C. Double cysteine mutants of Ssc1 were incubated with 0.8 molar ratio of donor and 1.2

molar ratio of acceptor dye to double label the protein stoichiometrically with donor (Atto-532 maleimide) and acceptor (Atto-647N maleimide) fluorophores. Unreacted dyes were removed by size exclusion chromatography through a NAP5 column.

2.5.2 Steady-state and Kinetic Ensemble FRET Measurements

Steady-state ensemble FRET measurements were performed on a Fluorolog 3 fluorometer (Spex) with Fluorescein, Alexa 594 or Atto532 as donor and Atto647N as fluorescent acceptor at 25°C. Stopped-flow experiments were done using an Applied Photo Physics SX.18MV with a 1:1 mixing ratio at 25°C. Kinetic traces shown are averages of 10-12 independent measurements.

2.5.3 Steady-state Ensemble FRET Efficiencies of Tim44:Ssc1, and P5:Ssc1 complexes

For calculating steady-state ensemble FRET efficiencies, the fluorescence of the donor (Alexa 594) was measured for donor labeled Tim44 and incubated with equal concentration of either unlabeled or acceptor labeled Ssc1 at 25°C on a Fluorolog 3 Spectrofluorometer (Spex). The donor fluorophore was excited at 590 nm and emission was monitored at 615 nm with slit widths of 2 nm and 5 nm, respectively. FRET efficiency was obtained using the following equation:

$$fE = 1 - (I_{DA}/I_D)$$

where fE is the FRET efficiency, I_{DA} and I_D are the fluorescence of the donor in presence of acceptor labeled and unlabeled Ssc1, respectively.

To obtain FRET efficiency between donor labeled P5 (P5-fl) and acceptor labeled Ssc1, the fluorescence of the donor (fluorescein) was followed upon incubation of P5-fl with acceptor labeled Ssc1. The donor fluorophore was excited at 480nm and the emission was monitored at 515nm with slit widths of 1nm and 5nm, respectively. The FRET efficiency was calculated according to the equation above.

2.5.4 Semi-quantitative intramolecular FRET measurement

To monitor intramolecular conformational changes using FRET, donor (Atto-532) and acceptor (Atto-647N) fluorescence of double labeled Ssc1 was monitored upon excitation

of the donor fluorophore at 532nm with a slit width of 2nm. Proximity ratio of the fluorophores was obtained using the following equation:

$$PR = I_{PA}/I_{PD}$$

Where PR is the proximity ratio, I_{PA} is the intensity of the acceptor peak and I_{PD} is the intensity of the donor peak.

2.5.5 Single Molecule FRET Experiments

Single molecule spectroscopy (fluorescence correlation spectroscopy (FCS) as well as single-pair FRET (spFRET) measurements) was performed on a confocal system based on an inverted microscope (Zeiss Axiovert 200) using pulsed interleaved excitation (PIE)(Muller et al., 2005). The concentration of double-labeled protein in the sample was diluted to ~60 pM to ensure that the probability of having more than one particle in the probe volume at the same time is negligible (<1 %). For each experiment, at least 500 particles were measured.

2.5.6 Determination of the Equilibrium Dissociation Constant of Tim44:Ssc1 Complexes

50nM of Tim44 (187C)-Alexa594 was mixed with different concentrations of Ssc1(448C)-647N or Ssc1-PBDp(448C)-Atto647N to obtain the decrease in Alexa-594 fluorescence due to energy transfer. Excitation was centered at 590 nm (1 nm slit width) and emission was monitored at 615nm (2nm slit width). Since the Alexa594-labeled Tim44 undergoes a change in fluorescence upon binding to labeled Ssc1, the bound proportion of the protein could be estimated by the change in fluorescence intensity. Equilibrium dissociation constants were obtained by quantifying the bound fraction of Tim44 (187C)-Alexa594 from the fluorescence amplitude change as a function of Ssc1 concentration, and fitting the resultant graph to the equation:

$$B = \frac{(c + x + K_D) - \sqrt{(c + x + K_D)^2 - 4xc}}{2}$$

where B is the concentration of Tim44(187C)-Alexa594 bound to Ssc1, c and x are the total concentrations of Ssc1 (or Ssc1-PDBp) and Tim44(187C)-Alexa594 respectively,

and K_D is the equilibrium dissociation constant of the Tim44:Ssc1 (or Tim44:Ssc1-PBDp) complex.

2.6 Far-UV CD spectroscopy

CD spectra were obtained on a Jasco-715 C spectropolarimeter (Jasco, Éaton, MD) flushed with nitrogen gas. The spectra were recorded using a 0.1cm pathlength cuvette with a scan rate of 10nm/min and a time constant of 8s. All data are an average over a minimum of 6 scans and are presented in terms of Mean Residue Ellipticity (MRE) as a function of wavelength. Far-UV CD spectra were taken in the range of 260nm to 200nm. The CD spectra of full length Tim44 (both labeled and non-labelled proteins) was taken in 50mM phosphate buffer containing 300mM NaCl, pH 7.8 and Hsp70 spectra were taken in 25mM HEPES/KOH, 100mM KCl, 5mM MgCl₂ and 5% glycerol, pH 7.4.

2.7 Screening of cellulose-bound peptides (Peptide scans)

Cellulose-bound peptide libraries from the sequences of firefly luciferase, ScMDH, ScHsp60 and ScHsp10 were synthesized (JPT Peptide Technologies GmbH, Berlin). Before screening the dry membranes were incubated with methanol for 5 min followed by 3×10 min washing steps in TBS (10mM Tris, 0.9% NaCl, pH 8.0). The membranes were blocked with 3% BSA in TBS pH8.0 at room temperature for 2h followed by a short washing step with TBS-T(0.05%, v/v). Purified Tim44 or Ssc1/ADP was then allowed to react with the peptide library in a concentration of 5µg/ml in blocking buffer for 2h at room temperature with gentle shaking. Unbound proteins were removed with washing with TBS-T and peptide bound Tim44 or Ssc1 were electro-transferred on to polyvinylene difluoride membrane (PVDF, Carl Roth GmbH) using a semi-dry blotting apparatus. The PVDF membrane was sandwiched between blotting papers soaked in Anode buffer I (30mM TRIS, 20% methanol), Anode buffer II (300mM TRIS, 20% methanol) and Cathode buffer (25mM TRIS, 40mM 6-aminohexanoic acid, 20% methanol). Electro-transfer was performed at a constant power of 1mA/cm² cellulose membrane for 30 min for three times. Transferred proteins were detected by immunodecoration with respective antibodies and chemiluminescence (ECL, Sigma).

2.8 Methods for enzymatic activity of purified proteins

2.8.1 Coupled assay for ATPase activity of Ssc1

A coupled ATP-regenerating enzyme system was employed following a method described by (Norby, 1988). In a total volume of 200 μ l, 2 μ M of Ssc1 was incubated together with 2 mM ATP, 0.12 mM NADH, 3 mM phosphoenolpyruvate, 10 μ g lactate dehydrogenase and 30 μ g pyruvate kinase (Sigma) in 20 mM HEPES/KOH, pH 7.0, 80mM KCl, 5mM MgCl₂ at 25°C and Δ Abs₃₆₀/ Δ t was monitored by a spectrophotometer (JASCO).

3 Results

3.1 Characterization of Pam17 and Tim21, the two non-essential subunits of the TIM23 complex

The TIM23 translocase is one of the major translocases of mitochondria situated in the inner mitochondrial membrane. It is responsible for translocation of precursors across and their insertion into the inner mitochondrial membrane. Traditionally TIM23 translocase is divided into a membrane embedded translocation part and the import motor. The membrane embedded part contains three essential subunits, Tim17, Tim23 and Tim50. mtHsp70, Tim44, Tim14, Tim16, and Mge1 form the import motor of the TIM23 translocase. In addition, the translocase contains two recently identified nonessential subunits, Pam17 and Tim21. The major aim of this part of the work was to analyze the roles of the two newly identified components Pam17 and Tim21.

3.1.1 Both Tim21 and Pam17 bind to the Tim17-Tim23 core of the TIM23 complex

Pam17 was identified as a component of the TIM23 translocase by co-purification with tagged Tim23 but its association to the parts of the translocase was not studied in detail (van der Laan et al., 2005). For that purpose, coimmunoprecipitation experiments with mitochondria isolated from wild type yeast cells (WT) were performed to analyze the association of Pam17 with the TIM23 translocase. At the same time, the association of the other nonessential component of the complex, Tim21, was analyzed. Mitochondria were solubilized in digitonin-containing buffer and incubated with affinity purified antibodies against Tim23, Tim17 and Tim16 or preimmune immunoglobulins bound to Protein A-Sepharose. These antibodies were previously shown to precipitate all known components of the TIM23 complex, however, with different efficiencies due to the reported instability of the complex upon solubilization. Upon digitonin solubilization the

vast majority of Tim21 could be coprecipitated using antibodies against Tim17 and Tim23 (Figure 3.1). Small but significant amounts could also be precipitated with antibodies to Tim16. In contrast, the majority of Pam17 remained in the supernatant, irrespective of the antibody used for precipitation, and only small amounts were detected in pellets after precipitation with Tim17 and Tim23 antibodies. There was no detectable Pam17 in the pellet after precipitation with Tim16 antibodies. All other components of the TIM23 translocase yielded precipitation patterns as described previously (Kozany et al., 2004; Mokranjac et al., 2003b).

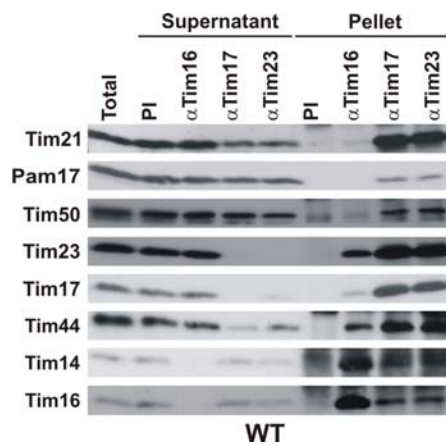


Figure 3.1: Pam17 and Tim21 associates with the Tim17-Tim23 core of the TIM23 complex. Mitochondria isolated from wild-type cells were solubilized with digitonin and incubated with affinity-purified antibodies against Tim16, Tim17, Tim23 or antibodies from preimmuneserum (PI) as a control. The proteins eluted from the ProteinA-Sepharose columns were analyzed by SDS-PAGE, Western blotting followed by immunodecoration with the indicated antibodies. Total fractions and supernatant represent 20% of the material used for immunoprecipitation.

To study the requirements of the association of Pam17 and Tim21 with the translocase, mitochondria depleted of one of the essential TIM23 components were used. In mitochondria depleted of either Tim17 (Figure 3.2A) or Tim23 (Figure 3.2B), association of Tim21 with the remaining one was lost. Essentially the same observation was made for Pam17. In contrast, depletion of any of the other essential components of the complex had no effect on the association of these two proteins with Tim17-Tim23 core (Figure 3.2C-F). These results suggest that stable association of Tim21 and Pam17 with the TIM23 translocase requires the assembled Tim17-Tim23 core of the complex and is not dependent on any other known essential component of the complex.

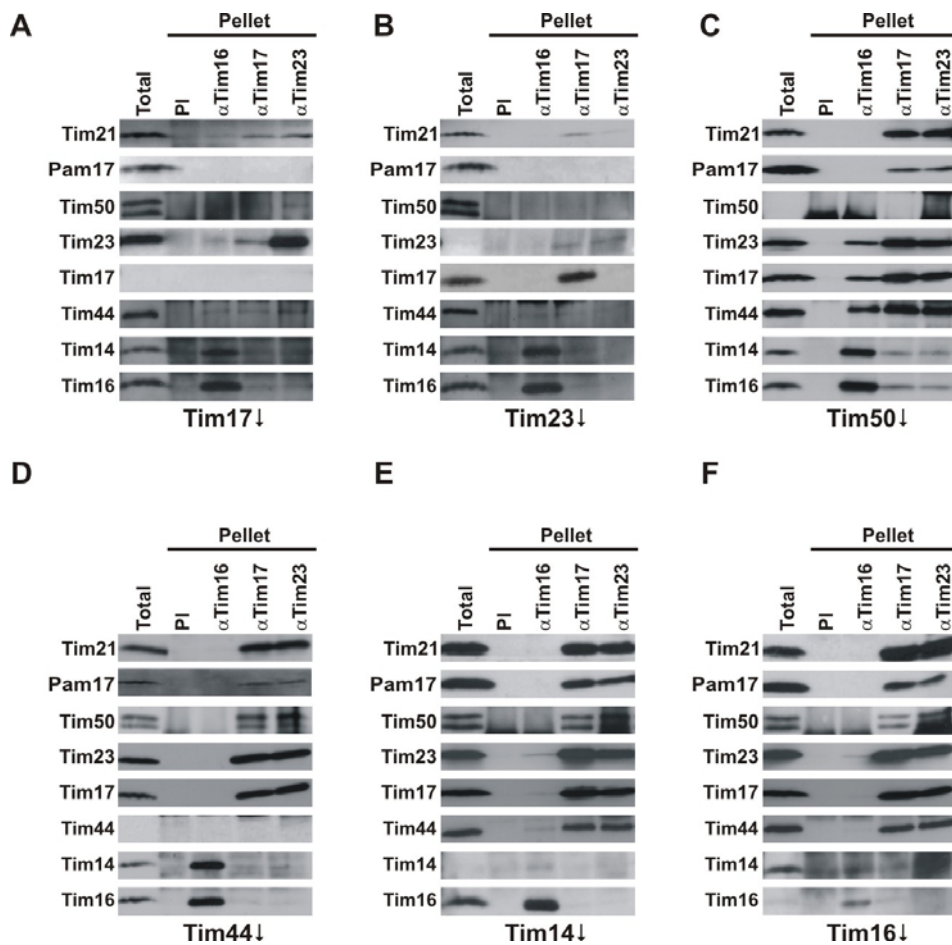


Figure 3.2: Pam17 and Tim21 interact with the intact Tim17-Tim23 core of the TIM23 complex. Mitochondria isolated from cells depleted of the TIM23 components: Tim17 (A), Tim23 (B), Tim50 (C), Tim44 (D), Tim14 (E) and Tim16 (F) were solubilized with digitonin and incubated with the affinity purified antibodies against Tim16, Tim17, Tim23 or antibodies from preimmune serum (PI) as a control. The eluted proteins from the ProteinA-Sepharose columns were analyzed by SDS-PAGE, Western blotting followed by immunodecoration with the indicated antibodies. Total fractions represent 20% of the material used for immunoprecipitation.

This association behavior of Pam17 with the Tim17-Tim23 core was also examined from the side of Pam17. Mitochondria containing N-terminally His₆-tagged Pam17 were solubilized and incubated with Ni-NTA beads. Tim50, Tim23 and Tim17 were specifically retained on the beads together with His₆Pam17 (Figure 3.3). None of the subunits of the import motor in particular Tim44, Tim16 and Tim14 were found in the

bound fraction. Interestingly, no co-isolation of Pam17 with Tim21 was observed, though both were found to bind to the Tim17-Tim23 core of the complex.

In summary, both Tim21 and Pam17 bind to the Tim17-Tim23 core of the TIM23 complex. However, they cannot be coisolated with each other. Furthermore, no evidence for a direct association of Pam17 with the TIM23 subunits traditionally assigned as the import motor components was obtained.

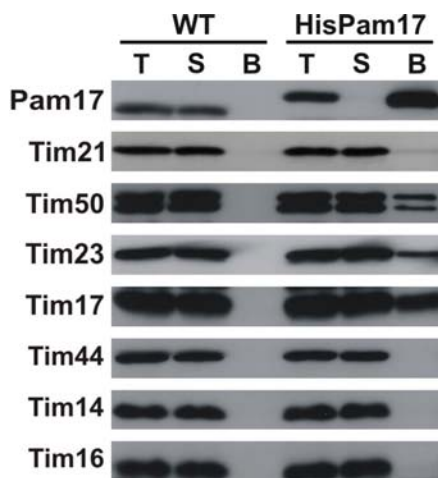


Figure 3.3: Only members of the membrane-integrated part of the TIM23 complex are co-isolated with His₆Pam17. Mitochondria isolated from wild-type cells and cells expressing His₆Pam17 were solubilised with digitonin and incubated with Ni-NTA agarose beads. The bound proteins were analyzed by SDS-PAGE followed by Western blot and immunodecoration with the indicated antibodies. Total fractions (T) and supernatant (S) represent 20% of the material used for binding to Ni-NTA.

3.1.2 The major cross-linked adduct of Tim23 is to Pam17

Upon cross-linking with DSG in wild type mitochondria, decoration with antibodies to Tim23 reveal two cross-linked adducts. The ca. 55 kDa adduct was previously identified as a Tim23 dimer (Bauer et al., 1996). The identity of the major crosslinking partner remained unknown. Considering the size of the adduct, we reasoned that the cross-linking partner of Tim23 could be Pam17. By chemical crosslinking in mitochondria isolated from wild type yeast cells and from cells containing N-terminally His-tagged Pam17 followed by Ni-NTA agarose pull down, the major cross-linked product of Tim23 was indeed found to be an adduct to Pam17 (Figure 3.4). This result obtained with intact mitochondria confirmed the close association of Pam17 to the membrane-embedded sector of the TIM23 translocase in lieu of the results obtained with solubilized

mitochondria. On the other hand, this result was surprising in view of a recent report describing Pam17 as a component of the import motor (van der Laan et al., 2005).

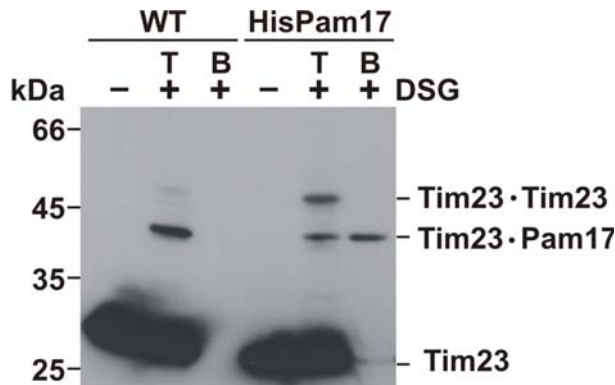


Figure 3.4: The major cross-linked adduct of Tim23 is to Pam17. Mitochondria isolated from wild-type cells and cells expressing His₆Pam17 were treated with 200 μ M DSG, solubilised with SDS-containing buffer and then incubated with Ni-NTA beads. The samples were analysed by SDS-PAGE followed by Western blotting and immunodecoration with anti-Tim23 antibodies. The cross-linked products are indicated. T: total material; B: material bound to Ni-NTA.

3.1.3 Deletion of Pam17 affects the conformation of both motor and membrane part of the TIM23 complex

To investigate the functions Pam17 and Tim21 in the TIM23 translocase, yeast strains were constructed in which these proteins were deleted alone, or in combination. Deletion of either protein alone or in combination did not alter the levels of the essential components of the TIM23 complex (Figure 3.5).

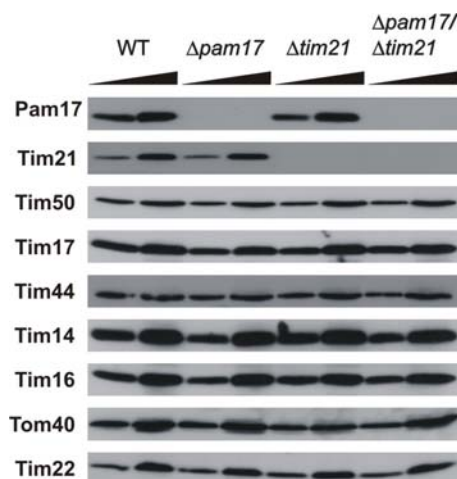


Figure 3.5: The endogenous levels of different mitochondrial proteins in strains lacking Pam17, Tim21 or both. 10 μ g and 50 μ g of isolated mitochondria from wild-type cells and cells lacking Pam17, Tim21 or both were analyzed by SDS-PAGE, Western blotting followed by immunodecoration with indicated antibodies.

In addition, the composition of the TIM23 complex was not changed as judged by co-immunoprecipitation experiments using digitonin solubilized mitochondria. This suggests

that neither of the two proteins has an essential role in assembly of the TIM23 complex (Figure 3.6).

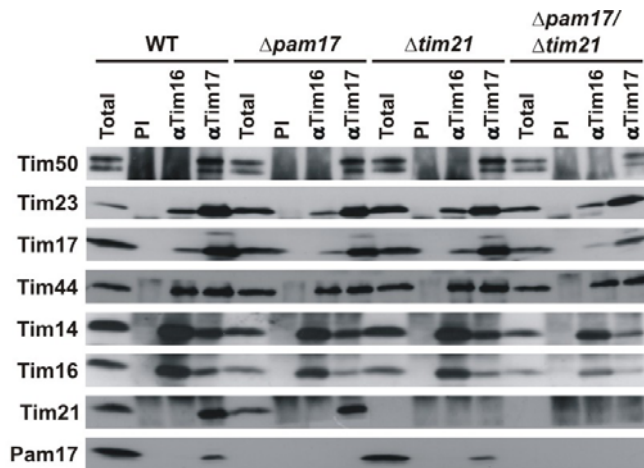


Figure 3.6: Deletion of Pam17 or Tim21 or both does not affect the assembly of the TIM23 translocase. Mitochondria were solubilized with digitonin and subjected to immunoprecipitation with antibodies against Tim16, Tim17 or with preimmune serum (PI) as a control. Total (20%) and precipitated material were analyzed by SDS-PAGE and immunodecoration with indicated antibodies.

However, when the conformation of the translocase was probed by chemical cross-linking in intact mitochondria isolated from $\Delta pam17$, $\Delta tim21$ and $\Delta pam17/\Delta tim21$ cells several differences from the wild-type pattern were observed. In mitochondria lacking Pam17, alone or in combination with Tim21, the crosslinking profile of Tim44 was changed (Figure 3.7).

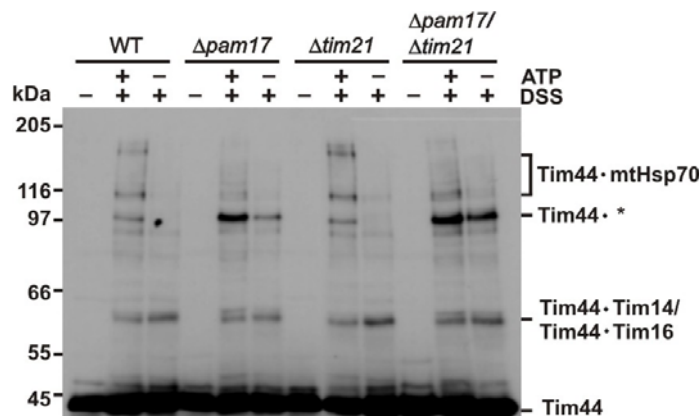


Figure 3.7: Molecular environment of Tim44 is drastically changed in mitochondria lacking Pam17, Tim21 or both proteins. Mitochondria isolated from the wild-type cells and cells lacking Pam17, Tim21 or both were subjected to cross-linking by disuccinimidyl suberate (DSS). After cross-linking the samples were analyzed by SDS-PAGE, Western blotting followed by immunodecoration with antibodies against Tim44.

Adducts to mtHsp70 were not visible and the intensity of the adduct presumably representing the Tim44 dimer was strongly increased in comparison to wild type. However, the Tim44-mtHsp70 subcomplex was still present when analyzed by coimmunoprecipitation (Figure 3.8).

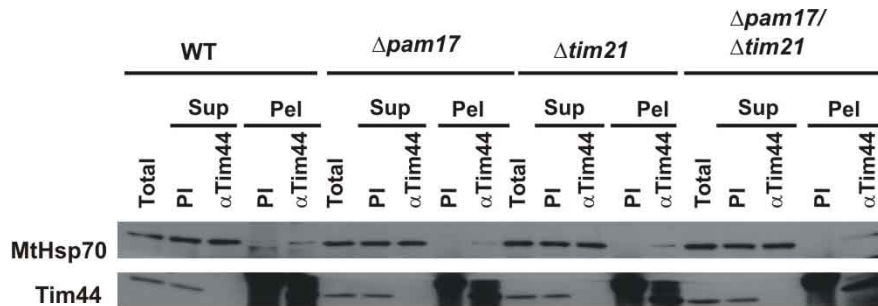


Figure 3.8: Deletion of Pam17 or Tim21 or both does not affect the formation of Tim44-mtHsp70 subcomplex. Mitochondria were solubilized with Tx-100 and subjected to immunoprecipitation with antibodies against Tim44 or with preimmune serum (PI) as a control. Total (20%), supernatant (sup) (20%) and precipitated material (Pel) were analyzed by SDS-PAGE and immunodecoration with indicated antibodies.

The environment of Tim16 also changed significantly upon deletion of Pam17 and Tim21 (Figure 3.9). There was a major shift from the Tim16-Tim14 adduct to the Tim16-Tim16 adduct in mitochondria lacking Pam17. This changed cross-linked pattern again indicated a conformational change within the Tim14-Tim16 sub-complex since no detectable difference was observed in the co-immunoprecipitation patterns of either Tim14 or Tim16 (Figure 3.6).

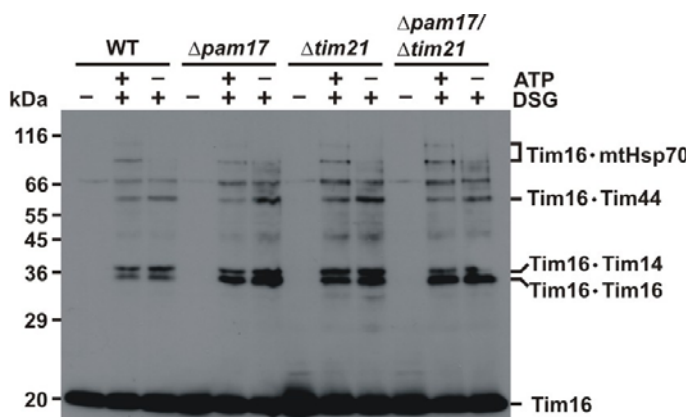


Figure 3.9: The molecular environment of Tim16 is significantly changed in mitochondria lacking Pam17, Tim21 or both proteins together. Mitochondria isolated from wild-type cells and cells lacking Pam17, Tim21 or both were subjected to cross-linking by disuccinimidyl glutarate (DSG). After cross-linking the samples were analysed by SDS-PAGE, Western blotting followed by immunodecoration with antibodies against Tim16.

When the environment of Tim23 was analyzed, in mitochondria lacking Pam17, the crosslinking adduct between Tim23 and Pam17 was, as expected, absent. In addition, an increased efficiency of Tim23-Tim23 adduct formation was observed (Figure 3.10). In $\Delta pam17/\Delta tim21$ the Tim23 dimer was even more abundant than in $\Delta pam17$ mitochondria. Thus, deletion of Pam17 not only influenced the import motor but also resulted in a conformational change of the membrane embedded part. On the other hand, deletion of Tim21 alone had no influence on the crosslinking pattern of any of the analyzed TIM23 components.

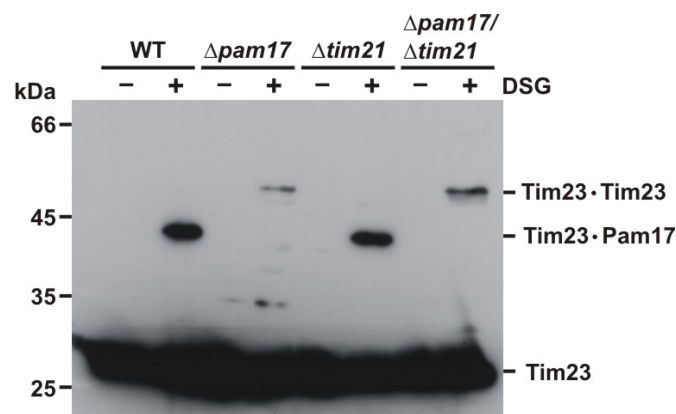


Figure 3.10: Molecular environment of Tim23 is drastically changed in mitochondria lacking Pam17, Tim21 or both proteins together. Mitochondria isolated from the wild-type cells and cells deleted of *PAM17*, *TIM21* or both were subjected to cross-linking by disuccinimidyl glutarate (DSG). After cross-linking the samples were analysed by SDS-PAGE, Western blotting followed by immunodecoration with antibodies against Tim23.

In summary, deletion of Pam17, either alone or in combination with Tim21, results in a structural reorganization of the TIM23 translocase that affects both the membrane embedded part and the motor part of the complex.

3.1.4 Binding of Tim21 and of Pam17 to the TIM23 complex is mutually exclusive

The effect of over-expression of Pam17, Tim21 or both at the same time on the TIM23 complex was analyzed. Interestingly, the extent of over-expression of the two proteins differed strongly in spite of the fact that they were expressed from the same promoter. The level of Pam17 was increased 3 to 4 fold as compared to the wild type level, whereas

the level of Tim21 was at least 10 fold higher than wild type level. The endogenous levels of various components of the TIM23 translocase and also of other mitochondrial proteins were unaltered under these conditions (Figure 3.11).

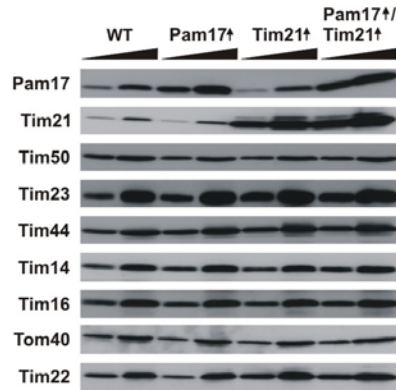


Figure 3.11: The endogenous levels of different mitochondrial proteins in strains over-expressing Pam17, Tim21 or both. 10µg and 50µg of isolated mitochondria from wild-type cells and cells over-expressing Pam17, Tim21 or both were analyzed by SDS-PAGE, Western blotting followed by immunodecoration with indicated antibodies.

Overexpression of Pam17 and Tim21 did not significantly influence the crosslinking patterns of different components of the import motor (Figure 3.12).

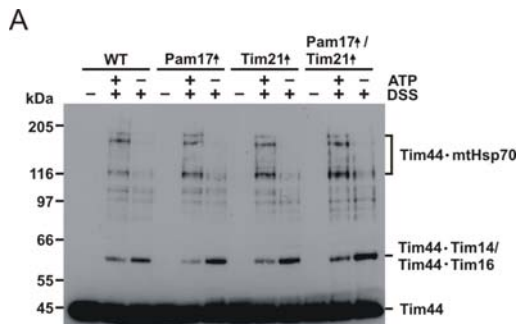
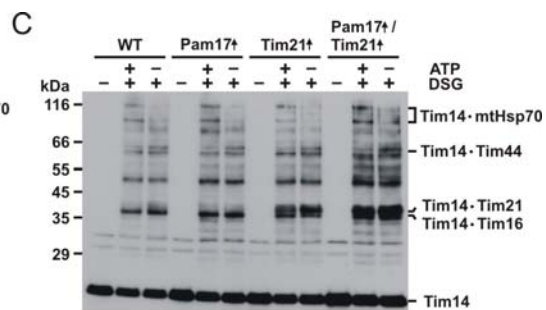
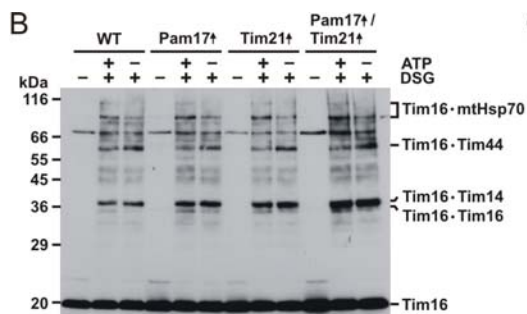


Figure 3.12: Over-expression of Pam17 or Tim21 or both do not significantly change the molecular environment of the import motor. A, Tim44; B, Tim16; C, Tim14. Mitochondria isolated from the indicated strains were subjected to chemical cross-linking with DSG or DSS. The samples were analysed by SDS-PAGE and Western blotting, followed by immunodecoration with indicated antibodies. The cross-linked products are indicated.



Upregulation of Pam17 did not result in a change of the crosslinking pattern of Tim23, not even in an increased efficiency of Tim23-Pam17 crosslinking (Figure 3.13). In contrast, overexpression of Tim21 led to a decreased efficiency of Tim23 crosslinking to Pam17 and also to a significantly increased dimerization of Tim23. Intriguingly, overexpressed Pam17 could counteract the effect of overexpression of Tim21. Dimers of Tim23 were virtually not visible anymore and the intensity of Tim23-Pam17 crosslink was returned to almost wild type level. This result suggests that Pam17 and Tim21 do not bind to the Tim17-Tim23 core of the complex at the same time.

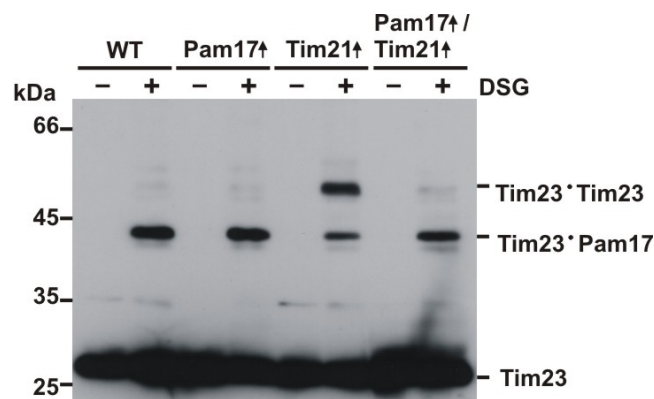


Figure 3.13: Conformational changes caused by over-expression of Tim21 are counteracted by overexpressing Pam17. Mitochondria isolated from the indicated strains were subjected to chemical cross-linking by DSG. The samples were analysed by SDS-PAGE and Western blotting, followed by immunodecoration with anti-Tim23 antibodies. The cross-linked products are indicated.

Next, coimmunoprecipitation experiments using digitonin solubilized mitochondria containing overexpressed Pam17, Tim21 or both (Figure 3.14) were performed. The assembly of the essential subunits of the complex was not affected under these conditions. Overexpression of Pam17 did not lead to a higher efficiency of its co-precipitation with the rest of the TIM23 translocase but it significantly reduced the amounts of Tim21, which could be precipitated with Tim17 antibodies. On the other hand, upregulation of Tim21 led to the virtual removal of Pam17 from the TIM23 complex under these conditions. Increased levels of Tim21 in mitochondria also resulted in a more efficient copurification of this protein with both Tim16 and Tim17 antibodies. In mitochondria containing increased levels of both Pam17 and Tim21, overexpressed

Pam17 could remove some of the overexpressed Tim21 from the complex in the way that coprecipitation of Pam17 with the TIM23 complex was again visible.

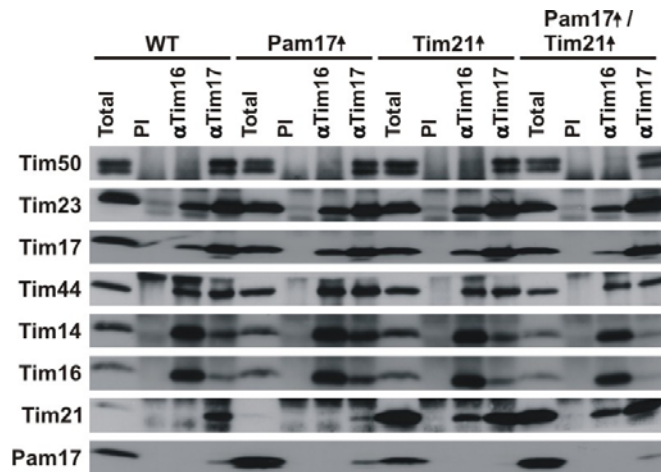


Figure 3.14: Presence of Tim21 and Pam17 in the TIM23 complex is mutually exclusive. Mitochondria were solubilized with digitonin and subjected to immunoprecipitation with antibodies against Tim16, Tim17 or with preimmune serum (PI) as a control. Total (20%) and precipitated material were analyzed by SDS-PAGE and immunodecoration with indicated antibodies.

In summary, Tim21 and Pam17 appear to either to have overlapping binding sites on the Tim17-Tim23 core of the complex or that binding of one of them induces a conformation not compatible with binding of the other one. This suggests interdependent regulatory roles for these two proteins in the import process (Popov-Celeketic et al., 2008a).

3.2 Reconstitution of the Tim44:Ssc1 interaction cycle of the mitochondrial import motor using the purified components

Complete translocation of preproteins into the mitochondrial matrix requires the import motor of the TIM23 translocase and consumes energy in the form of ATP. The ATP-consuming component of import motor is mtHsp70, also known as Ssc1 in yeast. Since the interaction of the translocating polypeptide chain with Ssc1 is thought to drive the translocation process, interaction between Ssc1 and its anchor point to the translocase, Tim44, forms a key element in the translocation of a matrix targeted pre-protein. The major aim of this part of the work was to uncover the dynamics of the Tim44-Ssc1

interaction. To explore the working mechanism of import motor, it was necessary to understand the kinetics of the processes along with the thermodynamics that drive these interactions. To understand the process of cycling of Ssc1 on Tim44 and relate it to the events of translocation, we need to uncover the kinetics of formation and dissociation of Tim44:Ssc1 complex. Towards this end, Fluorescence Resonance Energy Transfer (FRET) was used as a major tool to understand the real time kinetics of the cycling of Tim44:Ssc1 complex.

3.2.1 Recombinant Ssc1 and Tim44 are functional and can associate to form Tim44:Ssc1 complex *in vitro*

It has been previously reported that Tim44 and Ssc1 interact *in vitro* when purified from yeast (D'Silva et al., 2004; Liu et al., 2003). More recently, *in vitro* interaction of Tim44, purified from *E.coli*, and Ssc1, purified from yeast, has also been shown (Slutsky-Leiderman et al., 2007). As we intended to engineer cysteine mutants of both of these proteins for subsequent labeling with sulfhydryl-specific fluorophores for FRET studies, we expressed and purified both the components recombinantly from *E.coli* to facilitate the production of the various mutant proteins (Figure 3.15).

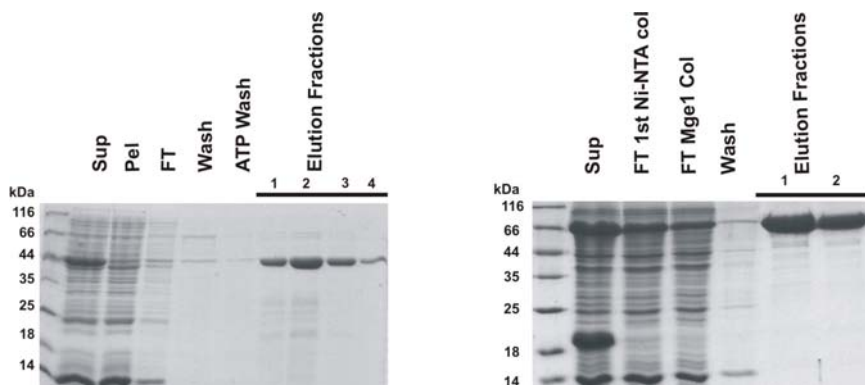


Figure 3.15: Purification of recombinantly expressed His₆Tim44 and Ssc1 from *E.coli*.

Left panel: Coomassie-Brilliant-Blue (CBB) stained gel illustrating the different steps of purification of His₆Tim44 over a Ni-NTA column. Sup: Supernatant fraction after cell lysis, Pel: Pellet fraction after cell lysis, FT: Flow-through from the Ni-NTA column after binding the Sup. **Right Panel:** Coomassie-Brilliant-Blue (CBB) stained gel illustrating the different steps of purification of Ssc1. Sup: Supernatant fraction after cell lysis, FT: Flow-through from the Ni-NTA column after binding the Sup.

It is noteworthy that Ssc1 could be expressed in soluble fraction only upon its co-expression along with Hep1 in the same bacterial cells (Sichting et al., 2005). Tim44 with a N-terminal His₆tag was expressed and purified from *E.coli* as described in Materials and Methods section. After expression, Ssc1 was purified by a novel approach using His₆-Mge1 column (discussed in detail in Materials and Methods).

Ssc1 purified from *E.coli* retained its full functionality in terms of its ATPase activity, stimulation of its ATPase activity in presence of Mdj1 (Figure 3.16), the J-domain co-chaperone of Ssc1 in the mitochondrial matrix, and its ability to bind substrate peptides (shown in a later section).

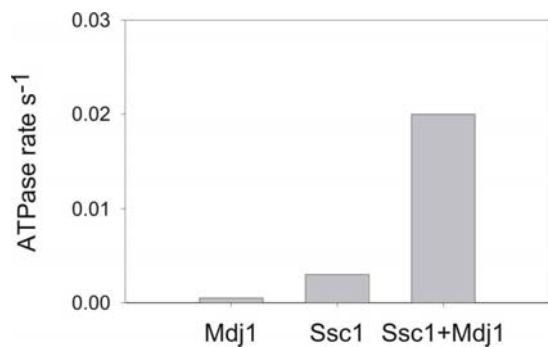


Figure 3.16: ATP hydrolysis activity of recombinantly expressed and purified Ssc1. ATP hydrolysis activity of Ssc1 was checked by coupled enzymatic detection of ADP produced as described in Materials and Methods. The rate of ATP hydrolysis reported is mole of ATP hydrolysed/mole of Ssc1/s.

Both the proteins showed distinct secondary structures in CD-spectra (Figure 3.17).

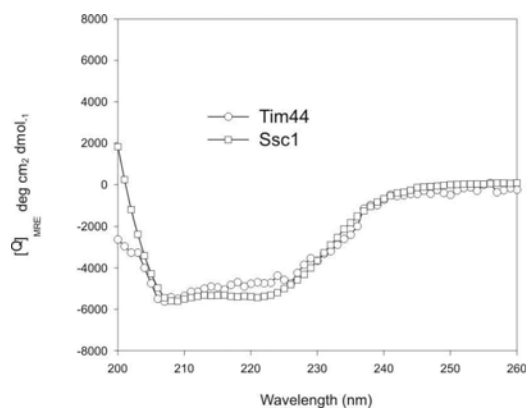


Figure 3.17: Recombinantly expressed and purified Tim44 and Ssc1 are folded. Comparison of far-UV CD spectra of purified Tim44 and Ssc1. The CD spectra were recorded on a Jasco-715 spectropolarimeter with a 2mm pathlength cuvette using 2μM protein in each case in appropriate buffer as mentioned in Materials and Methods.

Interaction between the purified proteins was checked by the ability of His₆-Tim44 to co-purify Ssc1 over a Ni-NTA column, when pre-incubated together (Figure 3.18). Tim44:Ssc1 complex was stable under Ssc1-ADP state and without addition of any

nucleotide to the reaction whereas addition of ATP made the complex unstable leading to absence of co-purification of Ssc1 with His₆Tim44 in agreement with the previously published data (Rassow et al., 1994; Schneider et al., 1994; Slutsky-Leiderman et al., 2007; von Ahsen et al., 1995; Voos et al., 1996).

Since the steady state interactions of Tim44 and Ssc1 under various conditions had been studied in some detail (D'Silva et al., 2004; Liu et al., 2003; Schneider et al., 1994; Slutsky-Leiderman et al., 2007; von Ahsen et al., 1995), we sought to uncover the dynamic properties of this complex in terms of the kinetic parameters involved in its formation and dissociation.

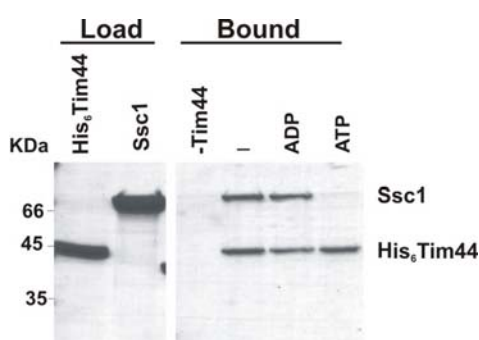


Figure 3.18: Recombinantly expressed and purified Tim44 and Ssc1 can interact *in vitro*. 1 μ M His₆-Tim44 was preincubated with 4 μ M of Ssc1 in absence of any added nucleotide or in presence of 2mM ATP or ADP at 25°C for 5 min to form the complex. The reactions were then incubated with Ni-NTA column and was eluted with buffer containing 300mM of imidazole followed by SDS-PAGE and CBB staining. 10% of the materials used for the reaction were used as load.

3.2.2 Development of a FRET based assay system to monitor Tim44-Ssc1 interaction cycle in real time

3.2.2.1 Generation of cysteine mutants of Tim44 and Ssc1 for maleimide specific fluorophore labeling

After the initial biochemical experiments had established that purified components can form a complex *in vitro*, the next step was to establish a system to monitor the interaction cycle in real-time in order to elucidate the exact order of events.

To study the Tim44-Ssc1 interaction cycle in real time, a Fluorescence resonance energy transfer (FRET) based assay system was developed. To monitor the interactions using FRET, exogenous Cysteine reactive fluorophores were incorporated at specific positions on Tim44 and Ssc1. As there is no structural information about the N-terminal domain of Tim44, the residues suitable for cysteine substitution and fluorophore labeling were

chosen by bio-informatic analysis. For choosing the residues which would be substituted to cysteines in case of Tim44, the sequences of Tim44s across different species were aligned. The residues that were not conserved in Tim44 across a representative set of species and contained Asp substitution in any of the species were chosen for mutagenesis to cysteines (Figure 3.19) (Bajaj et al., 2005).

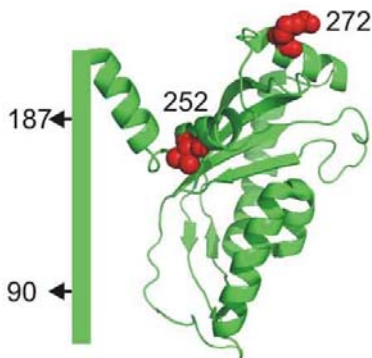


Figure 3.19: Positions of Cysteine mutations on Tim44. Schematic representation of N-terminal domain of yeast Tim44 along with the ribbon diagram of crystal structure of C-terminal indicating the positions of engineered cysteines is illustrated.

The Asp based cutoff, used in case of the absence of additional structural information, ensured that only surface residues are chosen so as to minimize the plausible deleterious effects of the exogenous fluorophores on the protein structure and function. The endogenous cysteine residue of Tim44 (C369) was not mutated, as the crystal structure of C-terminal of yeast Tim44 showed it to be buried in the hydrophobic core of the protein (Josyula et al., 2006) and was therefore inaccessible to fluorophores under native conditions (data not shown).

For labeling Ssc1, the surface exposed positions on the Ssc1 were chosen based on the homology modeled structure of Ssc1 on the crystal structures of Hsp110, an Hsp70 homologue (Liu and Hendrickson, 2007)(Figure 3.20).

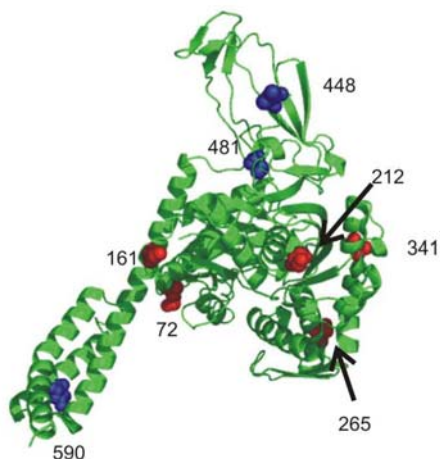


Figure 3.20: Positions of Cysteine substitutions on Ssc1. Homology model of Ssc1 based on the crystal structure of Hsp110 showing the residues mutated to cysteines for maleimide specific labeling. Engineered cysteines present in the NBD are represented in red and those present in PBD are shown in blue.

All cysteine substitutions of Tim44 and of Ssc1 were checked for functionality in yeast and all of them used for the study were found to be functional (Figure 3.21). The same mutants were then cloned in bacterial expression vector and expressed and purified as described above for wild type proteins.



Figure 3.21: All the single cysteine substitution mutants of Tim44 and Ssc1 are functional *in vivo*. **Left panel:** A haploid deletion strain of *TIM44* harbouring the wild type copy of *Tim44* on the *URA* plasmid was transformed with plasmids containing single cysteine mutants of Tim44. In vivo functionality of the mutant proteins was checked by plasmid shuffling on 5-fluoro-orotic acid plates. Plasmids carrying the wild type Tim44 or an empty plasmid were used as the positive and negative controls respectively. **Right panel:** A haploid deletion strain of *Ssc1* harbouring the wild type copy of *Ssc1* on the *URA* plasmid was transformed with plasmids containing single cysteine mutants of Ssc1. In vivo functionality of the mutant proteins was checked by plasmid shuffling on 5-fluoro-orotic acid plates. Plasmids carrying the wild type Ssc1 or an empty plasmid were used as the positive and negative controls respectively.

3.2.3 Interaction of Tim44 and Ssc1 can be monitored in real time by Fluorescence Resonance Energy Transfer

After the introduction of cysteines in different positions of both Tim44 and Ssc1, the next step was to label the proteins with fluorophores. Various maleimide specific fluorophores were tried for the labeling purpose and one donor-acceptor pair namely, Alexa-594-maleimide as the donor and Atto-647N-maleimide as the acceptor was found to be most sensitive for observing FRET between Tim44 and Ssc1. To perform FRET based binding assays, Tim44 was labeled with Alexa-594 as the donor fluorophore and Ssc1 was labeled with Atto-647N as the acceptor fluorophore. The labeling procedure (as described in the Materials and Methods section) did not affect the structural integrity of the proteins as observed by CD spectra of a representative labeled Tim44 and Ssc1 compared to the wild type proteins (Figure 3.25, left panel). Labeled Tim44s and Ssc1s formed complexes as shown by previously described Ni-NTA based pulldown experiment (Figure 3.22, Panel B).

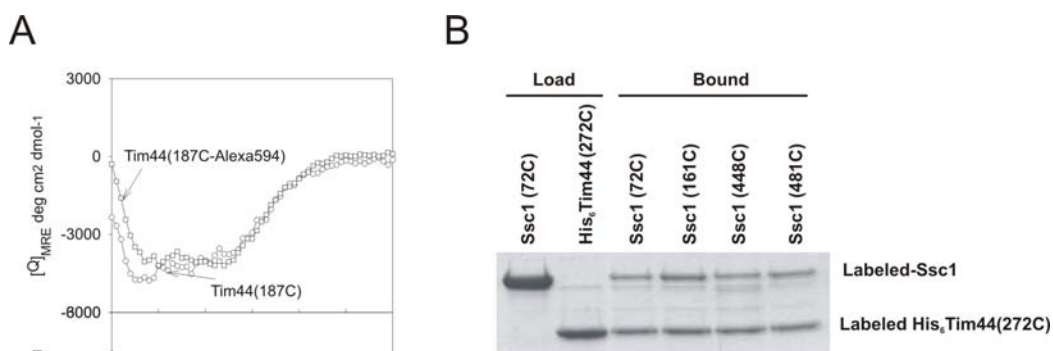


Figure 3.22: Panel A: Labelling with fluorophores does not affect the structures of purified Tim44 and Ssc1. Comparison of far-UV CD spectra of labeled and unlabeled Tim44 (top panel) and Ssc1 (bottom panel). The CD spectra were recorded on a Jasco-715 spectropolarimeter with a 2mm pathlength cuvette using 2 μ M protein in each case in the appropriate buffer as mentioned in materials and methods. **Panel B: Ni-NTA pulldown with the fluorophore-labeled protein.** 450nM of Alexa-594 labeled His₆Tim44(272C) was mixed with 1.8 μ M of Atto 647N labeled different Ssc1 mutants (72C, 161C, 448C and 481C) to form Tim44:Ssc1 in presence of 2mM ADP. The complex eluted from Ni-NTA column was subjected to SDS-PAGE followed by staining with coomassie brilliant blue (CBB).

Real time interaction between Tim44 and Ssc1 could be monitored by FRET by monitoring the quenching of donor fluorescence on Tim44 in presence of acceptor labeled Ssc1. Control experiments showed that unlabelled Ssc1 did not affect the fluorescence of donor labeled Tim44 (Figure 3.23).

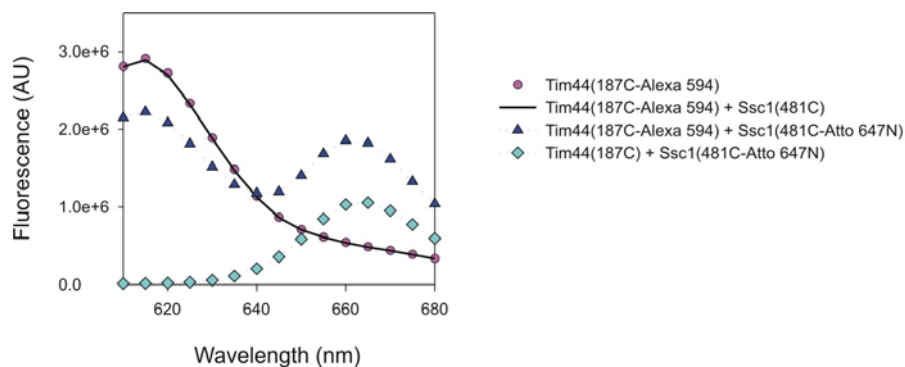


Figure 3.23: Tim44-Ssc1 interaction can be monitored by FRET. Intermolecular FRET between Tim44 (187C) and Ssc1 (481C). Quenching of donor fluorescence of 150nM Tim44 (187C-Alexa 594) was observed in presence of 300nM of acceptor-labeled Ssc1 (481C-647N). Unlabelled Ssc1 was used as a control.

3.2.4 Mapping of interaction sites in Tim44:Ssc1 complex

To understand the domain-wise interaction of Tim44 and Ssc1 in the context of full-length proteins, the proximities of the various domains of Tim44 and Ssc1 were obtained by quantifying the fluorescence quenching of donor labeled Tim44 in the presence of acceptor labeled Ssc1 in the ADP-bound state. FRET efficiencies (fE) were obtained for various donor-acceptor pairs to compare different distances between domains of the two proteins. FRET efficiencies (fE) were obtained for Tim44:Ssc1 pairs where the donor probes were placed in the N-terminal domain (NTD) (90C and 187C), and in C-terminal domain (252C and 272C) of Tim44. The acceptor fluorophores were positioned at different domains of Ssc1; subdomains of the nucleotide binding domain (NBD), base of the peptide binding domain (PBD-base) and the lid domain of PBD (PBD-lid). Comparison of fEs of different donor-acceptor pairs indicated that both domains of Tim44 molecule were closer to Ssc1-PBD-lid and Ssc1-PBD-base than Ssc1-NBD. FRET data obtained for the proximity of domains Tim44 with the different domains of Ssc1 also

suggested that there are regions of nucleotide binding domain of Ssc1 (subdomain Ia, position 161) that formed close contacts with Tim44 (Figure 3.24).

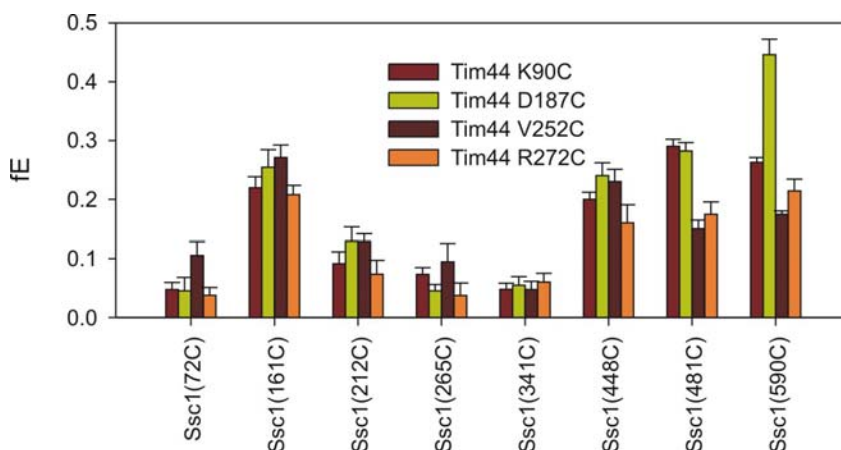


Fig. 3.24: Mapping of interaction sites of Tim44:Ssc1 complex. FRET efficiency (fE) of different positions of Ssc1 (both NBD and PBD) with either domains of Tim44 was determined by the amount of donor fluorescence quenching of 150nm of Tim44 (Alexa 594-maleimide) complexed with 4 μ M of acceptor labeled Ssc1 (Atto-647N maleimide). Four different bars represent the complex of particular donor labeled-Tim44 with the corresponding acceptor labeled Ssc1 (labeled position of Ssc1 is mentioned in X-axis.)

To negate the possibility of the contribution of uncomplexed Tim44 in the reaction, due to differences in binding affinity of the different mutants, fE was determined always at saturating concentrations of Ssc1, where the fE did not increase upon further addition of Ssc1.

3.2.5 Interaction of isolated domains of Ssc1 and Tim44

To determine the minimal domains required for Tim44-Ssc1 interaction and recapitulate the data obtained with full length proteins, individual domains of both Tim44 and Ssc1 were expressed and purified and interactions were examined.

3.2.5.1 *The solubility of Ssc1-NBD in E.coli strictly depends on its co-expression along with Hep1 and addition of the linker sequence*

Previous results from our laboratory suggested that the recombinant PBD of Ssc1 was soluble irrespective of the presence or absence of Hep1 whereas NBD was always found in the inclusion bodies (Sichting et al., 2005). Recent report showed that the hydrophobic linker sequence (VLLLD) stabilizes NBD of DnaK (Swain et al., 2007). The same was tested for NBD of Ssc1. Addition of the linker sequence to the NBD of Ssc1 did not improve the solubility of recombinant protein. Interestingly, this construct became soluble upon coexpression with Hep1, similar to the full length protein (Figure 3.25). Apparently, NBD along with the linker sequence is the minimal domain of Ssc1 which can be kept in functional conformation by Hep1.

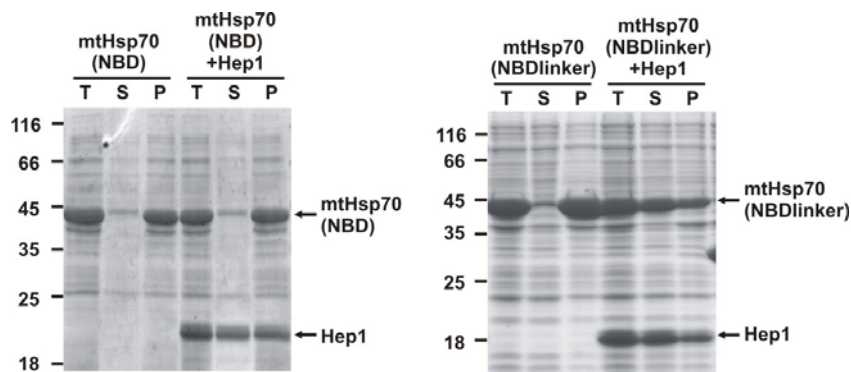


Figure 3.25: The solubility of Ssc1-NBD in *E.coli* strictly depends on addition of the linker sequence and its co-expression with Hep1. Ssc1-NBD with and without linker sequence was expressed alone or along with Hep1 from a Duet vector in *E.coli*. T: Total cell extract, S: Soluble fraction, P: Pellet fraction from the bacterial cell. The cell extracts and both the soluble and pellet fractions were subjected to SDS-PAGE followed by staining with Coomassie Brilliant blue (CBB).

3.2.5.2 *Isolated Ssc1-PBD can form a complex with Tim44 while the NBD does not interact*

Binding of the separate domains of Ssc1 to Tim44 was assessed using pull-down with His₆-Tim44 showed that the C-terminal PBD interacted with Tim44 in a nucleotide independent manner, as expected, whereas the N-terminal NBD was unable to form a complex with Tim44 under any of the experimental conditions analyzed (Figure 3.26, Panel A).

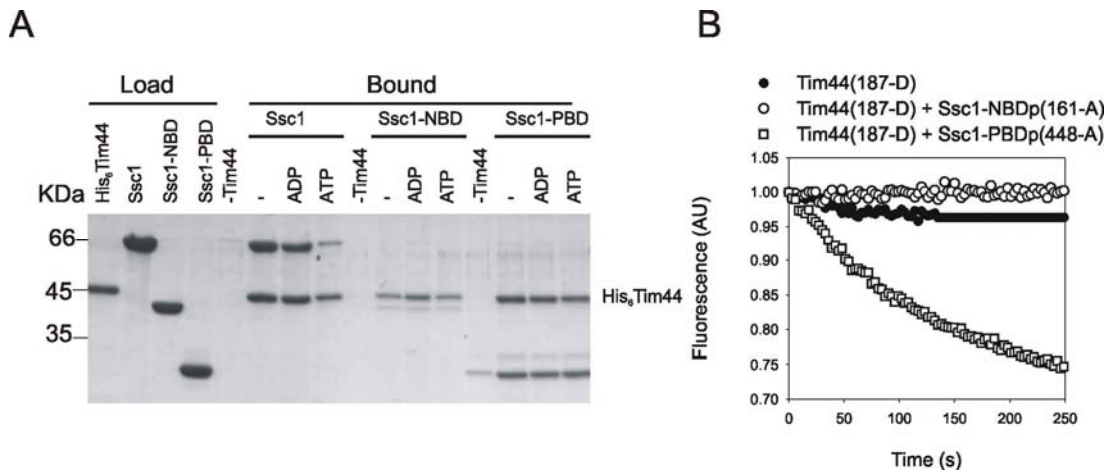


Figure 3.26: Interaction of isolated domains of Ssc1 with Tim44. **Panel A:** Ni-NTA pull-down of Ssc1 and Ssc1-NBD and Ssc1-PBD with His-tagged Tim44 in different nucleotide conditions. 2 μ M of His tagged Tim44 was mixed with 4 μ M of Ssc1 and 4 μ M of each of its isolated domains in presence of different nucleotides to form the complexes and subsequently bound and eluted from the Ni-NTA column. The eluted proteins were subjected to SDS-PAGE followed by staining with CBB. **Panel B:** Interaction of Ssc1 domains with Tim44 by FRET. Interactions of isolated domains of Ssc1 were monitored in real time by quenching of donor fluorescence of donor labeled Tim44 (187C-Alexa594) in presence of acceptor labeled Ssc1 domains, either Ssc1-NBD (161C-647N) or Ssc1-PBD (481C-647N).

The steady state observations obtained from the pull-down experiments were further supported by FRET based binding experiments to rule out any transient interactions with the NBD. Cysteine-reactive fluorophores were placed in the isolated domains in the same positions as in the full length protein which showed considerable FRET efficiency with Tim44 e.g. at the position 448 of PBD and position 161 on NBD. The donor fluorescence on Tim44 was only quenched with acceptor labeled Ssc1-PBD (481C) but not with acceptor labeled Ssc1-NBD (161C) reconfirming the results of the pull-down experiments (Figure 3.30, Panel B). Thus, both pull-down and FRET based binding assays showed that the peptide binding domain alone is able to interact with Tim44 reinstating the sufficiency of Ssc1-PBD for Tim44:Ssc1 interaction.

The K_D of Tim44:Ssc1 interaction was found to be $1.1 \pm 0.3 \mu$ M (Figure 3.27). Similarly, the K_D of Tim44:Ssc1-PBDp was determined to be $1.4 \pm 0.2 \mu$ M. Thus, the regions of

Ssc1-NBD, that are proximal to Tim44, do not contribute significantly towards the stabilization of Tim44:Ssc1 complex.

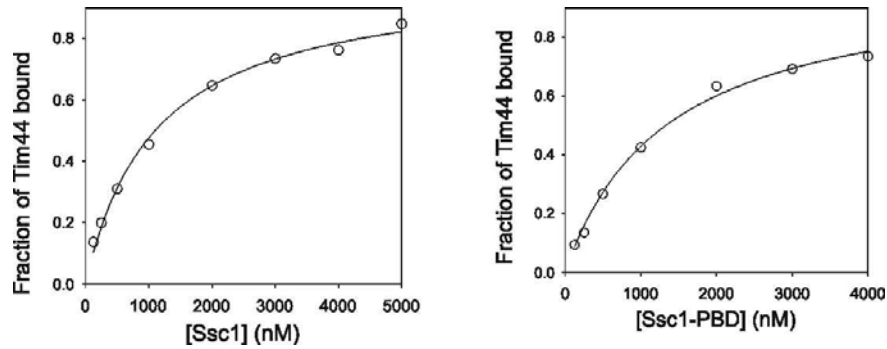


Figure 3.27: Determination of equilibrium dissociation constant (K_D) of Tim44:Ssc1 and Tim44:Ssc1-PBD. The experimentally determined concentrations of bound Tim44 were calculated in both cases based on FRET efficiency data obtained at different concentrations of Ssc1 and Ssc1-PBD. The data were fitted as described in Materials and Methods.

3.2.5.3 The N-terminal domain (NTD) of Tim44 is the major interacting domain with Ssc1

After dissecting the roles of domains of Ssc1 in Ssc1:Tim44 complex formation, it was interesting to delineate the roles of domains of Tim44. For that purpose, both domains of the protein, Tim44-NTD (aa 44-233) and Tim44-CTD (234-end), were expressed in *E.coli* (Tim44-NTDp and Tim44-CTDp respectively) and purified and their interaction with Ssc1 was monitored (Figure 3.28).

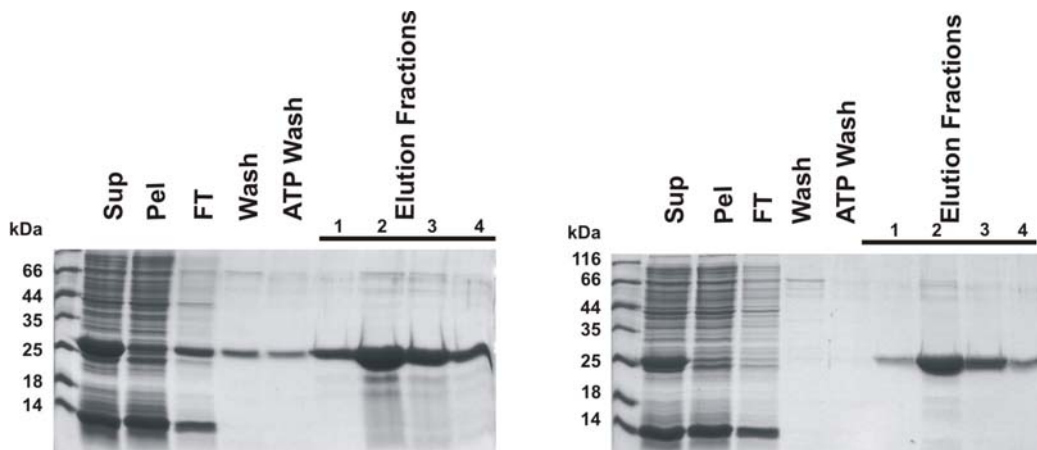


Figure 3.28: Purification of recombinantly expressed His₆Tim44-NTD and His₆Tim44-CTD from *E.coli*. **Left panel:** Coomassie-Brilliant-Blue (CBB) stained gel illustrating the different steps of purification of His₆Tim44-NTD over a Ni-NTA column. Sup: Supernatant fraction after cell lysis, Pel: Pellet fraction after cell lysis, FT: Flow-through from the Ni-NTA column after binding the Sup. **Right Panel:** Coomassie-Brilliant-Blue (CBB) stained gel illustrating the different steps of purification of His₆Tim44-CTD over a Ni-NTA column. Sup: Supernatant fraction after cell lysis, Pel: Pellet fraction after cell lysis, FT: Flow-through from the Ni-NTA column after binding the Sup.

Both the domains were with N-terminal His₆tags and the interaction with Ssc1 was first checked by Ni-NTA pull-down assays as was performed for full-length protein. Tim44-NTDp was sufficient to faithfully recapitulate the interaction of full length Tim44 with Ssc1. On the other hand, Tim44-CTDp exhibited only weak interaction with Ssc1 (Figure 3.29).

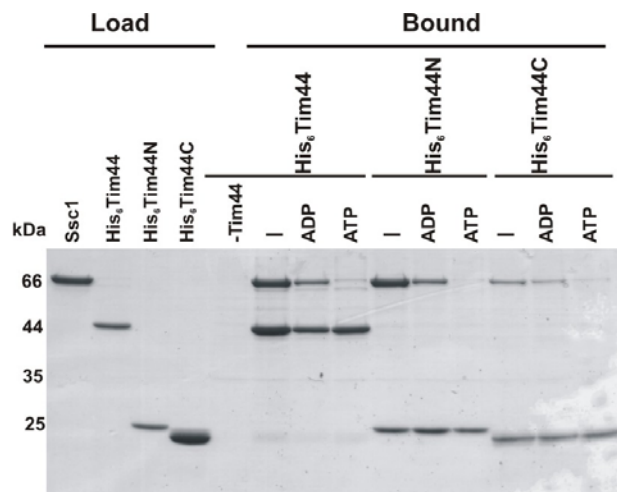


Figure 3.29: Ni-NTA pull-down of Ssc1 with Tim44 and isolated domains of Tim44. 2 μ M of His₆-tagged Tim44, Tim44-NTD and Tim44-CTD were mixed with 4 μ M of Ssc1 under different nucleotide conditions and subsequently incubated with the Ni-NTA beads. The bound proteins were subjected to SDS-PAGE followed by staining with CBB.

The same observation was made with FRET based binding assays by using donor-labelled Tim44 domains at position 187 in case of NTDp and 272 in case of CTDp. The equilibrium dissociation constant of Tim44-NTDp/Ssc1 was measured to be 2 \pm 0.4 μ M, which is very similar to K_D of Tim44:Ssc1 (1.1 \pm 0.3 μ M). (Figure 3.30, left panel), this further supports the finding that Tim44-CTD plays only a minor role in the stabilization of the Tim44:Ssc1 interaction. Also, Tim44-NTDp was able to bind to Ssc1-PBDp with affinity similar to the binding of Tim44 to Ssc1-PBDp (Figure 3.30, right panel). Thus, Tim44-NTD and Ssc1-PBD form the minimal interaction region in Tim44:Ssc1 complex.

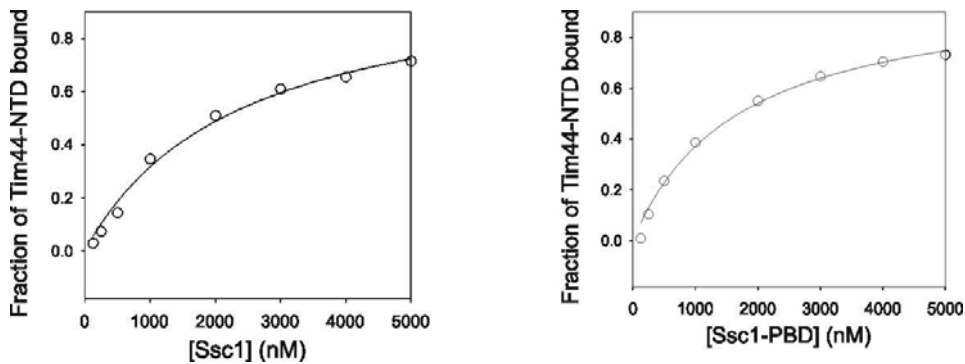


Figure 3.30: Determination of equilibrium dissociation constant (K_D) of Tim44-NTD/Ssc1 and Tim44-NTD/Ssc1-PBD. The experimentally determined concentrations of bound Tim44-NTD was calculated based on FRET efficiency data obtained at different concentrations of Ssc1 and Ssc1-PBD. The data were fitted as described in materials and methods.

3.2.5.4 Isolated domains of Tim44 cannot replace the full-length protein *in vivo* even when expressed together *in trans*

After establishing that the NTD of Tim44 is sufficient for interaction with Ssc1, it was interesting to check whether this part of Tim44 alone can replace the full-length protein in yeast cells. For that purpose nucleotide sequence coding for NTD and CTD were cloned into yeast vectors and transformed into the yeast cells lacking the wild type Tim44 but carrying the *TIM44* gene on the *URA* plasmid. The *in vivo* functionality of isolated domains was checked by plasmid shuffling on medium containing 5-FOA that selects against cells carrying *URA* plasmid. Neither of the isolated domains supported cell growth. Also, even when they were expressed together *in trans* they could not supplement for the function of the full length protein (Figure 3.31). This result indicated that both the domains of Tim44 act as *cis* acting elements *in vivo*.



Figure 3.31: full length Tim44 is required for its *in vivo* function. A haploid deletion strain of *TIM44* harbouring a wild type copy of *TIM44* on the *URA* plasmid was transformed with plasmids containing either Tim44-NTD or Tim44-CTD. Cells were plated into medium containing 5-fluoroorotic acid which specifically selects the cells that have lost the *URA* plasmid. Plasmids carrying the full length Tim44 or an empty plasmid were used as the positive and negative controls respectively.

3.2.6 Substrate induced dissociation of Tim44:Ssc1

Destabilization of Tim44:Ssc1 complex in presence of substrate protein is believed to be an essential feature for this complex to be competent for mitochondrial protein translocation. It has been observed earlier that binding of a substrate peptide P5 (CALLLSPARR) to Ssc1 leads to the dissociation of the Tim44 and Ssc1 complex (D'Silva et al., 2004; Liu et al., 2003). Dynamics of dissociation of the complex was followed by the recovery of quenched donor fluorescence of Tim44, in the Tim44 (187-Alexa594)/Ssc1 (481-Atto647N) complex, upon addition of P5 (Figure 3.32, Panel A). The complex between the minimal binding regions of Tim44 and Ssc1, namely the complex between Tim44-NTDp/Ssc1-PBDp, was able to faithfully reproduce the P5 induced dissociation of the Tim44:Ssc1 complex (Figure 3.32, Panel B). The substrate induced dissociation rate of Tim44/Ssc1/ADP complex was $\sim 0.004 \text{ s}^{-1}$ ($t_{1/2} \sim 173\text{s}$).

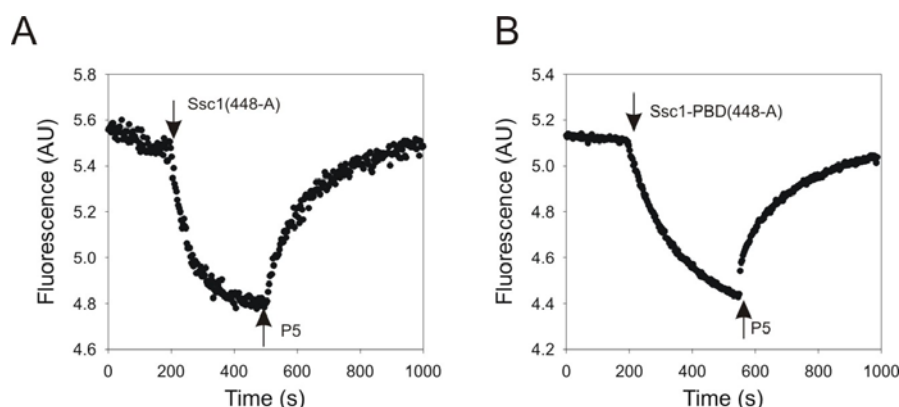


Figure 3.32: Substrate peptide (P5) induced dissociation of Tim44:Ssc1 and Tim44-NTD:Ssc1-PBD. Panel A: Substrate peptide (P5) induced dissociation of Tim44:Ssc1 was monitored in real-time by the recovery of quenched donor fluorescence of donor labeled Tim44 (187C-Alexa594) in presence of acceptor labeled Ssc1 (481C-647N). Arrows indicate the point of addition of Ssc1 or P5. Panel B: The experiment was done with Tim44-NTD and Ssc1-PBD.

To correlate the rate of substrate induced cycling with the physiological rate of protein translocation, we sought to obtain a rough indication of the rate of protein translocation across TIM23. A list of mitochondrial proteins was first generated using MITOPRED (Guda et al., 2004a; Guda et al., 2004b) followed by the use of the software Submito (<http://bioinfo.au.tsinghua.edu.cn/subMito/>) to generate a list of putative mitochondrial

matrix targeted preproteins. Hsp70-binding sites on these proteins were obtained using a DnaK-binding site prediction algorithm (Rudiger et al., 1997) as Ssc1 binding specificity was found to be similar to published reports for DnaK (see below). The average size of the mitochondrial matrix proteins thus obtained was 503aa with ~12 binding site per protein. With these data it was obtained that ~1800 pmol/mg of mitochondrial matrix targeted proteins are transported through 20 pmol/mg of TIM23 in ~210min, the doubling time of *S. cerevisiae* (Lim et al., 2001). This indicated that Ssc1 has to cycle off Tim44 in approximately 2-3s in order to support physiological rate of protein translocation. Surprisingly, the substrate induced dissociation rate ($t_{1/2} \sim 173s$) was two orders of magnitude slower than the expected rate of cycling of Tim44:Ssc1. This renders the substrate induced dissociation rate unsuitable to support physiological rate of protein translocation. To further rule out the possibility that extremely high local concentration of substrate proteins at the translocase channel would increase the off-rate of Ssc1 from the complex, the dissociation rate of the complex was obtained at different concentration of P5. The observed rates were found to be independent of P5 concentration (Figure 3.33, panel A), indicating further that even with high local concentrations of substrate at the translocase, substrate induced dissociation of the Tim44/Ssc1/ADP is too slow to support the physiological rate of protein translocation.

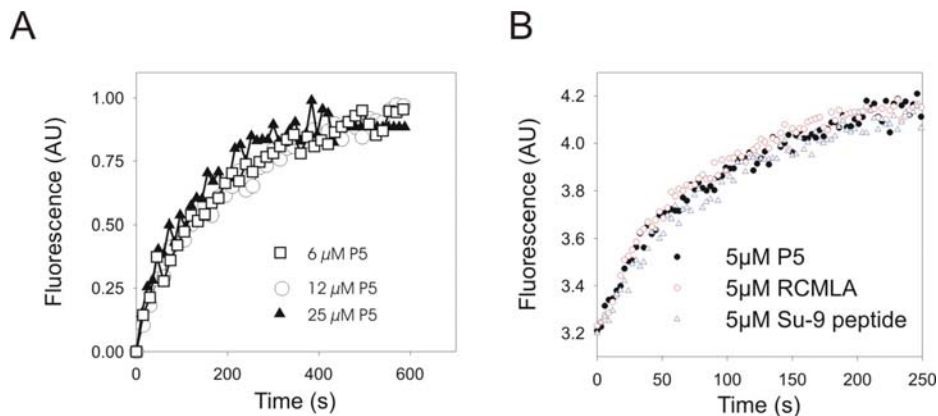


Figure 3.33: Panel A: Substrate induced dissociation of Tim44:Ssc1 is independent of substrate concentration. Substrate peptide (P5) induced dissociation of Tim44:Ssc1 was monitored in real-time by the recovery of quenched donor fluorescence of donor labeled Tim44 (187C-Alexa594) in presence of acceptor labeled Ssc1 (481C-647N). The substrate peptide induced dissociation was determined in presence of different concentrations of P5. **Panel B: Substrate induced dissociation of Tim44:Ssc1 is independent of type of substrate.** The same Tim44:Ssc1 was complex was formed and the dissociation kinetics was monitored in presence of 5 μM of either P5 peptide or RCMLA or peptide corresponding to the sequence of Su-9 sequence.

To rule out the possibility that substrate proteins would act differently from the peptide P5, RCMLA, a known substrate for Hsp70 chaperones and Su9 peptide, an authentic pre-sequence from a matrix targeted pre-protein, was used as a substrates. Identical rates of dissociation obtained in all these cases indicated that the rate of dissociation is independent of the nature of the substrate proteins further validating that substrate induced dissociation rate is unphysiological (Figure 3.33, panel B).

3.2.7 Nucleotide induced dissociation drives Tim44:Ssc1 reaction cycle

Extremely slow substrate induced dissociation of the Tim44:Ssc1 or Tim44-NTDp/Ssc1-PBDp complex in presence of ADP indicated the essentiality of nucleotide-induced conformational changes induced by Ssc1-NBD in the Tim44:Ssc1 cycle. Nucleotides have been shown to modulate the stability of Tim44:Ssc1 complex. To obtain kinetic information regarding the stability of the complex under different nucleotide conditions, off-rate of Ssc1 from the Tim44:Ssc1 complex was determined by recovery of donor fluorescence of Tim44 as described earlier. The spontaneous dissociation rate of the Tim44:Ssc1 complex in presence of an excess of unlabelled Tim44 or Ssc1 was not measurable with the technique. The dissociation rate was significantly accelerated in presence of ATP ($\sim 0.27 \text{ s}^{-1}$, $t_{1/2} \sim 2.5\text{s}$) whereas the dissociation was negligible in presence of either ADP or AMPPNP (Figure 3.34).

The small amplitude change in fE upon addition of AMPPNP was independent of the concentration of the nucleotide used, suggesting these processes to be a minor change in Ssc1-Tim44 distance rather than dissociation events. The dissociation rate of Tim44:Ssc1 complex in presence of ATP was ~ 70 fold faster than P5 induced dissociation and is more compatible with the rate of mitochondrial protein translocation. This dissociation is not coupled to the hydrolysis of ATP, as the spontaneous hydrolysis rate of ATP by Ssc1 in presence or absence of Tim44 was approximately ~ 150 fold slower than the observed rate of Tim44:Ssc1 dissociation (D'Silva et al., 2003). Interestingly, the observed rate of dissociation of Tim44:Ssc1 in presence of ATP was independent of ATP concentration indicating that the dissociation of the complex occurs subsequent to a conformational change upon ATP binding.

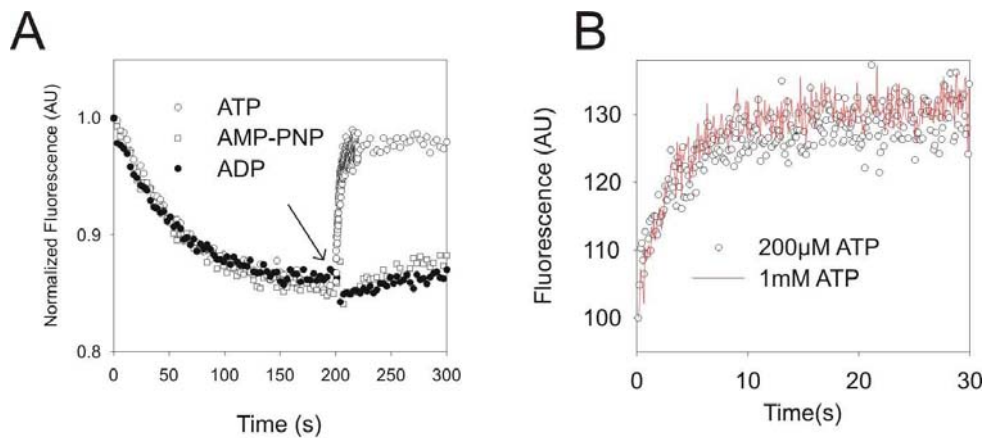


Figure 3.34: Nucleotide dependent dissociation of Tim44:Ssc1 complex. Panel A: Nucleotide dependent dissociation of Tim44:Ssc1 complex was followed by the recovery of donor fluorescence on labeled Tim44 (187C). 50nM of labeled Tim44 was mixed with 2µM of acceptor labeled Ssc1(448C) leading to quenching of donor fluorescence due to formation of Tim44:Ssc1. 2µM of Mge1 was present in buffer in order to facilitate nucleotide-charging of Ssc1 in subsequent steps. Different nucleotides, at a final concentration of 1mM, were then added at the indicated time point to obtain the rate of fluorescence recovery due to dissociation of the complex. **Panel B:** Tim44:Ssc1 complex was formed by donor- and acceptor-labeled Tim44 and Ssc1, respectively, as described in panel A. The dissociation of the complex was monitored by the recovery of donor fluorescence after addition of ATP at the final concentrations shown in the figure.

Consistent with the kinetic stability, the equilibrium dissociation constant of Tim44:Ssc1 in the presence of ATP is increased to the extent of being immeasurable with the assay. The calculated value for the K_D in presence of ADP is 1.2µM, which is in qualitative agreement with the biochemical evidence. The K_D in presence of ATP could not be calculated due to inner filter effect at the large concentrations of labeled Ssc1 needed for the measurement.

Consistent with the low affinity of Ssc1 and Tim44 in presence of ATP, *in organello* studies have shown that Tim44:Ssc1 complex is not stable under ATP rich conditions (Kronidou et al., 1994; Rassow et al., 1994; Schneider et al., 1994; Ungermann et al., 1996; von Ahsen et al., 1995). Pull-down experiment performed under different nucleotide conditions was corroborative of the kinetic stabilities of Tim44:Ssc1 complex under similar conditions (Figure 3.35).

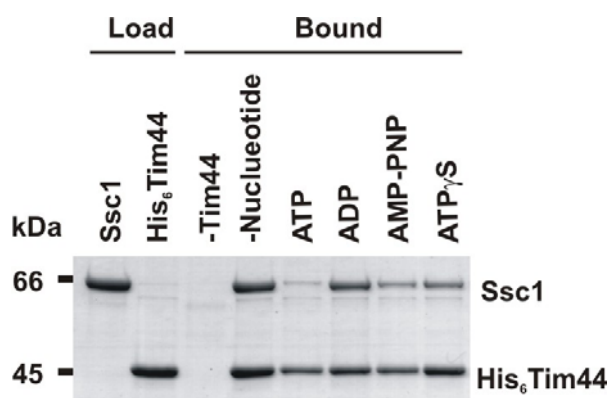


Figure 3.35: Ni-NTA pull-down of Ssc1 with Tim44 in different nucleotide conditions. 2 μ M of His₆-tagged Tim44 was mixed with 4 μ M of Ssc1 to form the complexes in absence of any nucleotide or in presence of 2mM of either of ATP or ADP or AMP-PNP or ATP γ S and subsequently bound and eluted from the Ni-NTA column. The eluted proteins were subjected to SDS-PAGE followed by staining with CBB. 10% of the materials used for the reactions were used as load.

The association of Tim44:Ssc1 monitored in presence of ADP indicated an extremely slow apparent on rate (Figure 3.36). The apparent rate of association in the presence of AMPPNP, was accelerated by a factor of ~ 4 with an apparent bimolecular rate constant (k_a) of $3 \times 10^4 \text{ M}^{-1}\text{s}^{-1}$, indicating an approximate binding time of $< 1\text{s}$ under physiological concentration of Ssc1 ($\sim 50\text{-}100\mu\text{M}$) (Rassow et al., 1994; Schmidt et al., 2001; Voisine et al., 2000). The equilibrium dissociation constant (K_D) of Tim44:Ssc1 calculated from the k_d and k_a of the complex formation was $\sim 10\mu\text{M}$ which was much higher than the concentrations of Ssc1 used for these experiments, hence binding Ssc1/ATP with Tim44 was not observable with the concentrations used. Higher concentrations of Ssc1 could not be used for the study due to the presence of inner filter effect. The high on-rate of Tim44 with Ssc1 in presence of AMPPNP, an ATP analog, suggests that the Ssc1-ATP complex is selected to bind to Tim44 in the presence of a mixture of Ssc1-ATP and Ssc1-ADP in the cellular milieu.

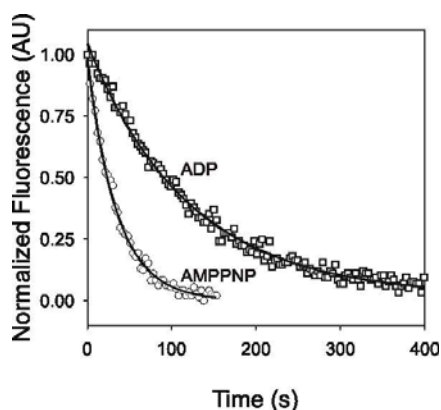


Figure 3.36: Apparent association rate of Tim44 with Ssc1 differs depending on the nucleotide state of the Ssc1. Comparison of apparent rate of association of Ssc1-AMPPNP or Ssc1-ADP with Tim44 was obtained by following the time dependent change of donor labeled Tim44 (481C) (50nm) in presence of 2.5 μ M of acceptor labeled Ssc1(481C) pre-incubated with 2mM of the different nucleotides.

The dissociation of Tim44/Ssc1/ATP occurs in the time-scale of ~ 2.5 s. This, taken together with the association rate of Tim44 and Ssc1/AMPPNP yields a K_D of $\sim 10\mu\text{M}$ for the complex, indicating that at physiological concentrations of Tim44 and Ssc1 most of the Tim44 would be saturated with Ssc1. The complex is transiently formed in presence of ATP which then undergoes dissociation to release Ssc1/ATP, the substrate acceptor state of Ssc1. The continuous on-off cycle of Ssc1 on Tim44 would maintain a high local concentration of Ssc1 near the translocase channel.

3.2.8 The dissociation of Tim44:Ssc1 complex is a single-step reaction

To obtain further insight into the kinetic intermediates populated during the dissociation of Tim44:Ssc1 complex under various conditions, the dissociation event was followed monitoring the different distance vectors in Tim44:Ssc1 complex. In presence of ATP, the rate of increase in distance along a distance vector between Tim44-NTD and Ssc1-NBD [Tim44 (187C)-Ssc1 (161C)], and between Tim44-NTD and Ssc1-PBD [Tim44 (187C)-Ssc1(448C)] followed identical kinetics (Figure 3.37, left panel). This indicates that both the domains of Ssc1 dissociate from the complex without populating an intermediate state where one of the domains remain bound to Tim44. Additionally, identical rates of decrease in fE between Tim44 (187C)-Ssc1 (448C) and Tim44 (252C)-Ssc1 (448C) (Figure 3.37, left panel) indicate further that there is no ordered dissociation event during the nucleotide dependent release of Tim44:Ssc1 complex. To rule out the possibility of segmental dissociation of the complex in presence of substrates, the same pairs of distance vectors were investigated during P5 induced dissociation of the Tim44:Ssc1 (Figure 3.37, right panel). Similar rates obtained by the increase in different distance vectors support a 2 state mechanism of dissociation of the complex in presence of substrate peptides. This experiment showed that the dissociation of Tim44:Ssc1 complex is a single step reaction.

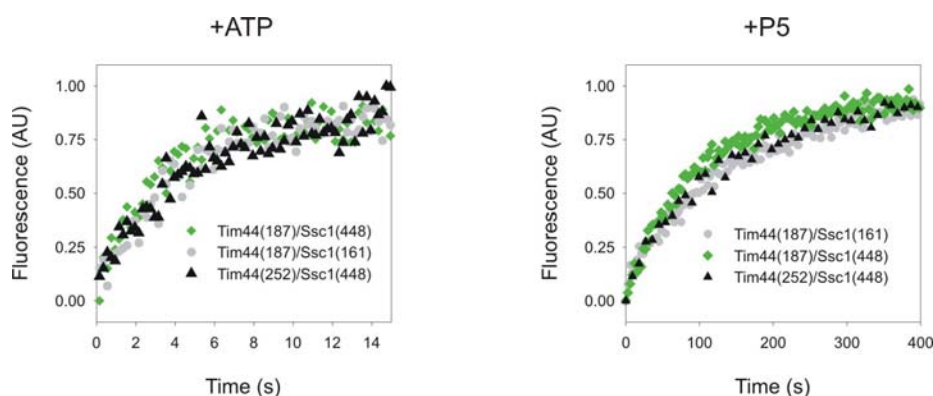


Figure 3.37: ATP or substrate induced dissociation of Tim44:Ssc1 is monophasic. Left and right panel: The dissociation of the Tim44:Ssc1 complex in presence of ATP (left panel) and P5 (right panel) was monitored by probing different distance vectors between Tim44 and Ssc1. The complexes were formed with donor labeled variants of Tim44 and acceptor labeled variants of Ssc1. The dissociation was initiated upon manually mixing either 2mM of ATP (left panel) or 6 μ M of P5 (right panel) and the recovery of donor fluorescence was obtained to follow the dissociation event. 2 μ M of Mge1 was present in buffer in order to facilitate ATP-charging of Ssc1 in subsequent step in case of ATP induced dissociation. The fluorescence recovery is normalized to compare the rate of increase in different distances.

3.2.9 Ssc1 and Tim44 share complementary binding sites on matrix targeted pre-proteins

Brownian ratchet mechanism posits that the vectorial translocation across TIM23 is driven by Ssc1 binding to substrates by preventing backsliding of pre-proteins to the cytosol (Ungermann et al., 1994). Earlier experiments have shown that a protein containing a large stretch of glutamates to which mtHsp70 cannot bind, can be imported efficiently (Okamoto et al., 2002). Stretches of negatively charged amino acids are known not to bind to Hsp70 group of chaperones and hence have a chance to slide back in the cytosol (Rudiger et al., 1997). This raises the question regarding the mechanism that prevents backsliding at non-Hsp70-interacting sequences. One possible solution might be the presence of other proteins at the TIM23 translocase that can bind transiently to these regions and prevent backsliding. Since Tim44 has been shown to be in the vicinity of preproteins in transit and interact with the unfolded polypeptides (Blom et al., 1993; Maarse et al., 1992; Rassow et al., 1994; Schneider et al., 1994), we sought to uncover if Tim44 binds to sequence specific regions within incoming preproteins. To

understand the distribution of Ssc1-and Tim44-binding site on mitochondrial matrix targeted protein, scanning of peptide array of luciferase, a bona-fide substrate of Hsp70 group of chaperones was performed. The binding specificity observed for Ssc1 was mostly similar to the reported specificities of other Hsp70 chaperones like DnaK (Gragerov and Gottesman, 1994; Gragerov et al., 1994; Rudiger et al., 1997) (Figure 3.38 A, upper panel). Surprisingly, when peptide scanning of luciferase was performed to probe for Tim44 binding (Figure 3.38 B, upper panel), it was observed that Ssc1 and Tim44 share complementary binding sites on luciferase. To probe the generality of the complementary binding specificity of Tim44 and Ssc1 peptide array scanning of two authentic mitochondrial matrix proteins, mMDH and Hsp60 (Figure 3.38 A, middle and lower panel) was performed. Near exact complementary binding sites in all these proteins indicated that Ssc1 binds to hydrophobic amino acids surrounded by positively charged residues whereas Tim44 binds to peptide sequences rich in negatively charged amino acids which do not bind to Hsp70 group of chaperones (Figure 3.38 B, middle and lower panel).

This result hinted towards the possibility that Tim44 would bind to stretches of amino acids where Ssc1 is incapable of binding, further implying that Tim44 plays a role in preventing back sliding of proteins during translocation. Notably, the binding between Tim44 and the peptides could not be detected in solution phase (data not shown), indicating that the binding affinities between Tim44 and these peptides are extremely low further supporting the previous finding that Tim44 binds to unfolded polypeptides with low affinity (Schneider et al., 1994). Physiologically, the low affinity would be consistent with transient binding of substrates to Tim44 at the TIM23 translocase channel where a high affinity binding would abrogate translocation leading to a stalled translocase.

DnaK-like binding site specificity of Ssc1 also justified the use of DnaK binding site prediction algorithm to obtain Ssc1-binding sites, on mitochondrial-matrix-targeted pre-proteins, in order to calculate the physiological rate of Ssc1 cycling at TIM23 translocase.

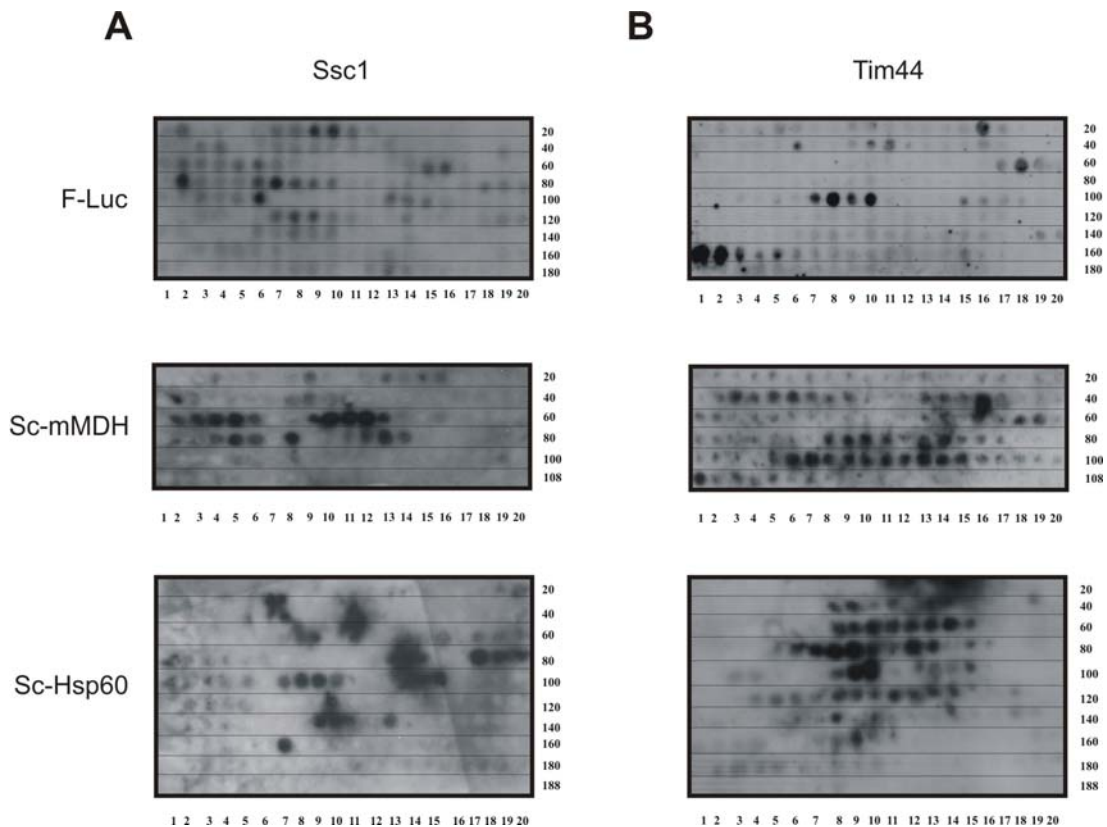


Figure 3.38: Peptide scans with purified Ssc1 and Tim44. Cellulose bound peptide scans derived from the sequences of Firefly-luciferase(top), Sc mitochondrial MDH(middle), Sc Hsp60 (bottom) were screened for binding with Ssc1(A) and Tim44(B). Last spot of each row is indicated with the number.

In summary, the *in vitro* reconstitution of Tim44:Ssc1 interaction cycle and its kinetic analysis suggested that cycling of Ssc1 on Tim44 is driven by nucleotide bound to Ssc1, rather than the substrate. It was evident that the N-terminal domain of Tim44 and PBD of Ssc1 constitute the minimal binding domains of Tim44:Ssc1 complex, as probed by pull-down experiments and FRET based binding analyses. However, in the context of full length proteins both the domains of Tim44 were found to be spatially proximal to the PBD of Ssc1 and sub-domain Ia of NBD of Ssc1. It was also evident that the dissociation of Ssc1 from Tim44 is a single-step process ruling out the possibility of Tim44-anchored conformational change of Ssc1. Additionally, peptide-array scanning of authentic mitochondrial matrix targeted proteins revealed the near exact complementarity of binding sites of Ssc1 and Tim44 on the precursors.

This result together with weak binding affinity of Tim44 to non-Hsp70 binding sites might explain how the backsliding of preproteins is prevented at the translocase channel. All the data can only be reconciled in the context of Brownian ratchet model of protein import motor.

3.3 Conformational dynamics of mtHsp70 (Ssc1) and the effects of co-chaperones and substrates on it

Different conformations of Hsp70 chaperones are evident from snapshots of the molecule in its different functional states revealing alteration of conformations as the key regulator of the chaperone allostery. Though the structural studies provided valuable insights into the end states of the chaperone in various stages of the functional chaperone cycle, information regarding the kinetics and dynamics of those events are severely lacking (Chang et al., 2008; Liu and Hendrickson, 2007; Swain et al., 2007). Moreover, even after extensive work on Hsp70s and their co-chaperones there is no unambiguous scheme that describes the chaperone cycle in terms of kinetics of binding of the co-chaperones and substrates.

3.3.1 Development of double cysteine substitution mutants of Ssc1 for fluorophore labelling

Recent findings suggest that ATP binding to Hsp70 induces docking of two domains and domain reorientation (Liu and Hendrickson, 2007; Swain et al., 2007). This has been proposed to be a key event in the conformational allostery between the NBD and PBD. Furthermore, opening and closing of the α -helical lid region have been observed in the crystal and NMR structures of different Hsp70 chaperones in the ATP and ADP-bound states respectively explaining the difference in substrate-binding-affinity in these states of the chaperones (Pellecchia et al., 2000; Stevens et al., 2003; Zhu et al., 1996). To monitor the inter-domain movements and lid movements, double cysteine substitution mutants of Ssc1 were constructed to label the protein with both donor and acceptor fluorophores.

With the double-labeled proteins semi-quantitative FRET assay was developed. To probe the inter-domain movements of Ssc1, it was stoichiometrically labeled with acceptor (Atto-647N) and donor fluorophore (Atto-532) at positions 448 and 341. The distance vector 341-448 was monitored in the construct, Ssc1 (341,448), where the position 341 is in subdomain IIa of NBD and position 448 is positioned at the base of PBD. In order to probe the evolutionary conservation of such conformational changes in the Hsp70 group of chaperones, DnaK from *E.coli* was analyzed in parallel. Before engineering cysteine substitutions in DnaK the endogenous cysteine (C15) was substituted to alanine. To study the domain movements in DnaK, positions 318 and 425 similar to the positions 341 and 448 of Ssc1 respectively, were substituted to cyteines to generate DnaK (318,425) (Figure 3.39).

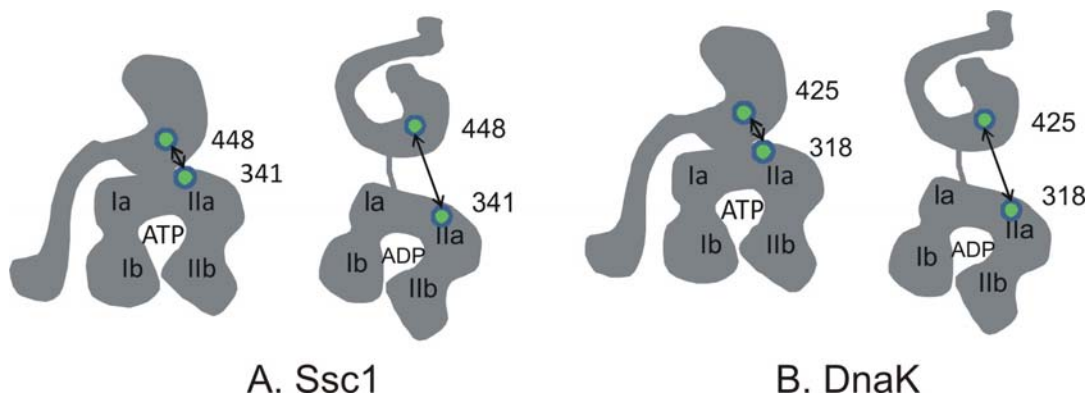


Figure 3.39: Schematic representation of Hsp70 molecules indicating the positions of engineered cyteines to monitor the inter-domain movements. Panel A. Ssc1 in both ATP (left panel) and ADP (right panel) bound forms indicating the positions of engineered cysteines to monitor the inter-domain movements. Arrows indicate the distance vectors monitored by intra-molecular FRET to follow the conformational changes. **Panel B.** Schematic representation of DnaK illustrating the corresponding positions for cysteine substitutions for monitoring the similar changes as Ssc1 is depicted.

To monitor the conformational changes in lid, the docking of lid to the peptide binding cleft was followed by monitoring the distance vector 448-590 in the construct Ssc1(448,590). The position 448 is in the base of PBD whereas the position 590 is in the α -helical lid domain. To probe for similar conformational changes in lid in DnaK, similar positions (amino acids 425 and 563) were substituted to cysteines in DnaK (Figure 3.40).

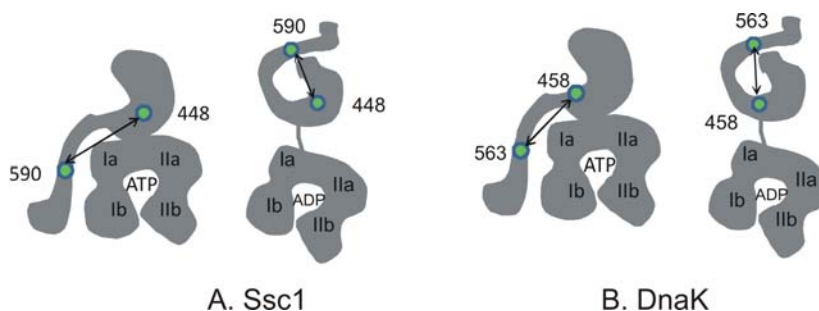


Figure 3.40: Schematic representation of Hsp70 molecules indicating the positions of engineered cysteines to monitor the movements of the α -helical lid in respect to the base of the PBD. Panel A. Ssc1 in both ATP (left panel) and ADP (right panel) bound form indicating the positions of engineered cysteines to monitor the movements in the α -helical lid in respect to the base of the PBD. Arrows indicate the distance vectors monitored by intra-molecular FRET to follow the conformational change. **Panel B.** Schematic representation of DnaK illustrating the corresponding positions for cysteine substitutions for monitoring the similar change as Ssc1 is depicted.

Ssc1 double cysteine mutants after labeling with two fluorophores retained its full functionality in terms of its ATPase activity, stimulation of its ATPase activity in presence of Mdj1 (Figure 3.41, Panel A) and its ability to bind substrate peptides (see below). All the double mutants were also checked for their *in vivo* functionality and all of them were able to support growth of yeast cells in the absence of wild type Ssc1 (Figure 3.41, Panel B).

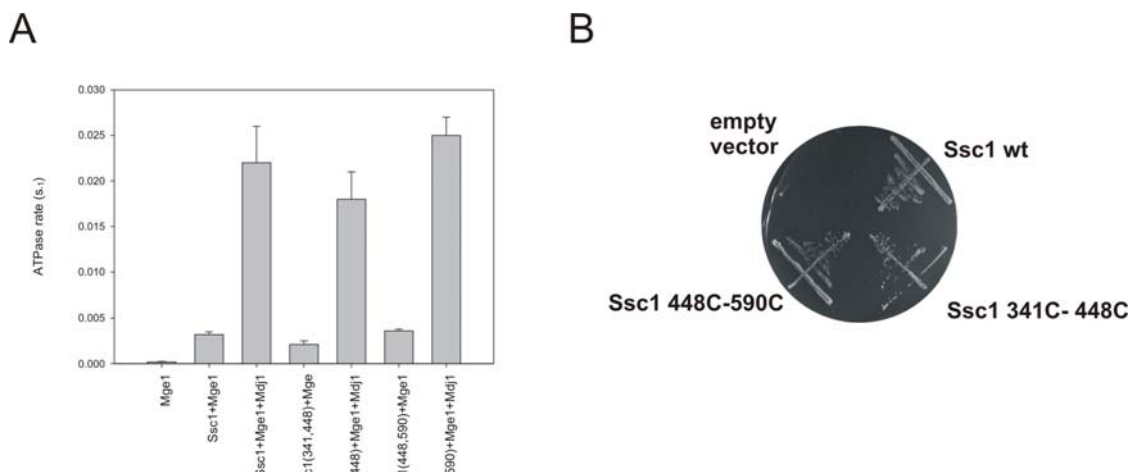


Figure 3.41: Panel A: ATP hydrolysis activity of fluorescently labelled Ssc1. Panel A: ATP hydrolysis activity of Ssc1 was checked by coupled enzymatic detection of ADP produced as described in Materials and Methods. The rate of ATP hydrolysis reported is per mole of ATP/mole of Ssc1/s. **Panel B: Double cysteine substitution mutants of Ssc1 are functional *in vivo*:** A haploid deletion strain of *Ssc1* harbouring the wild type copy of *Ssc1* on the *URA* plasmid was transformed with plasmids containing double cysteine mutants of Ssc1. *In vivo* functionality of the mutant proteins was checked by plasmid shuffling on 5-fluoroorotic acid plates. Plasmids carrying the wild type *Ssc1* or an empty plasmid were used as the positive and negative controls respectively.

3.3.2 Development of a FRET-based Ssc1 conformation sensor

Kinetic analysis of Hsp70 conformational changes in its functional chaperone cycle is an important step towards understanding the allosteric signaling in this molecular machine. Fluorescence resonance energy transfer (FRET) is a powerful technique that precisely allows for analysis of the sequence of conformational changes in real time. Towards this end, double cysteine mutants of Ssc1 were labeled with Atto-532 as the donor fluorophore and Atto-647N as the acceptor fluorophore. The ratio of acceptor to donor fluorescence after excitation of the donor fluorophore, subsequently mentioned as P_R (proximity ratio), has been used as a basis for comparing change in distance between the two positions. To obtain the P_R from spectrum measurements, donor fluorescence peak was normalized to 1 and the P_R was then read out from the acceptor peak height. An increase in P_R would correspond to a decrease in the distance between the two positions and *vice versa*. This relatively simple scheme was used instead of the more elaborate comparison of matched donor only and donor-acceptor labeled samples, as Ssc1 did not tolerate the specific double labeling steps due to its inherent instability.

Comparison of the P_R of GuHCl denatured protein and native protein showed a large decrease upon denaturation (Figure 3.42) demonstrating the validity of the approach for studying distance changes in Ssc1 and DnaK.

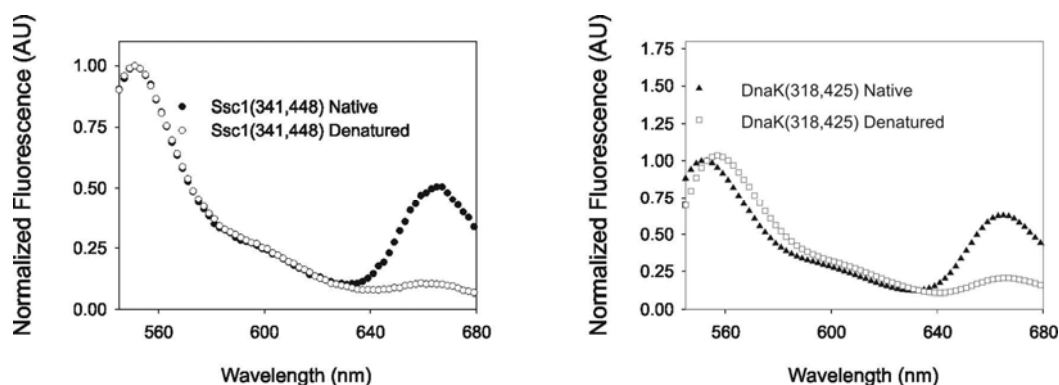


Figure 3.42: Fluorescence spectrum of double labeled native and denatured Hsp70s. Fluorescence spectra of 30nM of double labeled Ssc1 (341,448) (left panel) or DnaK (318,425) (right panel) were obtained after exciting the donor fluorophore at 530nm under native condition as well after denaturation with 6M GuHCl. Donor fluorescence was normalized to 1 to compare the Proximity ratio (P_R) of the different states as mentioned in the text.

3.3.3 Effect of nucleotides on the conformation of Ssc1 from ensemble FRET measurements

Conformational changes of Ssc1 were monitored in both the above mentioned distance vectors using the assay developed by ensemble FRET measurements.

The distance vector 341-448 showed that ATP binding led to a decrease in distance between the two domains (Figure 3.43) compared to the ADP-bound state. Similar results were obtained for DnaK (318,425) where the ADP-bound state exhibited lower P_R between the domains than the ATP-bound state. This was indeed consistent with the hypothesis that the NBD and PBD of Hsp70s, which are undocked in the presence of ADP, undergo docking in presence ATP.

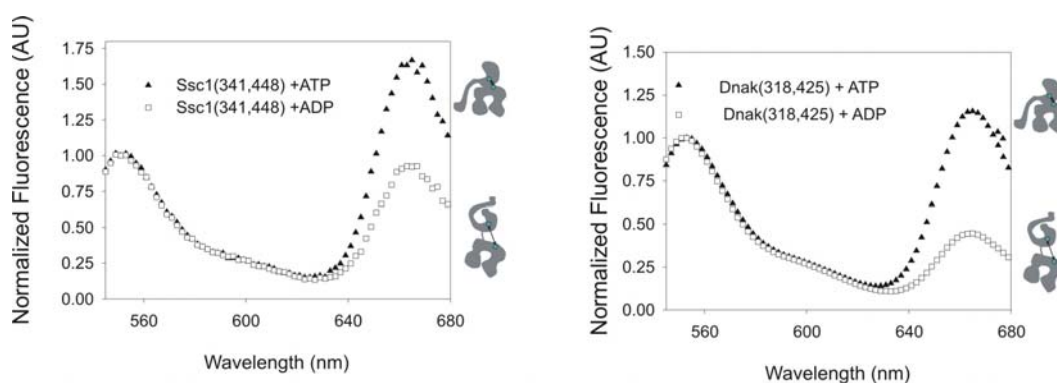


Figure 3.43: Changes in inter-domain distance of Ssc1 and DnaK as probed by intramolecular FRET experiments. Fluorescence spectrum of 30nM of double labeled Ssc1 (341,448) and DnaK (318,425) were obtained after exciting the donor fluorophore at 530nm in presence of 2mM ATP and 2mM ADP. Donor fluorescence was normalized to 1 to compare the P_R of the different nucleotide states.

To monitor the conformational changes in lid, the docking of lid to the peptide binding cleft was followed by monitoring the distance vector 448-590 in the construct Ssc1(448,590). As expected, a decrease in P_R upon ATP binding to Ssc1 indicated lid opening (Figure 3.44). In contrast, higher P_R in the ADP bound state demonstrated lid closure. Essentially the same results were obtained with the corresponding DnaK constructs.

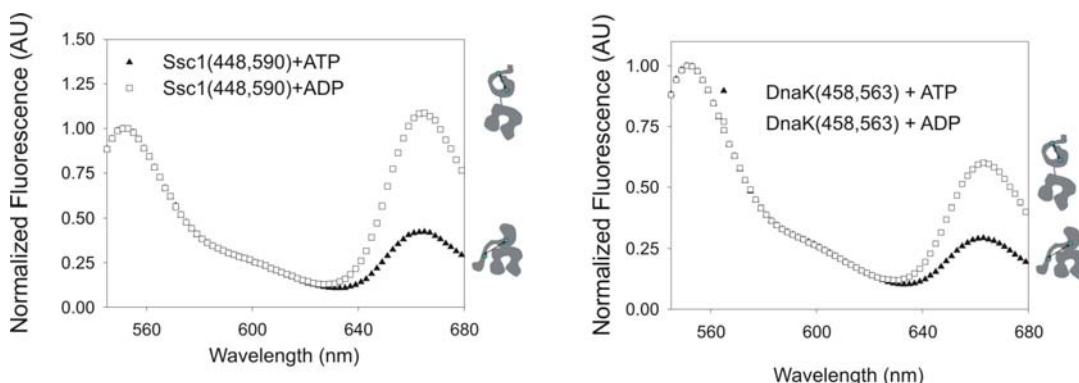


Figure 3.44: Changes in distance between the lid domain and base of PBD of Ssc1 and DnaK as probed by intra-molecular FRET experiments. Fluorescence spectrum of 30nM of double labeled Ssc1 (448,590) and DnaK (458,563) were obtained after exciting the donor fluorophore at 530nm in presence of 2mM ATP and 2mM ADP. Donor fluorescence was normalized to 1 to compare the P_R in presence of different nucleotides.

3.3.4 Effect of nucleotides on the conformation of Ssc1 from Single-molecule FRET measurements

As the ensemble measurements indicate an average of FRET-efficiencies of all the molecules being measured, changes in distance as read out from the P_R is only indicative of mean changes in distance. Single molecule FRET measurements are ideal in obtaining insights into the conformational distribution and heterogeneity. Towards elucidation of the conformational distribution, single particle FRET (SpFRET) measurements using PIE (Pulsed Interleaved Excitation) were performed (Muller et al., 2005).

For the distance vector 341-448, an unambiguous uni-modal distribution was observed upon ATP binding, suggesting majority of the molecules in the domain-docked state. Peak values of a Gaussian fit to the FRET efficiency distribution was 0.90 suggesting very compact state of majority of molecules. On the contrary, the ADP bound state was very broad and after Gaussian fitting two peaks were obtained one at 0.40 and other at 0.84 (Figure 3.45). This indicates that in the ADP-bound state the domains are flexible, populating conformations containing domain-undocked molecules as well as domain-docked molecules.

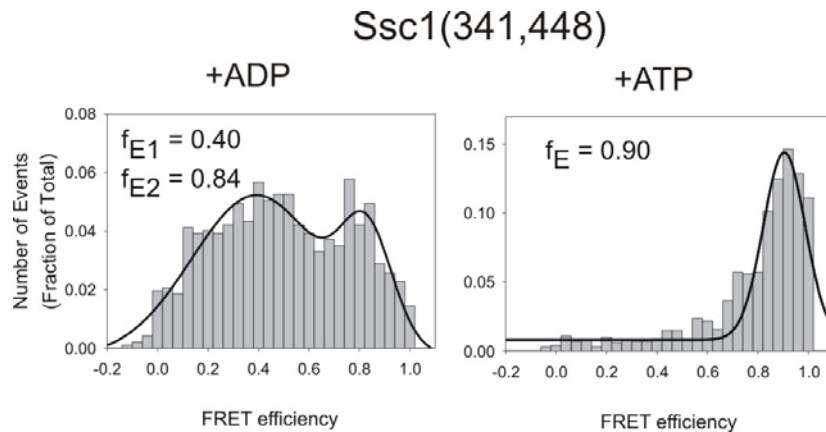


Figure 3.45: Nucleotide induced changes in inter-domain distance of Ssc1 as probed by SpFRET measurements. To obtain Single-molecule FRET measurements of double labeled Ssc1 (341,448) the protein was diluted in the appropriate buffer (as mentioned in the materials and methods) to a final concentration of 60 pM, containing either 2mM ATP or 2mM ADP. Representative histograms of two different nucleotide conditions are shown. Peak values of a Gaussian fit to the FRET efficiency distributions (f_E) are indicated.

In case of DnaK (318,425), for the distance vector 318-425, a bi-modal distribution was observed upon ATP binding. Peak values of a Gaussian fit to the FRET efficiency distribution were at 0.15 and at 0.80 which suggested a very compact state of majority of the molecules along with a small subpopulation of domain- undocked molecules. This distribution indicated some flexibility of the domains in the ATP state. On the contrary, the ADP bound state was clearly unimodal in distribution and after Gaussian fitting, a peak was obtained at 0.15 (Figure 3.46). Such a distribution is different from what was obtained for Ssc1 and suggests that the domains are fully undocked and are separated by a large distance in case of DnaK.

DnaK (318,425)

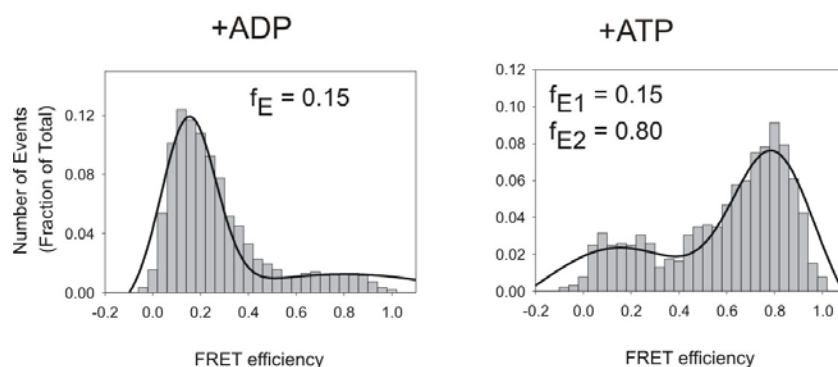


Figure 3.46: Nucleotide induced changes in inter-domain distance of DnaK as probed by SpFRET measurements. To obtain Single-molecule FRET measurements of double labeled DnaK (318,425) the protein was diluted in the appropriate buffer (as mentioned in the materials and methods) to a final concentration of 60 pM, containing either 2mM ATP or 2mM ADP. Representative histograms of two different nucleotide conditions are shown. Peak values of a Gaussian fit to the FRET efficiency distributions (f_E) are indicated.

For the distance vector 448-590 in Ssc1 (448,590) probing for the movements of the α -helical lid in respect to the base of the PBD, a unimodal distribution was observed upon ATP binding. Peak values of a Gaussian fit to the FRET efficiency distribution was 0.15 suggesting lid-open state of majority of molecules. On the contrary, the distribution for ADP bound state was very broad and it was not possible to fit the f_E distribution to Gaussian fits (Figure 3.47). The flexibility of the lid in the ADP-bound state hinted that the lid was not firmly locked on to PBD, as envisioned for canonical Hsp70s.

Ssc1(448,590)

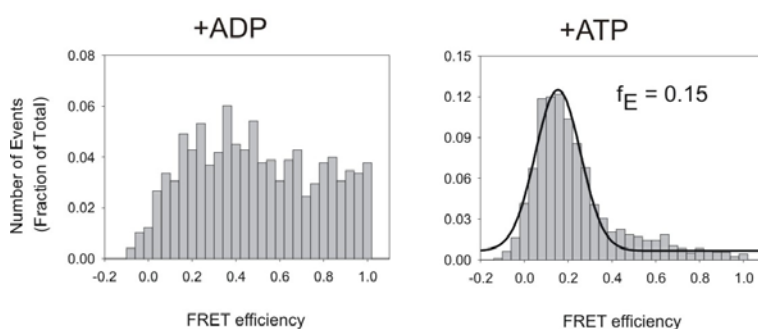


Figure 3.47: Nucleotide induced changes in distance between lid domain and base of the PBD of Ssc1 as probed by SpFRET measurements. To obtain Single-molecule FRET measurements of double labeled Ssc1 (448,590) the protein was diluted in the appropriate buffer (as mentioned in the materials and methods) to a final concentration of 60 pM, containing either 2mM ATP or 2mM ADP. Representative histograms of two different nucleotide conditions are shown. Peak values of a Gaussian fit to the FRET efficiency distributions (f_E) are indicated.

Similar observations were made for the 425-563 in DnaK (425,563). A uni-modal distribution was observed upon ATP binding. Peak values of a Gaussian fit to the FRET efficiency distribution was 0.20. Like Ssc1, the distribution of f_E for the ADP bound state was very broad and could be fit to bimodal Gaussian distribution with one peak at 0.16 and another at 0.58 suggesting large flexibility of the lid in the ADP-bound state (Figure 3.48).

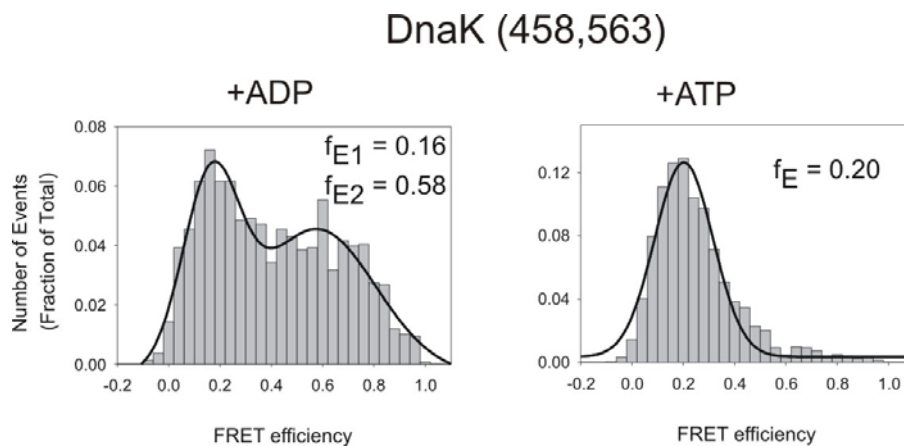


Figure 3.48: Nucleotide induced changes in distance between lid domain and base of the PBD of DnaK as probed by SpFRET measurements. To obtain Single-molecule FRET measurements of double labeled DnaK (458,563) the protein was diluted in the appropriate buffer (as mentioned in the materials and methods) to a final concentration of 60 pM, containing either 2mM ATP or 2mM ADP. Representative histograms of two different nucleotide conditions are shown. Peak values of a Gaussian fit to the FRET efficiency distributions (f_E) are indicated.

Thus, with the ensemble and SpFRET analyses, the nucleotide dependent changes in conformations of Ssc1 and its bacterial homologue DnaK could be probed. Using the same assay developed, we went further to look for effects of J domain co-chaperone and substrate on the conformations of Ssc1 in respect to its functional chaperone cycle. Simultaneously, the same experiments were performed with DnaK to compare similarities in two systems.

3.3.5 Effect of J-domain co-chaperone and peptide substrate on the conformation of Ssc1

3.3.5.1 Binding of substrate and Mdj1 to Ssc1

The domain-docked lid-open state of Hsp70 formed after ATP binding is thought to act as the substrate acceptor state *in vivo*. Since Hsp70s have high association and dissociation rates for substrate in the ATP-bound state, binding of substrates to Hsp70s in its ATP bound state requires the presence of J-domain co-chaperones that can assist efficient capture of the substrates by the chaperone through their ability to stimulate ATP hydrolysis of Hsp70s (Karzai and McMacken, 1996; Laufen et al., 1999; Liberek et al., 1991; Wittung-Stafshede et al., 2003). To monitor the binding of substrate-peptide P5 to Ssc1, in context of nucleotide- and co-chaperone-bound states of Ssc1, we developed a FRET based binding assay. Binding of substrate peptide P5 to Ssc1 was monitored by the quenching of fluorescence of fluorescein labeled P5 (P5-fl) in the presence of acceptor (Atto-647N) labeled Ssc1 [Ssc1 (448-A)] (Figure 3.49, panel A). To simplify the interpretation of the experiments with Ssc1, which are inherently convoluted with residual nucleotide-exchange-induced cycling, all the measurements with P5 and Mdj1 were monitored under single turnover conditions, unless mentioned otherwise. To design single-turnover ATP-hydrolysis based binding experiments, Ssc1 binding to ATP was followed by the quenching of excess ATP by the addition of glucose and hexokinase. Subsequently P5 or Mdj1 or Mdj1/P5 was added to monitor the affect of J-domain co-chaperone and substrate. As observed for other Hsp70s, P5-fl was able to bind Ssc1/ATP significantly faster in presence of Mdj1 confirming that the J-domain co-chaperone assists substrate binding to Ssc1/ATP (Figure 3.49, panel A). Binding rate of substrate to Ssc1/ATP was identical to the ATP-hydrolysis rate of Ssc1 in presence of the substrate (Figure 3.49, panel B) suggesting that the substrate capture is rate determined by the ATP-hydrolysis rate of Ssc1. This is further supported by the fact that the accelerated binding of substrate to Ssc1/ATP in presence of Mdj1 is also identical to the ATP-hydrolysis rate of Ssc1 in presence of Mdj1 (Figure 3.49, panel B). Substrate association with Ssc1 can be formulated as a two step reaction (Figure 3.49, panel C) with ATP-hydrolysis being the rate-determining step for substrate capture.

Since, dissociation rate of P5 from Ssc1/P5/ADP is extremely slow (Figure 3.49, panel D), substrate stays locked with Ssc1 once this complex is formed. To show that a similar complex is formed even in presence of Mdj1, we obtained the off-rate of P5 from the complex formed in presence of Mdj1 (Figure 3.49, panel D). Identical off-rates of P5 from Ssc1-ADP and from the Ssc1-ADP-P5 complex formed in presence of Mdj1 indicates that Mdj1 does not alter the conformational properties of Ssc1 to induce substrate locking but promotes substrate association with Ssc1 through the stimulation of ATPase activity of Ssc1.

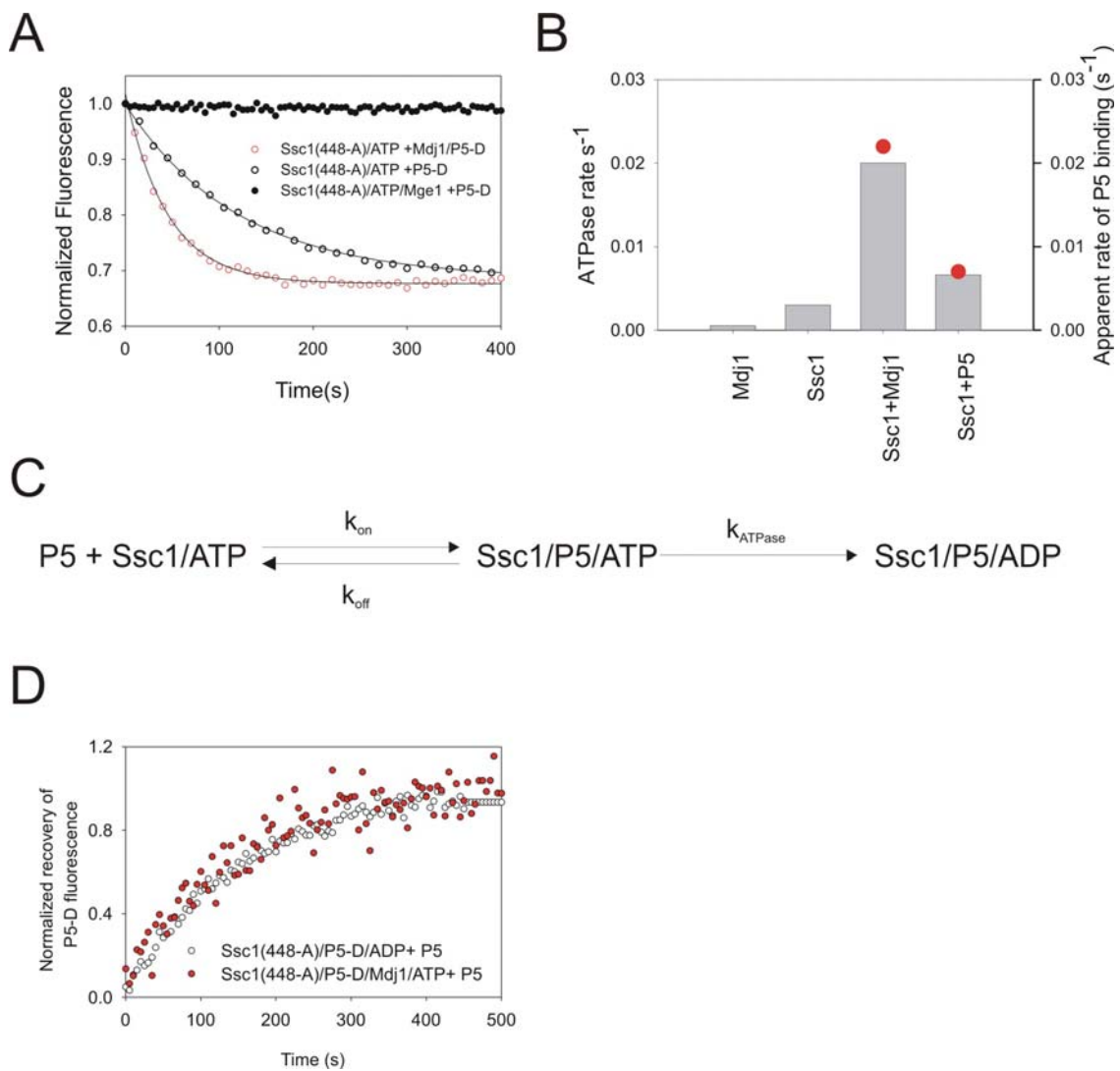


Figure 3.49: Substrate binding to Ssc1 is facilitated by ATP-hydrolysis mediated capture. Panel A: Ssc1(448-A)(500nM) was briefly incubated with ATP(2mM) followed by the addition of hexokinase(2U)/glucose(20mM), to quench excess ATP. Subsequently, either 20nM of P5-D(black open circles) or P5-D(20nM)/Mdj1(500nM)(red open circles) was added to observe the binding of P5-D as monitored by the quenching of donor fluorescence of P5-D. Ssc1-A(500nM) was incubated with Mge1(500nM) and ATP(2mM), followed by the addition of P5-D(20nM) where no binding was observed due to continuous cycling of Ssc1 to the ATP-bound state. **Panel B:** Steady state ATP hydrolysis rate was measured with a coupled enzymatic detection of ADP produced, as described in materials and methods. The rate of ATP hydrolysis reported is mole of ATP hydrolysed per mole of Ssc1 per second. All the conditions shown had 2 μ M of Mge1 in the buffer to support nucleotide exchange and hence steady-state ATP hydrolysis by Ssc1. The red circles refer to the right axis which is the apparent rate of P5 binding to Ssc1 but under conditions of single turnover ATP hydrolysis, as observed in panel A. **Panel C:** Schematic of Ssc1 binding to P5 to indicate the k_{ATPase} , the ATP-hydrolysis rate if Ssc1, dictates the final binding rate in case of fast on- (k_{on}) and off-rates(k_{off}) of substrate binding to Ssc1. **Panel D:** Dissociation of P5-D from preformed Ssc1(448-A)(500nM)/P5-D(20nM)/ADP(2mM) or Ssc1(448-A)(500nM)/P5-D(20nM)/Mdj1(1 μ M)/ATP, formed as described in panel A, was monitored by the recovery of P5-D after addition of unlabelled P5.

J-domain co-chaperones and substrates have been proposed to induce conformational changes in Hsp70s that affect the allosteric communication between the two domains of Hsp70s. To probe for the changes in interdomain distance in Ssc1 resulting from interactions with the J-cochaperone Mdj1 and substrate (P5 peptide), ensemble and single molecule FRET measurements were performed. The binding of P5 and Mdj1 to Ssc1/ATP led to the formation of a domain-undocked state in Ssc1 (Figure 3.50) whereas Mdj1 alone was insufficient to effect a similar change in conformation. In case of Mdj1, a heterogeneous bimodal distribution could be observed. This distribution was similar to the distributions obtained for Ssc1 in its ADP-bound state. This result indicated that Mdj1 alone is insufficient to change the interdomain distance of Ssc1/ATP but causes a change in the conformation due to the formation of Ssc1/ADP. The inability of Mdj1 to modulate the conformational change could be due to the inability of Mdj1 to form a stable complex with Ssc1/ATP after the hydrolysis. However, the presence of substrate led to a change in conformation which was not brought about by Mdj1 or ADP, indicating that substrates play an active role in modulating interdomain communication in Ssc1.

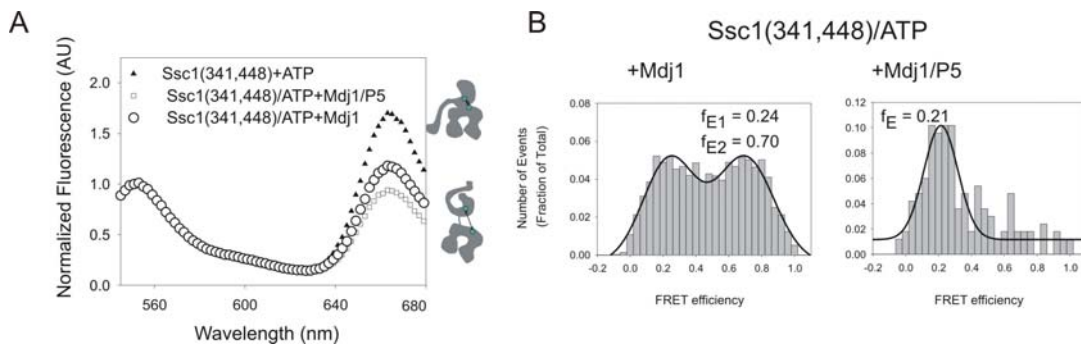


Figure 3.50: Effect of J-protein and substrate peptide on the inter-domain distance of Ssc1 as probed by ensemble and SpFRET measurements. Panel A: Fluorescence spectra of 30nM of double labeled Ssc1 (341,448) was obtained in presence of ATP (2mM), ATP (2mM)/Mdj1(5 μ M) or ATP(2mM)/Mdj1(5 μ M)/P5(50 μ M) after exciting the donor fluorophore. In all the cases, except the ATP-bound state, in order to maintain single turnover conditions, prior to addition of Mdj1 or Mdj1/P5, excess ATP was quenched by hexokinase (2U)/glucose(20mM) after briefly incubating Ssc1 with 2mM ATP. **Panel B:** SpFRET analysis of double labeled Ssc1(341,448) was performed after the protein was diluted in the appropriate buffer, to a final concentration of 60pM, containing either ATP(2mM)/Mdj1(5 μ M) (left panel) or ATP(2mM)/Mdj1(5 μ M)/P5(50 μ M) (right panel). In all the cases, except the ATP-bound state, in order to maintain single turnover conditions, prior to addition of Mdj1 or Mdj1/P5, excess ATP was quenched by hexokinase(2U)/glucose(20mM) after briefly incubating Ssc1 with 2mM ATP.

The conformational modulation of Ssc1 upon substrate binding was further observed in terms of lid-closure. Similar to domain-undocking, the complete lid-closure was induced only in the presence of Mdj1 and P5 whereas Mdj1 alone could not induce this state. This is also consistent with the observation that Ssc1-ADP and Ssc1/ADP/Mdj1 also has very similar conformational distributions underlining the inability of Mdj1 to affect large allosteric changes in terms of inter-domain communication or lid-movement. The two major modes of conformational changes in Ssc1, the domain-docking and lid-closure, were majorly affected in the presence of substrates indicating the active role of substrates in changing the conformations of Ssc1 (Figure 3.51).

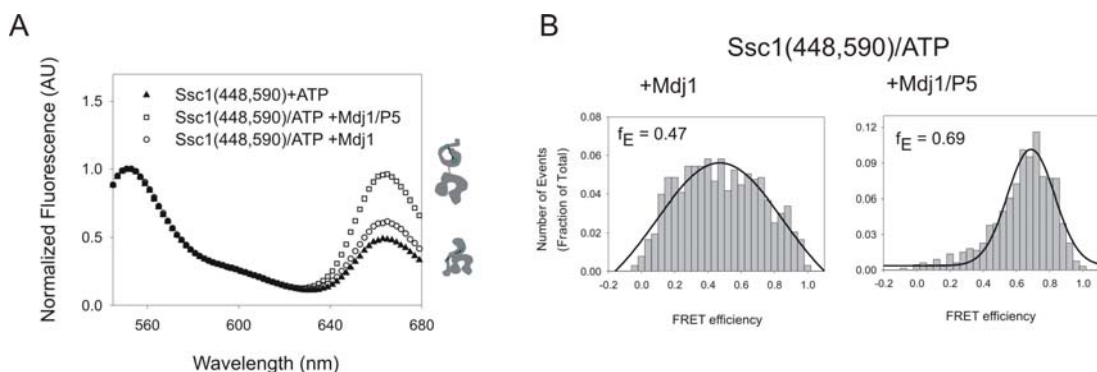


Figure 3.51: Effect of J-protein and substrate peptide on the distance between lid domain and base of the PBD of Ssc1 as probed by ensemble and SpFRET measurements. Panel A: Fluorescence spectra of 30nM of double labeled Ssc1 (448,590) was obtained in presence of ATP(2mM), ATP/Mdj1(5 μ M) or ATP(2mM)/Mdj1(5 μ M)/P5(50 μ M) after exciting the donor fluorophore. In all the cases, except the ATP-bound state, in order to maintain single turnover conditions, prior to addition of Mdj1 or Mdj1/P5, excess ATP was quenched by hexokinase(2U)/glucose(20mM) after briefly incubating Ssc1 with 2mM ATP. **Panel B:** SpFRET analysis of double labeled Ssc1(448,590) was performed after the protein was diluted in the appropriate buffer, to a final concentration of 60pM, containing either ATP(2mM)/Mdj1(5 μ M) (left panel) or ATP(2mM)/Mdj1(5 μ M)/P5(50 μ M) (right panel). In all the cases, except the ATP-bound state, in order to maintain single turnover conditions, prior to addition of Mdj1 or Mdj1/P5, excess ATP was quenched by hexokinase(2U)/glucose(20mM) after briefly incubating Ssc1 with 2mM ATP.

Since Ssc1-ADP state did not differ from the state of Ssc1 when Mdj1 was added to Ssc1/ATP there remained a possibility that Mdj1 dissociates from Ssc1 after it has stimulated the ATP hydrolysis of Ssc1. The step of dissociation of J-domain co-chaperone from Hsp70s in context of the chaperone cycle is not well defined so far and there have been propositions stating that J-domain proteins leave Hsp70s upon completion of ATP hydrolysis by Hsp70s. To investigate whether Mdj1 remains associated with Ssc1 after ATP hydrolysis and more generally to monitor the dynamics of binding and release of J-protein in context of the Hsp70 chaperone cycle, we developed a FRET based assay to probe Mdj1 binding to Ssc1. Towards this end, Mdj1 was labeled with cysteine specific Alexa-488 maleimide (Mdj1-D) and the functionality of this molecule was checked by its ability to induce hydrolysis of Ssc1 (Figure 3.52) to the same extent as that of the unlabeled protein.

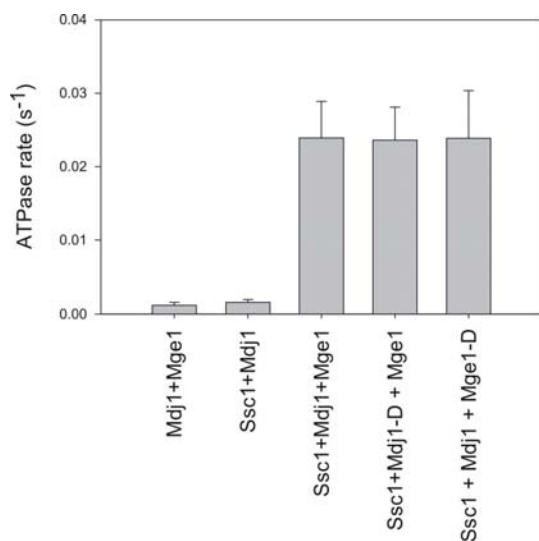


Figure 3.52: Fluorescently labeled co-chaperones are functionally active in inducing the ATPase activity of Ssc1. ATP hydrolysis activity of Ssc1 was checked by coupled enzymatic detection of ADP produced as described in Materials and Methods with the fluorescently labeled Mdj1(Mdj1-D) and Mge1(Mge1-D). The rate of ATP hydrolysis reported is per mole of ATP/mole of Ssc1/s. In all the cases the concentrations of Ssc1, Mdj1(or Mdj1-D), Mge1 (or Mge1-D) were 500nM, 500nM and 1 μ M, respectively.

Binding of Mdj1-D to acceptor labeled Ssc1 [Ssc1(448-A)] could be followed by the quenching of donor fluorescence on Mdj1 (Figure 3.53, panel A). In terms of association rate, Mdj1 only weakly bound to Ssc1-ADP (Figure 3.53, panel A) consistent with previous observations (Mayer et al., 1999), indicating that Mdj1 would preferentially bind to Ssc1-ATP complex over Ssc1-ADP complex. Ssc1(448-A)/P5/Mdj1-D could be kinetically populated in the presence of ATP, though Mdj1 subsequently dissociated from the complex with a rate of $8 \times 10^{-3} \text{ s}^{-1}$ (Figure 3.53, panel B). Importantly, the spontaneous dissociation rate of Mdj1 from Ssc1/P5/Mdj1 complex is ~ 7 fold slower than the chaperone cycle of Ssc1 in presence of Mdj1, as observed by steady state ATP-hydrolysis rate. Hence, in context of the functional Ssc1 cycle, the spontaneous dissociation of Mdj1 from the substrate captured complex of Ssc1 would not support the chaperone cycle. Notably, when Ssc1(448-A)/Mdj1-D complex was formed in presence of ATP but in absence of substrate, Mdj1 dissociation from the complex was slower by a factor of ~ 2 , indicating that substrates also modulate the interaction between the J-domain co-chaperone and Hsp70. Hence the single molecule distributions obtained with Mdj1 is a result of the conformation of Ssc1 solely affected by ATP-hydrolysis without the presence of any bound Mdj1. Since single molecule experiments lack the time resolution needed to look at the Mdj1-bound conformation of Ssc1, we performed ensemble kinetic measurements to monitor the change in domain (Figure 3.53, panel C) and lid

conformation (Figure 3.53, panel D). It was observed that Mdj1 binding to Ssc1/ATP led a rapid undocking of the domains and closure of the lid which was similar in magnitude to the change observed with Mdj1 and P5 together. Subsequent to this, the domains docked and the lids opened up with a rate of $2 \times 10^{-1} \text{s}^{-1}$, which is slower than the rate of Mdj1 dissociation from Ssc1 in presence of ATP. This indicated that though Mdj1 is able to affect the same conformational change on Ssc1 like P5, it cannot remain stably associated with Ssc1 upon ATP hydrolysis and hence dissociates from the complex allowing Ssc1 to relax back to the ADP-bound conformation. Since the excess ATP in these reactions was quenched by glucose/hexokinase, possibility of residual cycling by replacement of ADP with ATP on Ssc1 was abrogated. Hence, these experiments are analogous to single turnover hydrolysis experiments and under these conditions Mdj1 dissociates from Ssc1 after a single round of ATP hydrolysis.

The kinetic stability of Ssc1/P5/Mdj1 complex suggests that in the context of Ssc1 cycling, Mdj1 does not leave Ssc1 after ATP hydrolysis and forms an authentic substrate-captured complex with Ssc1. This opens up the possibility that J-domain release from Ssc1 is modulated at the next step of the chaperone cycle, the binding of Mge1 and the nucleotide exchange.

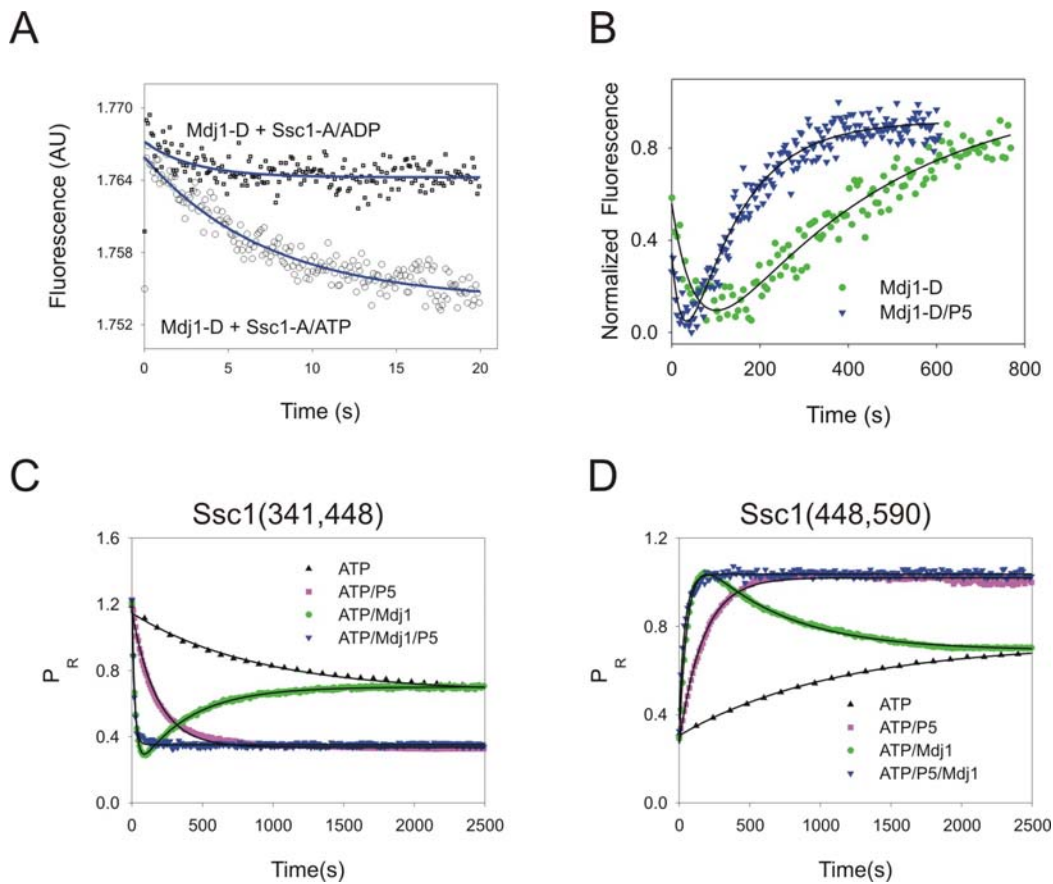


Figure 3.53: Association-dissociation kinetics of Mdj1 and kinetics of conformational changes by Mdj1 or Mdj1/P5 in context of Ssc1 chaperone cycle. Panel A: Binding kinetics of Mdj1 was followed by the quenching of donor fluorescence of donor fluorophore-labelled (Alexa 488-maleimide) Mdj1(Mdj1-D after 1:1 mixing of 200nM Mdj1-D with 500nM acceptor labeled (Atto 647N-maleimide) Ssc1(Ssc1-A), Ssc1(448-A)/ATP or Ssc1(448-A)/ADP in a stopped flow mixing device. **Panel B:** To monitor of the off rate of Mdj1 from the Ssc1/P5/Mdj1 or Ssc1/Mdj1 complex the binding kinetics of Mdj1-D to Ssc1-A/ATP was followed upon manual mixing of 200nM Mdj1 with 500nM of Ssc1-A/ATP (green curve). To observe the dissociation of Mdj1 in presence of substrate 200nM Mdj1 and 50 μ M P5 were simultaneously mixed with 500nM of Ssc1-A/ATP (blue curve). Since Mdj1-D does not rebind to Ssc1-ADP formed upon ATP hydrolysis, the off-rate could be observed even in absence of added unlabeled Mdj1. **Panel C:** The kinetics of domain undocking of double labeled Ssc1(341,448) was followed by monitoring the change in P_R . Single turnover ATP hydrolysis condition was established by charging Ssc1(100nM) with ATP(1mM) in presence of Mge1(1 μ M). Immediately after the addition of Mge1, excess ATP was quenched with Hexokinase(2U)/Glucose(10mM). The change in P_R was then monitored as such or after addition of Mdj1(4 μ M), P5(50 μ M) or simultaneous addition of both Mdj1 and P5. **Panel D:** The kinetics of lid-closing in double labeled Ssc1(448,590) was followed by monitoring the change in P_R analogous to panel C.

3.3.5.2 Binding of Mge1 to the substrate captured complex of Ssc1

Since exchange factors have been proposed to lead to release of substrates resulting in the start of a new Hsp70 cycle, we sought to uncover if an ordered series of events in terms of conformational changes are initiated upon Mge1 binding. Mge1 binding to Ssc1 was monitored using a FRET based assay. Mge1 was labeled at the N-terminus with Alexa-488 (Mge1-D) and its ability to support steady-state ATP hydrolysis rate of Ssc1 was found to be identical to that of wild-type Mge1 indicating no perturbation of Mge1 function upon fluorophore labeling (Figure 3.52). Quenching of donor fluorescence of Mge1-D was monitored to observe the binding of Mge1-D to the acceptor labeled Ssc1 [Ssc1(448-A)] in Ssc1(448-A)/P5/Mdj1/ADP.Pi complex (Figure 3.54, Panel A). This was possible as the rate of binding of Mge1, at the concentration used, was much faster than the dissociation of Mdj1 from the Ssc1(448-A)/P5/Mdj1/ADP.Pi complex. There was a stable interaction indicating that Mge1 stably associates with the substrate-captured complex of Ssc1 in absence of excess ATP.

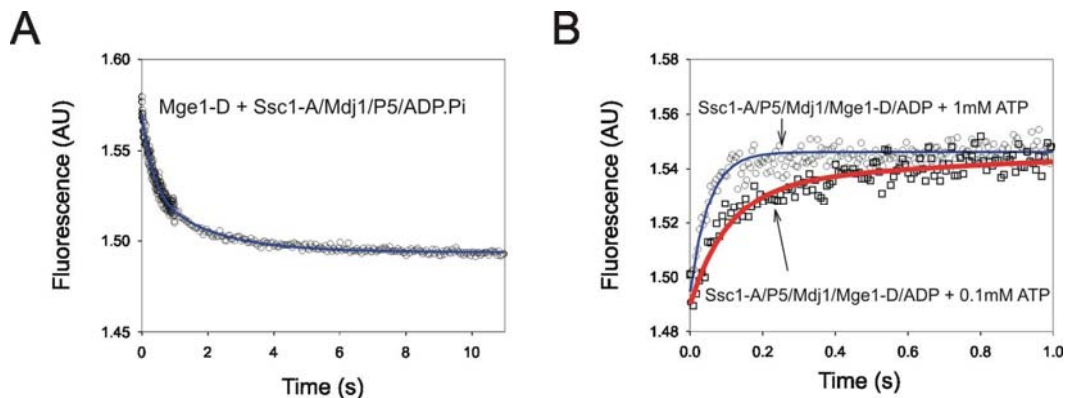


Figure 3.54: Association and dissociation kinetics of Mge1 in the functional cycle of Ssc1. **Panel A:** Decrease in fluorescence of Mge1-D is followed after a 1:1 mixing of 200nM Mge1-D with 500nM of Ssc1(448-A)/ADP in a stopped flow mixing device. **Panel B:** Increase in fluorescence of Mge1-D is followed after 1:1 mixing of 100nm preformed complex of Ssc1(448-A)/P5/Mdj1/Mge1-D/ADP with either 1mM or 100 μ M of ATP in a stopped flow device.

In presence of ATP, the Ssc1/P5/Mdj1/Mge1/ADP complex dissociates rapidly. The rate of dissociation of Mge1 was followed by the recovery of donor fluorescence of Mge1-D upon dissociation from Ssc1(448-A)/P5/Mdj1/Mge1-D/ADP complex (Figure 3.54, Panel

B) in presence of ATP and excess of unlabelled Mge1. It was observed that in presence of 1mM ATP, Mge1 dissociated from the complex rapidly ($t_{1/2} \sim 35\text{ms}$), the rate being dependent on ATP concentration, indicating that the dissociation closely follows the association of ATP with Ssc1(448-A)/P5/Mdj1/Mge1-D/ADP complex. To obtain insight into the order of release of substrate and Mdj1 from Ssc1 in context of this cycle, we investigated the dissociation rate of Mdj1 and P5 separately using the corresponding labeled protein/peptide to obtain the substrate captured complex with Ssc1. The dissociation of Mdj1-D (Figure 3.55, blue curve) or P5-fl (Figure 3.55, red curve) from Ssc1(448-A)/P5/Mdj1-D/Mge1/ADP or Ssc1(448-A)/P5-fl/Mdj1/Mge1/ADP respectively, was followed by the recovery of the respective donor fluorescences of either

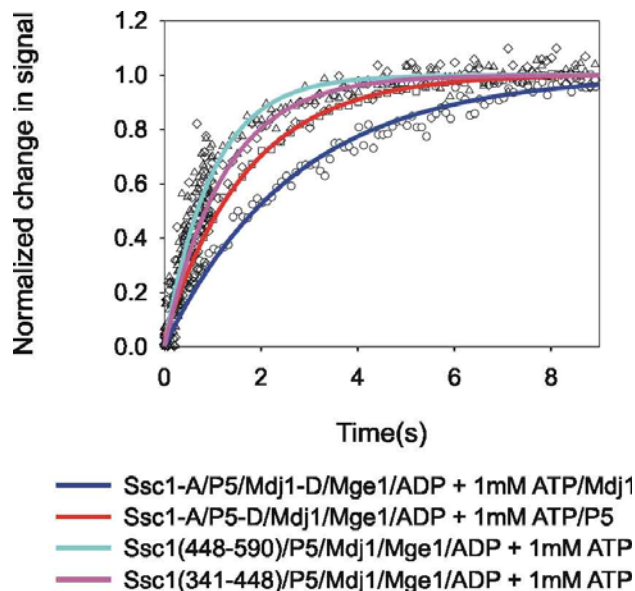


Figure 3.55: Kinetics of Conformational changes and dissociation of Mdj1 and P5 during the dissociation of Ssc1/ADP/Mdj1/P5/Mge1 complex in the functional cycle of Ssc1. The conformational changes are measured as proximity ratios and the dissociation of Mdj1 and P5 are measured as recovery of donor fluorescence of donor labeled Mdj1 or P5 respectively. To provide visual comparison of the different rates, normalized changes in signals for all of them are plotted. Change in fluorescence of Mdj1-D is followed after 1:1 mixing of 100nM of preformed Ssc1(448-A)/Mdj1-D/P5/Mge1/ADP with 2mM ATP and 1 μ M Mdj1 in a stopped flow mixing device(Blue curve). Change in fluorescence of P5-fl is followed after 1:1 mixing of 100nM of preformed Ssc1(448-A)/Mdj1/P5-fl/Mge1/ADP with 2mMATP and 5 μ M P5 in a stopped flow mixing device(Red curve). Change in the P_R monitored along the distance vector 341-448 is followed after a 1:1 mixing of 100nM preformed Ssc1 (341,448)/Mdj1/P5/Mge1/ADP with 2mM of ATP in a stopped flow mixing device(Pink curve). Change in the P_R monitored along the distance vector 448-590 is followed after a 1:1 mixing of 100nm preformed Ssc1 (448,590)/Mdj1/P5/Mge1/ADP with 2mM of ATP in a stopped flow mixing device (Cyan curve).

Mdj1-D or P5-fl. It was observed that the rate of dissociation of P5 from the complex ($t_{1/2} \sim 1.2$ s) was slightly faster than the rate of dissociation of Mdj1 ($t_{1/2} \sim 2$ s) indicating that the substrate leaves the complex followed by the dissociation of the J-domain co-chaperone. Both the rates are significantly slower than the rate of dissociation of Mge1 ($t_{1/2} \sim 35$ ms) from the complex suggesting the ordered release to exchange factor followed by the substrate and J-domain protein from the complex.

Since the semi-quantitative measure of intra-molecular FRET efficiency for Ssc1 provided analogous results as the SpFRET measurements, we used P_R to obtain the kinetics of domain-docking and lid-opening during the dissociation of the substrate-captured complex of Ssc1. To obtain the rate of domain-docking and lid-opening, the complex Ssc1/P5/Mdj1/Mge1/ADP was formed with double labeled Ssc1 (341,448) and Ssc1(448,590) respectively, and dissociation was initiated with ATP. Time dependent changes in P_R were obtained on a stopped-flow apparatus to obtain the rates of domain-docking and lid-opening. The rates of domain-docking (Figure 3.55, pink curve) and lid-opening (Figure 3.55, cyan curve) during this process were near simultaneous ($t_{1/2} \sim 700$ ms) and preceded the dissociation of P5 or Mdj1 indicating that domain docking and lid-opening leads to the dissociation of Mdj1 and P5 from Ssc1. The rate was significantly slower than the dissociation rate of Mge1 suggesting that Mge1 dissociation upon ATP binding precedes all the other changes that restart the cycle.

Here, with the aid of FRET based conformational analysis and binding studies we obtained a more complete picture of the Ssc1 chaperone cycle. From the conformational analysis of Ssc1 it is also evident that conformational transitions in Ssc1 are dually regulated by the nucleotide and substrate. Notably, the timing of the various events, in terms of conformational changes on Ssc1 and binding of co-chaperones, could be resolved in context of the chaperone cycle.

4 Discussion

4.1 Characterization of Pam17 and Tim21, the non-essential components of the TIM23 complex

Extensive research in the field of protein translocation into mitochondria, during the last 15 years has advanced our knowledge about the subject considerably. Especially, after the availability of the complete genome sequence of yeast (*S. cerevisiae*), many new components of the different translocases have been discovered within a very short span of time. In recent years many essential as well as non-essential components of the TIM23 complex of mitochondria have been discovered. These discoveries have furthered our knowledge about the mode of function of the TIM23 complex.

The original idea behind the present work was to reconstitute the events of the TIM23 translocase using the purified components. *In vitro* Reconstitution of the whole translocase is necessary to understand the detailed mechanism of action. The reconstitution is experimentally difficult because of unavailability of purified membrane components and plausible missing components of the translocase. As the principal components of the import motor Tim44 and Ssc1 could be purified recombinantly in functional forms, we started the reconstitution of the events of the import motor. Recently, Pam17 was identified as a component of the import motor of the TIM23 translocase (van der Laan et al., 2005). Before initiating the reconstitution of the import motor, Pam17 was characterized in detail. For that purpose, the association of Pam17 and its possible role in the translocase was studied systematically. Along with Pam17, the role of another nonessential component Tim21 was studied, in parallel.

Different experiments performed in the present work, showed that Pam17 is associated exclusively with the membrane embedded sector of the translocase. The Tim17-Tim23 core is the minimal domain of its association within the translocase. Importantly, Pam17 is not located in close vicinity of the motor part of the translocase. This is in contrast to the proposed role of Pam17 in the TIM23 translocase (van der Laan et al., 2005). In parallel, Tim21 is also mainly associated with the membrane sector of the translocase. Interestingly, in spite of the fact that both Pam17 and Tim21 were found to be associated

with the Tim17-Tim23 core of the membrane sector of the translocase, these proteins could never be co-isolated. In contrast to Pam17, a small but detectable fraction of Tim21 was coisolated with the motor component Tim16. This finding strongly argues against the proposed ‘railroad-switch model’ or ‘two translocase theory’ of TIM23 translocase (Chacinska et al., 2005). According to this model TIM23 translocase exists in two modular states in mitochondria: the first module is sorting competent and consists of Tim23, Tim17, Tim50 and Tim21 but lacks the import motor. On the contrary, for translocation into the matrix, Tim21 leaves the sorting module and the import motor joins the rest to make the matrix translocation module. This model implies Tim21 to be specifically found in a motor free form of the translocase and would therefore exclude co-purification with motor components. Furthermore, based on the ‘two translocase theory’, Pam17 was classified as a motor component because of its lack of co-isolation with Tim21 (van der Laan et al., 2005). The results presented in the current study show that indeed Tim21 and Pam17 were not co-isolated though both were associated with the membrane sector of the translocase. Furthermore, a functional interrelationship between these two nonessential components was found out. Both proteins interact with the TIM23 complex in a dynamic manner and binding of one modulates the membrane embedded part in such a manner that is not competent for binding of the other. Furthermore the results presented here show that Pam17 is needed for obtaining a conformation of the membrane sector of the translocase which is competent for efficient translocation of precursor proteins into the mitochondrial matrix (Popov-Celeketic et al., 2008a). This function of Pam17 would explain the observed defects in the translocation of matrix targeted precursors (van der Laan et al., 2005).

Taken together, the non essential components of the translocase, Pam17 and Tim21, associate with the Tim17-Tim23 core, which is the minimal domain needed for their association with the TIM23 complex. Finally, although both Pam17 and Tim21 are dispensable for cell viability, they do modulate the functionality of the translocase in an antagonistic manner.

4.2 *In vitro* reconstitution of the Tim44:Ssc1 interaction cycle

In the *in vitro* reconstitution of the events of import motor, we describe the kinetic and structural characteristics of the interaction of Tim44 and Ssc1, the key components of it. The results presented here identify the interacting domains and regions of both components. Furthermore, the findings provide insights into the dynamics of association and dissociation advancing our understanding of the translocation process. The results presented here are in agreement with the Brownian ratchet model of the import motor. Understanding the contributions of the individual domains of Tim44 and Ssc1 is critical for understanding the mechanism of proein translocation to mitochondrial matrix by the TIM23 translocase (Neupert and Brunner, 2002). Several studies have addressed this question previously, however, have led to conflicting conclusions. A study using yeast two hybrid assay and *in vitro* import of intact Ssc1 and its domains showed that Tim44 interacts with the Ssc1-NBD, yet with much lower affinity as compared to full length Ssc1 (Krimmer et al., 2000). Other results have shown that Tim44 interacts with the β -sandwich core of the PBD of Ssc1 (Moro et al., 2002). An *in vitro* analysis using purified proteins led to the conclusion that both domains of Ssc1 can interact independently with Tim44 (D'Silva et al., 2004). In the current study, for the first time, the proximities of the different domains of Tim44 and Ssc1 in the context of the full length proteins were determined using domain specific FRET efficiency (FE) measurements. Ssc1-PBD turned out to be more proximal to Tim44 than Ssc1-NBD. Experiments with isolated domains were in agreement with the results obtained with full-length proteins. Ssc1-PBD was able to interact with Tim44 with the same affinity as the full-length Ssc1, whereas Ssc1-NBD did not interact. This interaction of Tim44 with Ssc1-PBD exhibited the same substrate sensitive dissociation observed with the Tim44:Ssc1 complex, excluding necessity of Ssc1-NBD for substrate-assisted dissociation of Tim44:Ssc1. The proximity of Tim44 to Ssc1-PBD and the subdomain Ia of Ssc1-NBD suggests interaction of Tim44 with the junction of the Ssc1-NBD and Ssc1-PBD, with PBD contributing the majority of the interacting residues. Recent structural studies on Tim44-CTD suggested this domain to be the most plausible part involved in membrane binding of Tim44, in line with biochemical evidence for a lack of

Tim44-CTD in contributing to complex formation with Ssc1 (Josyula et al., 2006; Schiller et al., 2008; Slutsky-Leiderman et al., 2007). According to the results presented here, indeed isolated Tim44-CTD does not display significant binding to Ssc1, although this domain is spatially close to Ssc1 as is Tim44-NTD in the context of full length protein which indicates that Tim44-NTD is the major Ssc1-interacting domain.

Substrate induced dissociation of the Ssc1:Tim44 complex has been intuitively considered to be a key step in the cycling of Ssc1 at the translocase. However, in light of the results presented in this study, substrate induced dissociation is unlikely to be the basis of Ssc1 cycling. A two order of magnitude difference between the rates at which substrates can dissociate Ssc1 from Tim44:Ssc1 as compared to the proposed rate of Ssc1 cycling at the TIM23 translocase has been reported. Notably, Tim44 was found to bind transiently to Ssc1-ATP with a half life of 2-3s. This kinetics is consistent with the rate of Ssc1 cycling required for a physiological rate of protein translocation. The dissociation of the complex followed single-step kinetics excluding the possibility of a large conformational change of Ssc1 during the dissociation process. This is consistent with the Brownian ratchet mechanism, which does not imply large conformational changes in Ssc1, in contrast to a lever-type function in a power-stroke mechanism.

Hsp70 chaperones are known to assume in a lid-closed conformation when in the ADP-bound state, with extremely slow association rates for substrates. The ATP-bound state, though having lower affinity for substrates, is believed to be the substrate acceptor state as it has a high association rate for substrates. The higher association rate of Tim44 for Ssc1-ATP compared to that for Ssc1-ADP implies kinetic selection of Ssc1-ATP complexes. The resulting increase in local concentration of Ssc1-ATP at the translocase channel, in conjunction with ATP-bound Hsp70 as substrate acceptor *in vivo*, leads to a model in which Tim44 functions in positioning Ssc1 at the site of entrance of substrate into the matrix space, in consistence with previous proposals (Schneider et al., 1994; Ungermann et al., 1994). Similar mechanism of kinetic selection associated with transient interaction may have evolved for other Hsp70s, associated with protein translocation systems such as present in the ER and chloroplasts.

Binding of substrates to Ssc1 at the translocase was proposed to be the trigger of Brownian ratchet mediated translocation by TIM23. The ability of Tim44 to bind with low affinity to sequences of precursor proteins which are not recognized by Hsp70-binding described here may assist in preventing retrograde movement.

Taken together, this study gave new insights into the domain contribution of Tim44 and Ssc1 in Tim44:Ssc1 complex formation in the context of full-length proteins. Furthermore, kinetic analyses of association and dissociation events of Tim44:Ssc1 indicated that the interaction is a transient one where Tim44 mainly localizes the substrate-acceptor forms of Ssc1 near the translocase channel. The one-step dissociation of Ssc1 from Tim44:Ssc1 and sharing of complementary substrate specificity between Tim44 and Ssc1 were in agreement with the Brownian ratchet mediated protein translocation across the TIM23 translocase.

4.3 The chaperone cycle of Ssc1 in the mitochondrial matrix

The complete chaperone cycle of the prototypical Hsp70 chaperone, DnaK, has been worked on for over a decade and controversies still exist as to the order of events in the functional chaperone cycle (Genevaux et al., 2007; Swain et al., 2007). Armed with a multitude of conformational sensors positioned on the mitochondrial Hsp70, Ssc1, we were able to monitor the principal modes of conformational changes of Ssc1 in real time and also elucidate the order of events that lead to a productive chaperone cycle.

ATP-bound state is known to be the substrate acceptor state of Hsp70s with low affinity but high exchange rate for substrate proteins (Wittung-Stafshede et al., 2003; Zhu et al., 1996). In this work we were able to present convincing evidence that Ssc1, a bona-fide member of the Hsp70 group of chaperones, exist in a domain docked and lid open state in the ATP-bound form as hypothesized from numerous biochemical and biophysical evidences (Schmid et al., 1994; Swain et al., 2007; Zhu et al., 1996) or from the crystal structure of Hsc70 or Hsp110 (Jiang et al., 2005; Liu and Hendrickson, 2007), an Hsp70 homolog. This form is extremely homogeneous without any evidence of heterogeneity in the distances as probed by single-molecule fluorescence spectroscopy. On the contrary,

the ADP bound form was found to be more heterogenous in respect to the interdomain distance and distance of lid domain to the base of the PBD.

Substrate was found to efficiently bind to Ssc1 in the presence of its J-domain co-chaperone Mdj1 reconfirming the previous reports on the essentiality of J-domain proteins in assisting substrate binding (Karzai and McMacken, 1996; Laufen et al., 1999; Liberek et al., 1991; Wittung-Stafshede et al., 2003). The binding of the substrate peptide, P5, to Ssc1 in presence of Mdj1 led to the formation of a lid-closed and domain undocked structure. Binding of Mdj1 to Ssc1-ATP complex led to the transient formation of lid-closed, domain-undocked conformation, followed by the release of Mdj1 to form a heterogeneous population of Ssc1 molecules which was extremely similar to the conformational distribution of Ssc1-ADP complex, suggesting the possible effect of Mdj1 on Ssc1 conformation to be driven solely by ATP-hydrolysis. Bimodal distribution of the inter-domain distance of Ssc1 for Ssc1/ADP indicates that Ssc1 might be a dynamic molecule in this state, fluctuating between the domain-docked and the undocked state. Contrary to observations made with DnaK (Chang et al., 2008; Swain et al., 2007), we found that that ADP binding to Ssc1 is not able to efficiently undock the domains or lock the lid onto the base of the PBD which was affected efficiently only upon substrate binding. This indicates that substrate binding to Ssc1 is essential to bring about conformational changes and is corroborative with previous studies that examined the effect of substrate binding to isolated domains of DnaK (Tanaka et al., 2005).

Even though it is well understood that binding of J-domain co-chaperone is essential for substrate capture by Hsp70s, the timing of the exit of this J-domain protein in the chaperone cycle is unknown. We were able to develop a FRET based sensor for Mdj1-Ssc1 interaction and reproduce the reported observation that J-domain co-chaperones bind much faster to Hsp70s in the ATP-bound state than in the ADP-bound state (Mayer et al., 1999). Using the same sensors we observed that Mdj1 does not dissociate from the Ssc1/P5/Mdj1/ATP complex soon after hydrolysis of ATP. Even though Mdj1 was found to dissociate from Ssc1/P5, the off-rate measured was extremely slow to account for the functional chaperone cycle. Interestingly, it was observed that substrate can modulate the interaction between Ssc1 and Mdj1, with Mdj1 having a higher off-rate from Ssc1 in presence of the substrate Mge1, the bona fide nucleotide exchange factor of

Ssc1, could bind to Ssc1 only in the ADP bound state of Ssc1. It was also found that after the exogenous ATP was depleted, Mge1 could form a quaternary complex, Ssc1/P5/Mdj1/Mge1, which dissociated upon addition of ATP. This is consistent with a model of the cycle in which the cycle ends with the binding of the exchange factor to the ternary complex of Hsp70, substrate and J-domain co-chaperone.

Exchange factor assisted ATP-binding to Hsp70 is known to restart the cycle by releasing bound substrates (Brehmer et al., 2001; Harrison et al., 1997), however the sequence of release of the exchange factor and the substrate is not well studied. We were able to show that addition of ATP to Ssc1/P5/Mdj1/Mge1 leads to an instantaneous release of Mge1 from the complex followed by lid opening and domain-docking. This further leads to the dissociation of Mdj1 and P5 from Ssc1. In this work we were able to discern the dissociation of the J-domain protein from Hsp70 in a time resolved manner and show that contrary to some previously held convention (Genevaux et al., 2007), the J-domain co-chaperone dissociates from the Hsp70 at the end of the cycle simultaneous to substrate dissociation. This sequence of events restarts the cycle of Ssc1 which comes back to the substrate-acceptor state. The re-binding rate of a substrate would be dependent on the association rates and the concentrations of Ssc1, substrate and Mdj1. The rebinding rate in turn would dictate the time scale a substrate remains free in solution to be partitioned into folding competent state. Highly hydrophobic stretches, present at high concentrations, would have an inherent tendency to aggregate and since the Ssc1-binding rate for these would also be high, they would spend lesser time unbound from Ssc1 in an aggregation competent state. Based on all the results obtained, a comprehensive model for Ssc1 chaperone cycle in the mitochondrial matrix is summarized (Fig.4.1).

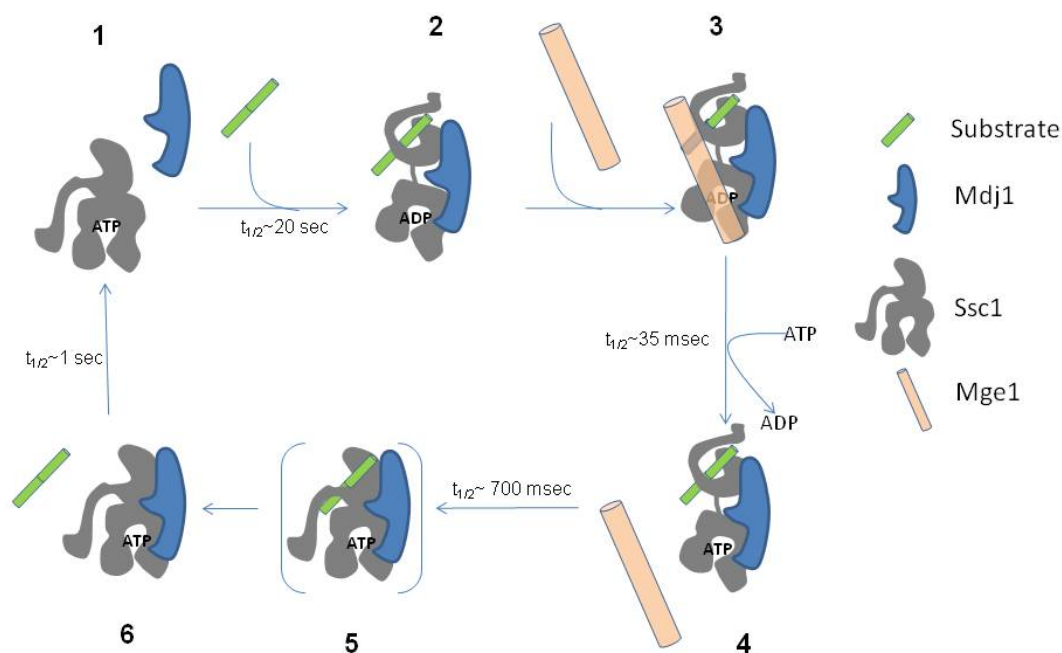


Figure 4.1: A comprehensive model of the Ssc1 chaperone cycle in the mitochondrial matrix. (1). Ssc1 in the ATP-bound state (domain-docked, lid-open state) interacts with the substrate via its PBD with low affinity which becomes effective only in presence of Mdj1. **(2).** Binding of Mdj1 and substrate and acceleration of hydrolysis of ATP by Mdj1 and substrate closes the PBD leading to high affinity binding of the substrate forming a ternary complex of Ssc1/Mdj1/substrate. **(3).** Mge1 can bind to this ternary complex in absence of an exogenous ATP. **(4).** Addition of ATP to the quaternary complex leads to instantaneous exchange of ADP with the ATP in the NBD of Ssc1 with release of Mge1. **(5 & 6).** Subsequently, ATP induced conformational changes of Ssc1 take place followed by near simultaneous dissociation of substrate and Mdj1 from Ssc1 in the ATP-state which starts a new cycle.

In this study the comparison between DnaK and Ssc1 reveals interesting new insights into the conformational differences between the two chaperones. In presence of ADP, the conformation of Ssc1 is highly heterogeneous implying that the domain connectivity might be dynamic under these conditions, whereas in the case of DnaK the domains are fully disjoined. Residual domain connectivity in Ssc1-ADP state suggests that although ATP is needed in DnaK to facilitate physical contact and hence allosteric signaling between the two domains, it might not be an essential feature in Ssc1 and in general of the Hsp70 chaperones.

5 Summary

The vast majority of mitochondrial proteins are synthesized by the cytosolic ribosomes as precursor proteins which have to be transported into the organelle to reach their sites of function. The whole process of recognition, translocation, intra-mitochondrial sorting of and assembly of precursor proteins is achieved by the concerted action of different mitochondrial translocases. All proteins destined for the mitochondrial matrix and some inner membrane proteins are imported first by the TOM complex of the outer membrane and subsequently by the TIM23 complex of the inner membrane in an energy-driven process. The TIM23 complex was found to consist of ten components, conventionally divided into two sectors: membrane sector harbouring the translocation channel and the import motor on the matrix side of the membrane sector.

In the first part of the present work, the two most recently discovered subunits of the TIM23 complex, Pam17 and Tim21 were characterized. A systematic characterization revealed that both of these non-essential subunits of the translocase are associated with Tim17-Tim23 core of the membrane sector of the TIM23 translocase. A functional connection between the two non-essential components was discovered. Results presented in this part showed that Pam17 and Tim21 modulate the functions of the TIM23 complex in an antagonistic manner.

The second part of the work was directed towards understanding the motor sector of the translocase in terms of the regulated interaction between Tim44 and Ssc1. Previous studies on the Tim44:Ssc1 interaction were able to discern the steady-state properties of Tim44:Ssc1 interaction *in organello* and *in vitro*. However, due to the limitations of the techniques used, they were unable to shed light on the kinetics and dynamics of the process. The translocation event is a dynamic event with conformational cycling of the various components. Therefore, the kinetic components essential in defining the cycle of events in the motor sector were explored. A FRET based assay to analyze the Tim44:Ssc1 interaction in real time was developed. The same set of tools was also used to resolve the regions of the two proteins that determine their interaction. The substrate

induced dissociation of Tim44:Ssc1 complex was found to be too slow to support a physiological rate of protein translocation. ATP-induced dissociation was observed to be fast enough to be physiologically relevant. The dissociation of Ssc1 from Tim44 occurred in a one step manner without Tim44 anchored conformational changes. Furthermore, peptide-array scanning of mitochondrial matrix proteins revealed that Ssc1 and Tim44 share complementary binding sites on the precursor proteins which could prevent backsliding of preproteins. The data support the Brownian ratchet model mediated translocation of preproteins into the mitochondrial matrix.

The third part of the work aimed at dissecting the chaperone cycle of Ssc1 in the mitochondrial matrix, in terms of conformational changes and binding of co-chaperones. Using the FRET sensors developed, the inter-domain conformation and lid-base conformations of the PBD of Ssc1 could be investigated. Single particle FRET (SpFRET) analysis showed that in the ATP-bound form Ssc1 populates a homogeneous conformational state with respect to the inter-domain conformation and conformation of the lid to base of the PBD. On the contrary, in the ADP-bound state the conformation of the chaperone is heterogenous. Using the same sensors on bacterial homologue DnaK, specific differences in conformational distributions were observed. Furthermore, the active role of substrates in determining the inter-domain conformation and lid-closing was evident from the SpFRET based conformational analyses. Using ensemble time resolved FRET, the kinetics and dynamics of conformational changes along with binding of co-chaperones were explored. This provided a better understanding of the conformational dynamics of Ssc1 in the context of functional chaperone cycle in the mitochondrial matrix.

6 Zusammenfassung

Die meisten mitochondrialen Proteine werden von cytosolischen Ribosomen als Vorstufenproteine synthetisiert, die anschließend in das Organell transportiert werden, um den Ort ihrer Funktion zu erreichen. Der gesamte Prozess der Erkennung, Translokation, intramitochondrialer Sortierung sowie der Assemblierung der Vorstufenproteine wird durch die aufeinander abgestimmte Aktivität verschiedener mitochondrialer Proteintranslokasen erreicht.

Alle für die Matrix bestimmten sowie einige Innenmembranproteine werden in einem energieabhängigen Prozess zunächst vom TOM-Komplex der äußeren Membran und anschließend vom TIM23-Komplex der inneren Membran transportiert. Der TIM23-Komplex, der im Zentrum dieser Arbeit steht, setzt sich aus zehn Komponenten zusammen. Er wird gewöhnlich in zwei Sektoren unterteilt; den den Translokationskanal beinhaltenden Membran-Sektor und den Import-Motor an der zur Matrix gerichteten Seite des Membran-Sektors.

Im ersten Teil der vorliegenden Arbeit werden die beiden erst kürzlich entdeckten Untereinheiten Pam17 und Tim21 des TIM23-Komplexes charakterisiert. Eine systematische Untersuchung dieser beiden nicht-essentiellen Proteine der Translokase ergab eine direkte Assoziation der beiden Untereinheiten mit dem Tim17-Tim23-Kern des Membran-Sektors der TIM23-Translokase. Des Weiteren konnte eine funktionelle Verbindung der beiden nicht-essentiellen Untereinheiten miteinander aufgedeckt werden. Pam17 und Tim21 modulieren demnach die Funktion des TIM23-Komplexes.

Der zweite Teil der Arbeit richtet sich auf das Verständnis des Motor-Sektors und seine Rolle in der regulierten Interaktion zwischen Tim44 und Ssc1. Tim44 kann als Protein angesehen werden, das die dynamische Interaktion mit den diversen anderen Komponenten des Importmotors reguliert. Das mitochondriale Chaperon mtHsp70, in Hefe als Ssc1 bezeichnet, ist die Energie-transduzierende ATP-abhängige und gleichzeitig die zu translozierenden Polypeptide bindende Komponente des

Importmotors. Sie besteht aus zwei Domänen, der Nukleotid-bindenden Domäne (NBD) und der Peptid-bindenden Domäne (PBD). Vorausgegangene Studien der Tim44:Ssc1-Interaktion hatten die Eigenschaften des stationären Zustands *in organello* und *in vitro* beschrieben. Über die Kinetik und Dynamik des Prozesses konnte kein Aufschluss geben werden. Der Translokationsvorgang ist jedoch ein dynamischer Prozess, welcher einen zyklischen Wechsel der Konformationen der Untereinheiten beinhaltet. Folglich wurden die Kinetiken der Teilreaktionen des Zyklus des Motor-Sektors untersucht. Dazu wurde ein auf Fluoreszenz-Resonanz-Elektronen-Transfer (FRET) basiertes Messverfahren zur Echtzeit-Analyse der Tim44:Ssc1-Interaktion entwickelt. Dieses Verfahren wurde auch zur Festlegung der die Interaktion bedingenden Regionen beider Proteine angewandt, die der Interaktion zu Grunde liegen. Dabei stellte sich heraus, dass die Substrat-induzierte Dissoziation des Tim44:Ssc1-Komplex zu langsam abläuft, um eine physiologische Translokationsrate der Vorstufenproteine zu ermöglichen. Die *in vitro* gemessene ATP-induzierte Dissoziation hingegen erwies sich als ausreichend schnell, um die physiologische Translokationsrate zu erklären. Die Loslösung des Ssc1 von Tim44 erfolgt in einem einstufigen Prozess ohne zu beobachtende Tim44-gebundene Konformationsintermediate. Weiterhin wurden Experimente durchgeführt, in denen mitochondriale Matrixproteine hinsichtlich der Präsenz von Bindungsstellen für Ssc1 und Tim44 durchmustert wurden. Jeweils wurden mehrere solche Bindungsstellen beobachtet, die nicht überlappend waren. Diese Bindungsspezifität kann erklären, warum bei der Translokation eine retrograde Bewegung der Polypeptidketten verhindert wird. Somit unterstützen diese Befunde das Modell des Brown'schen Ratchet (Sperrklinke) als plausiblen Translokationsmechanismus.

Der dritte Abschnitt dieser Arbeit zielt auf die Aufklärung des Chaperonzyklus des Matrix-ständigen Ssc1. Insbesondere ging es dabei um die Erfassung konformativer Änderungen und die Bindung der Co-Chaperone Tim14 und Tim16. Der Einsatz von FRET-Sonden ermöglichte die Untersuchung der Domänen sowie der "lid-base"-Konformation der PBD des Ssc1. Messungen mittels Einzelpartikel-FRET (single particle FRET, spFRET) zeigen, dass Ssc1 in der ATP-gebundenen Form einen homogenen Zustand einnimmt, und zwar in Bezug auf das Verhalten der beiden Domänen als auch in

Bezug auf die "lid-base"-Interaktion. Im Gegensatz dazu erwies sich der Konformationszustand der ADP-gebundenen Form als heterogen. Das bakterielle Ssc1-Homologe, DnaK, wurde mit derselben Technik untersucht; trotz der sehr großen strukturellen Ähnlichkeit wurden ausgeprägte Unterschiede hinsichtlich der Verteilung der Konformere beobachtet. Ferner wurde eine aktive Rolle der Proteinsubstrate bei der Verteilung der Konformationszustände von Ssc1 festgestellt. Die Dynamik und Kinetik der Konformationsänderungen aufgelöst in Real Time-FRET und die Bindung der Co-Chaperone Tim14 und Tim16 wurden ebenfalls untersucht. Insgesamt führen die hier beschriebenen Ergebnisse zu einem genaueren Verständnis der Funktion des Ssc1 als zentrale Komponente des Chaperonzyklus der Mitochondrien.

7 References:

Ahting, U., Thieffry, M., Engelhardt, H., Hegerl, R., Neupert, W., and Nussberger, S. (2001). Tom40, the pore-forming component of the protein-conducting TOM channel in the outer membrane of mitochondria. *J Cell Biol* *153*, 1151-1160.

Ahting, U., Thun, C., Hegerl, R., Typke, D., Nargang, F.E., Neupert, W., and Nussberger, S. (1999). The TOM core complex: the general protein import pore of the outer membrane of mitochondria. *J Cell Biol* *147*, 959-968.

Ainavarapu, S.R., Li, L., Badilla, C.L., and Fernandez, J.M. (2005). Ligand binding modulates the mechanical stability of dihydrofolate reductase. *Biophys J* *89*, 3337-3344.

Alder, N.N., Jensen, R.E., and Johnson, A.E. (2008). Fluorescence mapping of mitochondrial TIM23 complex reveals a water-facing, substrate-interacting helix surface. *Cell* *134*, 439-450.

Bajaj, K., Chakrabarti, P., and Varadarajan, R. (2005). Mutagenesis-based definitions and probes of residue burial in proteins. *Proc Natl Acad Sci U S A* *102*, 16221-16226.

Bauer, M.F., Sirrenberg, C., Neupert, W., and Brunner, M. (1996). Role of Tim23 as voltage sensor and presequence receptor in protein import into mitochondria. *Cell* *87*, 33-41.

Becker, L., Bannwarth, M., Meisinger, C., Hill, K., Model, K., Krimmer, T., Casadio, R., Truscott, K.N., Schulz, G.E., Pfanner, N., *et al.* (2005). Preprotein translocase of the outer mitochondrial membrane: reconstituted Tom40 forms a characteristic TOM pore. *J Mol Biol* *353*, 1011-1020.

Becker, T., Pfannschmidt, S., Guiard, B., Stojanovski, D., Milenkovic, D., Kutik, S., Pfanner, N., Meisinger, C., and Wiedemann, N. (2008a). Biogenesis of the mitochondrial TOM complex: Mim1 promotes insertion and assembly of signal-anchored receptors. *J Biol Chem* *283*, 120-127.

Becker, T., Vogtle, F.N., Stojanovski, D., and Meisinger, C. (2008b). Sorting and assembly of mitochondrial outer membrane proteins. *Biochim Biophys Acta* *1777*, 557-563.

Blobel, G. (1980). Intracellular protein topogenesis. *Proc Natl Acad Sci U S A* *77*, 1496-1500.

Blom, J., Kubrich, M., Rassow, J., Voos, W., Dekker, P.J., Maarse, A.C., Meijer, M., and Pfanner, N. (1993). The essential yeast protein MIM44 (encoded by MPI1) is involved in an early step of preprotein translocation across the mitochondrial inner membrane. *Mol Cell Biol* *13*, 7364-7371.

Bolliger, L., Deloche, O., Glick, B.S., Georgopoulos, C., Jenö, P., Kronidou, N., Horst, M., Morishima, N., and Schatz, G. (1994). A mitochondrial homolog of bacterial GrpE interacts with mitochondrial hsp70 and is essential for viability. *Embo J* 13, 1998-2006.

Brehmer, D., Rudiger, S., Gassler, C.S., Klostermeier, D., Packschies, L., Reinstein, J., Mayer, M.P., and Bukau, B. (2001). Tuning of chaperone activity of Hsp70 proteins by modulation of nucleotide exchange. *Nat Struct Biol* 8, 427-432.

Casadaban, M.J., and Cohen, S.N. (1980). Analysis of gene control signals by DNA fusion and cloning in *Escherichia coli*. *J Mol Biol* 138, 179-207.

Chacinska, A., Lind, M., Frazier, A.E., Dudek, J., Meisinger, C., Geissler, A., Sickmann, A., Meyer, H.E., Truscott, K.N., Guiard, B., *et al.* (2005). Mitochondrial presequence translocase: switching between TOM tethering and motor recruitment involves Tim21 and Tim17. *Cell* 120, 817-829.

Chacinska, A., Pfannschmidt, S., Wiedemann, N., Kozjak, V., Sanjuan Szklarz, L.K., Schulze-Specking, A., Truscott, K.N., Guiard, B., Meisinger, C., and Pfanner, N. (2004). Essential role of Mia40 in import and assembly of mitochondrial intermembrane space proteins. *Embo J* 23, 3735-3746.

Chan, N.C., Likic, V.A., Waller, R.F., Mulhern, T.D., and Lithgow, T. (2006). The C-terminal TPR domain of Tom70 defines a family of mitochondrial protein import receptors found only in animals and fungi. *J Mol Biol* 358, 1010-1022.

Chang, Y.W., Sun, Y.J., Wang, C., and Hsiao, C.D. (2008). Crystal structures of the 70-kDa heat shock proteins in domain disjoining conformation. *J Biol Chem* 283, 15502-15511.

Coppock, D.L., and Thorpe, C. (2006). Multidomain flavin-dependent sulfhydryl oxidases. *Antioxid Redox Signal* 8, 300-311.

Craig, E.A., Kramer, J., and Kosc-Smithers, J. (1987). SSC1, a member of the 70-kDa heat shock protein multigene family of *Saccharomyces cerevisiae*, is essential for growth. *Proc Natl Acad Sci U S A* 84, 4156-4160.

Cyr, D.M., Stuart, R.A., and Neupert, W. (1993). A matrix ATP requirement for presequence translocation across the inner membrane of mitochondria. *J Biol Chem* 268, 23751-23754.

D'Silva, P., Liu, Q., Walter, W., and Craig, E.A. (2004). Regulated interactions of mtHsp70 with Tim44 at the translocon in the mitochondrial inner membrane. *Nat Struct Mol Biol* 11, 1084-1091.

D'Silva, P.D., Schilke, B., Walter, W., Andrew, A., and Craig, E.A. (2003). J protein cochaperone of the mitochondrial inner membrane required for protein import into the mitochondrial matrix. *Proc Natl Acad Sci U S A* 100, 13839-13844.

- Daum, G., Bohni, P.C., and Schatz, G. (1982a). Import of proteins into mitochondria. Cytochrome b2 and cytochrome c peroxidase are located in the intermembrane space of yeast mitochondria. *J Biol Chem* *257*, 13028-13033.
- Daum, G., Gasser, S.M., and Schatz, G. (1982b). Import of proteins into mitochondria. Energy-dependent, two-step processing of the intermembrane space enzyme cytochrome b2 by isolated yeast mitochondria. *J Biol Chem* *257*, 13075-13080.
- Dekker, P.J., Ryan, M.T., Brix, J., Muller, H., Honlinger, A., and Pfanner, N. (1998). Preprotein translocase of the outer mitochondrial membrane: molecular dissection and assembly of the general import pore complex. *Mol Cell Biol* *18*, 6515-6524.
- Deshaies, R.J., Koch, B.D., and Schekman, R. (1988). The role of stress proteins in membrane biogenesis. *Trends Biochem Sci* *13*, 384-388.
- Dietmeier, K., Honlinger, A., Bomer, U., Dekker, P.J., Eckerskorn, C., Lottspeich, F., Kubrich, M., and Pfanner, N. (1997). Tom5 functionally links mitochondrial preprotein receptors to the general import pore. *Nature* *388*, 195-200.
- Donzeau, M., Kaldi, K., Adam, A., Paschen, S., Wanner, G., Guiard, B., Bauer, M.F., Neupert, W., and Brunner, M. (2000). Tim23 links the inner and outer mitochondrial membranes. *Cell* *101*, 401-412.
- Dower, W.J., Miller, J.F., and Ragsdale, C.W. (1988). High efficiency transformation of *E. coli* by high voltage electroporation. *Nucleic Acids Res* *16*, 6127-6145.
- Duchniewicz, M., Germaniuk, A., Westermann, B., Neupert, W., Schwarz, E., and Marszalek, J. (1999). Dual role of the mitochondrial chaperone Mdj1p in inheritance of mitochondrial DNA in yeast. *Mol Cell Biol* *19*, 8201-8210.
- Emtage, J.L., and Jensen, R.E. (1993). MAS6 encodes an essential inner membrane component of the yeast mitochondrial protein import pathway. *J Cell Biol* *122*, 1003-1012.
- Frazier, A.E., Dudek, J., Guiard, B., Voos, W., Li, Y., Lind, M., Meisinger, C., Geissler, A., Sickmann, A., Meyer, H.E., *et al.* (2004). Pam16 has an essential role in the mitochondrial protein import motor. *Nat Struct Mol Biol* *11*, 226-233.
- Fujiki, M., and Verner, K. (1991). Coupling of protein synthesis and mitochondrial import in a homologous yeast in vitro system. *J Biol Chem* *266*, 6841-6847.
- Fujiki, M., and Verner, K. (1993). Coupling of cytosolic protein synthesis and mitochondrial protein import in yeast. Evidence for cotranslational import in vivo. *J Biol Chem* *268*, 1914-1920.
- Gallas, M.R., Dienhart, M.K., Stuart, R.A., and Long, R.M. (2006). Characterization of Mmp37p, a *Saccharomyces cerevisiae* mitochondrial matrix protein with a role in mitochondrial protein import. *Mol Biol Cell* *17*, 4051-4062.

- Gambill, B.D., Voos, W., Kang, P.J., Miao, B., Langer, T., Craig, E.A., and Pfanner, N. (1993). A dual role for mitochondrial heat shock protein 70 in membrane translocation of preproteins. *J Cell Biol* 123, 109-117.
- Geissler, A., Krimmer, T., Bomer, U., Guiard, B., Rassow, J., and Pfanner, N. (2000). Membrane potential-driven protein import into mitochondria. The sorting sequence of cytochrome b(2) modulates the deltapsi-dependence of translocation of the matrix-targeting sequence. *Mol Biol Cell* 11, 3977-3991.
- Geissler, A., Rassow, J., Pfanner, N., and Voos, W. (2001). Mitochondrial import driving forces: enhanced trapping by matrix Hsp70 stimulates translocation and reduces the membrane potential dependence of loosely folded preproteins. *Mol Cell Biol* 21, 7097-7104.
- Genevaux, P., Georgopoulos, C., and Kelley, W.L. (2007). The Hsp70 chaperone machines of *Escherichia coli*: a paradigm for the repartition of chaperone functions. *Mol Microbiol* 66, 840-857.
- Gentle, I., Gabriel, K., Beech, P., Waller, R., and Lithgow, T. (2004). The Omp85 family of proteins is essential for outer membrane biogenesis in mitochondria and bacteria. *J Cell Biol* 164, 19-24.
- Glick, B.S. (1995). Pathways and energetics of mitochondrial protein import in *Saccharomyces cerevisiae*. *Methods Enzymol* 260, 224-231.
- Gragerov, A., and Gottesman, M.E. (1994). Different peptide binding specificities of hsp70 family members. *J Mol Biol* 241, 133-135.
- Gragerov, A., Zeng, L., Zhao, X., Burkholder, W., and Gottesman, M.E. (1994). Specificity of DnaK-peptide binding. *J Mol Biol* 235, 848-854.
- Grumbt, B., Stroobant, V., Terziyska, N., Israel, L., and Hell, K. (2007). Functional characterization of Mia40p, the central component of the disulfide relay system of the mitochondrial intermembrane space. *J Biol Chem* 282, 37461-37470.
- Guda, C., Fahy, E., and Subramaniam, S. (2004a). MITOPRED: a genome-scale method for prediction of nucleus-encoded mitochondrial proteins. *Bioinformatics* 20, 1785-1794.
- Guda, C., Guda, P., Fahy, E., and Subramaniam, S. (2004b). MITOPRED: a web server for the prediction of mitochondrial proteins. *Nucleic Acids Res* 32, W372-374.
- Habib, S.J., Waizenegger, T., Lech, M., Neupert, W., and Rapaport, D. (2005). Assembly of the TOB complex of mitochondria. *J Biol Chem* 280, 6434-6440.
- Habib, S.J., Waizenegger, T., Niewianda, A., Paschen, S.A., Neupert, W., and Rapaport, D. (2007). The N-terminal domain of Tob55 has a receptor-like function in the biogenesis of mitochondrial beta-barrel proteins. *J Cell Biol* 176, 77-88.

- Hachiya, N., Komiya, T., Alam, R., Iwahashi, J., Sakaguchi, M., Omura, T., and Mihara, K. (1994). MSF, a novel cytoplasmic chaperone which functions in precursor targeting to mitochondria. *Embo J* *13*, 5146-5154.
- Harrison, C.J., Hayer-Hartl, M., Di Liberto, M., Hartl, F., and Kuriyan, J. (1997). Crystal structure of the nucleotide exchange factor GrpE bound to the ATPase domain of the molecular chaperone DnaK. *Science* *276*, 431-435.
- Hartl, F.U., and Hayer-Hartl, M. (2002). Molecular chaperones in the cytosol: from nascent chain to folded protein. *Science* *295*, 1852-1858.
- Hell, K. (2008). The Erv1-Mia40 disulfide relay system in the intermembrane space of mitochondria. *Biochim Biophys Acta* *1783*, 601-609.
- Hell, K., Herrmann, J., Pratje, E., Neupert, W., and Stuart, R.A. (1997). Oxa1p mediates the export of the N- and C-termini of pCoxII from the mitochondrial matrix to the intermembrane space. *FEBS Lett* *418*, 367-370.
- Hell, K., Herrmann, J.M., Pratje, E., Neupert, W., and Stuart, R.A. (1998). Oxa1p, an essential component of the N-tail protein export machinery in mitochondria. *Proc Natl Acad Sci U S A* *95*, 2250-2255.
- Hell, K., Neupert, W., and Stuart, R.A. (2001). Oxa1p acts as a general membrane insertion machinery for proteins encoded by mitochondrial DNA. *Embo J* *20*, 1281-1288.
- Herrmann, J.M., Kauff, F., and Neuhaus, H.E. (2008). Thiol oxidation in bacteria, mitochondria and chloroplasts: Common principles but three unrelated machineries? *Biochim Biophys Acta*.
- Hill, K., Model, K., Ryan, M.T., Dietmeier, K., Martin, F., Wagner, R., and Pfanner, N. (1998). Tom40 forms the hydrophilic channel of the mitochondrial import pore for preproteins [see comment]. *Nature* *395*, 516-521.
- Hofhaus, G., Lee, J.E., Tews, I., Rosenberg, B., and Lisowsky, T. (2003). The N-terminal cysteine pair of yeast sulfhydryl oxidase Erv1p is essential for in vivo activity and interacts with the primary redox centre. *Eur J Biochem* *270*, 1528-1535.
- Hofmann, S., Rothbauer, U., Muhlenbein, N., Baiker, K., Hell, K., and Bauer, M.F. (2005). Functional and mutational characterization of human MIA40 acting during import into the mitochondrial intermembrane space. *J Mol Biol* *353*, 517-528.
- Hwang, D.K., Claypool, S.M., Leuenberger, D., Tienson, H.L., and Koehler, C.M. (2007). Tim54p connects inner membrane assembly and proteolytic pathways in the mitochondrion. *J Cell Biol* *178*, 1161-1175.
- Ishikawa, D., Yamamoto, H., Tamura, Y., Moritoh, K., and Endo, T. (2004). Two novel proteins in the mitochondrial outer membrane mediate beta-barrel protein assembly. *J Cell Biol* *166*, 621-627.

Jia, L., Dienhart, M., Schramp, M., McCauley, M., Hell, K., and Stuart, R.A. (2003). Yeast Oxa1 interacts with mitochondrial ribosomes: the importance of the C-terminal region of Oxa1. *Embo J* 22, 6438-6447.

Jiang, J., Prasad, K., Lafer, E.M., and Sousa, R. (2005). Structural basis of interdomain communication in the Hsc70 chaperone. *Mol Cell* 20, 513-524.

Josyula, R., Jin, Z., Fu, Z., and Sha, B. (2006). Crystal structure of yeast mitochondrial peripheral membrane protein Tim44p C-terminal domain. *J Mol Biol* 359, 798-804.

Junker, J.P., Hell, K., Schlierf, M., Neupert, W., and Rief, M. (2005). Influence of substrate binding on the mechanical stability of mouse dihydrofolate reductase. *Biophys J* 89, L46-48.

Karzai, A.W., and McMacken, R. (1996). A bipartite signaling mechanism involved in DnaJ-mediated activation of the Escherichia coli DnaK protein. *J Biol Chem* 271, 11236-11246.

Komiya, T., Rospert, S., Koehler, C., Looser, R., Schatz, G., and Mihara, K. (1998). Interaction of mitochondrial targeting signals with acidic receptor domains along the protein import pathway: evidence for the 'acid chain' hypothesis. *Embo J* 17, 3886-3898.

Kovermann, P., Truscott, K.N., Guiard, B., Rehling, P., Sepuri, N.B., Muller, H., Jensen, R.E., Wagner, R., and Pfanner, N. (2002). Tim22, the essential core of the mitochondrial protein insertion complex, forms a voltage-activated and signal-gated channel. *Mol Cell* 9, 363-373.

Kozany, C., Mokranjac, D., Sichting, M., Neupert, W., and Hell, K. (2004). The J domain-related cochaperone Tim16 is a constituent of the mitochondrial TIM23 preprotein translocase. *Nat Struct Mol Biol* 11, 234-241.

Kozjak, V., Wiedemann, N., Milenkovic, D., Lohaus, C., Meyer, H.E., Guiard, B., Meisinger, C., and Pfanner, N. (2003). An essential role of Sam50 in the protein sorting and assembly machinery of the mitochondrial outer membrane. *J Biol Chem* 278, 48520-48523.

Krimmer, T., Rassow, J., Kunau, W.H., Voos, W., and Pfanner, N. (2000). Mitochondrial protein import motor: the ATPase domain of matrix Hsp70 is crucial for binding to Tim44, while the peptide binding domain and the carboxy-terminal segment play a stimulatory role. *Mol Cell Biol* 20, 5879-5887.

Kronidou, N.G., Oppliger, W., Bolliger, L., Hannavy, K., Glick, B.S., Schatz, G., and Horst, M. (1994). Dynamic interaction between Isp45 and mitochondrial hsp70 in the protein import system of the yeast mitochondrial inner membrane. *Proc Natl Acad Sci U S A* 91, 12818-12822.

Kubo, Y., Tsunehiro, T., Nishikawa, S., Nakai, M., Ikeda, E., Toh-e, A., Morishima, N., Shibata, T., and Endo, T. (1999). Two distinct mechanisms operate in the reactivation of

heat-denatured proteins by the mitochondrial Hsp70/Mdj1p/Yge1p chaperone system. *J Mol Biol* 286, 447-464.

Kunkele, K.P., Heins, S., Dembowski, M., Nargang, F.E., Benz, R., Thieffry, M., Walz, J., Lill, R., Nussberger, S., and Neupert, W. (1998a). The preprotein translocation channel of the outer membrane of mitochondria. *Cell* 93, 1009-1019.

Kunkele, K.P., Juin, P., Pompa, C., Nargang, F.E., Henry, J.P., Neupert, W., Lill, R., and Thieffry, M. (1998b). The isolated complex of the translocase of the outer membrane of mitochondria. Characterization of the cation-selective and voltage-gated preprotein-conducting pore. *J Biol Chem* 273, 31032-31039.

Kutik, S., Stojanovski, D., Becker, L., Becker, T., Meinecke, M., Kruger, V., Prinz, C., Meisinger, C., Guiard, B., Wagner, R., *et al.* (2008). Dissecting membrane insertion of mitochondrial beta-barrel proteins. *Cell* 132, 1011-1024.

Laufen, T., Mayer, M.P., Beisel, C., Klostermeier, D., Mogk, A., Reinstein, J., and Bukau, B. (1999). Mechanism of regulation of hsp70 chaperones by DnaJ cochaperones. *Proc Natl Acad Sci U S A* 96, 5452-5457.

Lee, C.M., Sedman, J., Neupert, W., and Stuart, R.A. (1999). The DNA helicase, Hmi1p, is transported into mitochondria by a C-terminal cleavable targeting signal. *J Biol Chem* 274, 20937-20942.

Li, Y., Dudek, J., Guiard, B., Pfanner, N., Rehling, P., and Voos, W. (2004). The presequence translocase-associated protein import motor of mitochondria. Pam16 functions in an antagonistic manner to Pam18. *J Biol Chem* 279, 38047-38054.

Liberek, K., Marszalek, J., Ang, D., Georgopoulos, C., and Zylicz, M. (1991). Escherichia coli DnaJ and GrpE heat shock proteins jointly stimulate ATPase activity of DnaK. *Proc Natl Acad Sci U S A* 88, 2874-2878.

Lim, J.H., Martin, F., Guiard, B., Pfanner, N., and Voos, W. (2001). The mitochondrial Hsp70-dependent import system actively unfolds preproteins and shortens the lag phase of translocation. *Embo J* 20, 941-950.

Lithgow, T., Glick, B.S., and Schatz, G. (1995). The protein import receptor of mitochondria. *Trends Biochem Sci* 20, 98-101.

Liu, Q., D'Silva, P., Walter, W., Marszalek, J., and Craig, E.A. (2003). Regulated cycling of mitochondrial Hsp70 at the protein import channel. *Science* 300, 139-141.

Liu, Q., and Hendrickson, W.A. (2007). Insights into Hsp70 chaperone activity from a crystal structure of the yeast Hsp110 Sse1. *Cell* 131, 106-120.

Lu, H., Golovanov, A.P., Alcock, F., Grossmann, J.G., Allen, S., Lian, L.Y., and Tokatlidis, K. (2004). The structural basis of the TIM10 chaperone assembly. *J Biol Chem* 279, 18959-18966.

Maarse, A.C., Blom, J., Grivell, L.A., and Meijer, M. (1992). MPI1, an essential gene encoding a mitochondrial membrane protein, is possibly involved in protein import into yeast mitochondria. *Embo J* 11, 3619-3628.

Martin, J., Mahlke, K., and Pfanner, N. (1991). Role of an energized inner membrane in mitochondrial protein import. Delta psi drives the movement of presequences. *J Biol Chem* 266, 18051-18057.

Martinez-Caballero, S., Grigoriev, S.M., Herrmann, J.M., Campo, M.L., and Kinnally, K.W. (2007). Tim17p regulates the twin pore structure and voltage gating of the mitochondrial protein import complex TIM23. *J Biol Chem* 282, 3584-3593.

Matouschek, A., Pfanner, N., and Voos, W. (2000). Protein unfolding by mitochondria. The Hsp70 import motor. *EMBO Rep* 1, 404-410.

Mayer, A., Nargang, F.E., Neupert, W., and Lill, R. (1995). MOM22 is a receptor for mitochondrial targeting sequences and cooperates with MOM19. *Embo J* 14, 4204-4211.

Mayer, M.P., Laufen, T., Paal, K., McCarty, J.S., and Bukau, B. (1999). Investigation of the interaction between DnaK and DnaJ by surface plasmon resonance spectroscopy. *J Mol Biol* 289, 1131-1144.

Meier, S., Neupert, W., and Herrmann, J.M. (2005). Conserved N-terminal negative charges in the Tim17 subunit of the TIM23 translocase play a critical role in the import of preproteins into mitochondria. *J Biol Chem* 280, 7777-7785.

Meinecke, M., Wagner, R., Kovermann, P., Guiard, B., Mick, D.U., Hutu, D.P., Voos, W., Truscott, K.N., Chacinska, A., Pfanner, N., *et al.* (2006). Tim50 maintains the permeability barrier of the mitochondrial inner membrane. *Science* 312, 1523-1526.

Merlin, A., Voos, W., Maarse, A.C., Meijer, M., Pfanner, N., and Rassow, J. (1999). The J-related segment of tim44 is essential for cell viability: a mutant Tim44 remains in the mitochondrial import site, but inefficiently recruits mtHsp70 and impairs protein translocation. *J Cell Biol* 145, 961-972.

Milenkovic, D., Kozjak, V., Wiedemann, N., Lohaus, C., Meyer, H.E., Guiard, B., Pfanner, N., and Meisinger, C. (2004). Sam35 of the mitochondrial protein sorting and assembly machinery is a peripheral outer membrane protein essential for cell viability. *J Biol Chem* 279, 22781-22785.

Model, K., Prinz, T., Ruiz, T., Radermacher, M., Krimmer, T., Kuhlbrandt, W., Pfanner, N., and Meisinger, C. (2002). Protein translocase of the outer mitochondrial membrane: role of import receptors in the structural organization of the TOM complex. *J Mol Biol* 316, 657-666.

Mokranjac, D., Bourenkov, G., Hell, K., Neupert, W., and Groll, M. (2006). Structure and function of Tim14 and Tim16, the J and J-like components of the mitochondrial protein import motor. *Embo J* 25, 4675-4685.

- Mokranjac, D., and Neupert, W. (2008). Thirty years of protein translocation into mitochondria: Unexpectedly complex and still puzzling. *Biochim Biophys Acta*.
- Mokranjac, D., Paschen, S.A., Kozany, C., Prokisch, H., Hoppins, S.C., Nargang, F.E., Neupert, W., and Hell, K. (2003a). Tim50, a novel component of the TIM23 preprotein translocase of mitochondria. *Embo J* 22, 816-825.
- Mokranjac, D., Popov-Celeketic, D., Hell, K., and Neupert, W. (2005). Role of Tim21 in mitochondrial translocation contact sites. *J Biol Chem* 280, 23437-23440.
- Mokranjac, D., Sighting, M., Neupert, W., and Hell, K. (2003b). Tim14, a novel key component of the import motor of the TIM23 protein translocase of mitochondria. *Embo J* 22, 4945-4956.
- Moro, F., Okamoto, K., Donzeau, M., Neupert, W., and Brunner, M. (2002). Mitochondrial protein import: molecular basis of the ATP-dependent interaction of MtHsp70 with Tim44. *J Biol Chem* 277, 6874-6880.
- Muller, B.K., Zaychikov, E., Brauchle, C., and Lamb, D.C. (2005). Pulsed interleaved excitation. *Biophys J* 89, 3508-3522.
- Muller, J.M., Milenkovic, D., Guiard, B., Pfanner, N., and Chacinska, A. (2008). Precursor oxidation by Mia40 and Erv1 promotes vectorial transport of proteins into the mitochondrial intermembrane space. *Mol Biol Cell* 19, 226-236.
- Murakami, H., Pain, D., and Blobel, G. (1988). 70-kD heat shock-related protein is one of at least two distinct cytosolic factors stimulating protein import into mitochondria. *J Cell Biol* 107, 2051-2057.
- Nakai, M., Kato, Y., Ikeda, E., Toh-e, A., and Endo, T. (1994). Yge1p, a eukaryotic Grp-E homolog, is localized in the mitochondrial matrix and interacts with mitochondrial Hsp70. *Biochem Biophys Res Commun* 200, 435-442.
- Neupert, W., and Brunner, M. (2002). The protein import motor of mitochondria. *Nat Rev Mol Cell Biol* 3, 555-565.
- Neupert, W., and Herrmann, J.M. (2007). Translocation of proteins into mitochondria. *Annu Rev Biochem* 76, 723-749.
- Norby, J.G. (1988). Coupled assay of Na⁺,K⁺-ATPase activity. *Methods Enzymol* 156, 116-119.
- Okamoto, K., Brinker, A., Paschen, S.A., Moarefi, I., Hayer-Hartl, M., Neupert, W., and Brunner, M. (2002). The protein import motor of mitochondria: a targeted molecular ratchet driving unfolding and translocation. *Embo J* 21, 3659-3671.

- Ott, M., Prestele, M., Bauerschmitt, H., Funes, S., Bonnefoy, N., and Herrmann, J.M. (2006). Mba1, a membrane-associated ribosome receptor in mitochondria. *Embo J* 25, 1603-1610.
- Paschen, S.A., Waizenegger, T., Stan, T., Preuss, M., Cyrklaff, M., Hell, K., Rapaport, D., and Neupert, W. (2003). Evolutionary conservation of biogenesis of beta-barrel membrane proteins. *Nature* 426, 862-866.
- Pellecchia, M., Montgomery, D.L., Stevens, S.Y., Vander Kooi, C.W., Feng, H.P., Gierasch, L.M., and Zudierweg, E.R. (2000). Structural insights into substrate binding by the molecular chaperone DnaK. *Nat Struct Biol* 7, 298-303.
- Popov-Celeketic, D., Mapa, K., Neupert, W., and Mokranjac, D. (2008a). Active remodelling of the TIM23 complex during translocation of preproteins into mitochondria. *Embo J* 27, 1469-1480.
- Popov-Celeketic, J., Waizenegger, T., and Rapaport, D. (2008b). Mim1 functions in an oligomeric form to facilitate the integration of Tom20 into the mitochondrial outer membrane. *J Mol Biol* 376, 671-680.
- Preuss, M., Leonhard, K., Hell, K., Stuart, R.A., Neupert, W., and Herrmann, J.M. (2001). Mba1, a novel component of the mitochondrial protein export machinery of the yeast *Saccharomyces cerevisiae*. *J Cell Biol* 153, 1085-1096.
- Prip-Buus, C., Westerman, B., Schmitt, M., Langer, T., Neupert, W., and Schwarz, E. (1996). Role of the mitochondrial DnaJ homologue, Mdj1p, in the prevention of heat-induced protein aggregation. *FEBS Lett* 380, 142-146.
- Ramage, L., Junne, T., Hahne, K., Lithgow, T., and Schatz, G. (1993). Functional cooperation of mitochondrial protein import receptors in yeast. *Embo J* 12, 4115-4123.
- Rapaport, D. (2002). Biogenesis of the mitochondrial TOM complex. *Trends Biochem Sci* 27, 191-197.
- Rapaport, D. (2003). Finding the right organelle. Targeting signals in mitochondrial outer-membrane proteins. *EMBO Rep* 4, 948-952.
- Rassow, J., Maarse, A.C., Krainer, E., Kubrich, M., Muller, H., Meijer, M., Craig, E.A., and Pfanner, N. (1994). Mitochondrial protein import: biochemical and genetic evidence for interaction of matrix hsp70 and the inner membrane protein MIM44. *J Cell Biol* 127, 1547-1556.
- Rehling, P., Model, K., Brandner, K., Kovermann, P., Sickmann, A., Meyer, H.E., Kuhlbrandt, W., Wagner, R., Truscott, K.N., and Pfanner, N. (2003). Protein insertion into the mitochondrial inner membrane by a twin-pore translocase. *Science* 299, 1747-1751.

Rowley, N., Prip-Buus, C., Westermann, B., Brown, C., Schwarz, E., Barrell, B., and Neupert, W. (1994). Mdj1p, a novel chaperone of the DnaJ family, is involved in mitochondrial biogenesis and protein folding. *Cell* 77, 249-259.

Rudiger, S., Germeroth, L., Schneider-Mergener, J., and Bukau, B. (1997). Substrate specificity of the DnaK chaperone determined by screening cellulose-bound peptide libraries. *Embo J* 16, 1501-1507.

Ryan, K.R., Leung, R.S., and Jensen, R.E. (1998). Characterization of the mitochondrial inner membrane translocase complex: the Tim23p hydrophobic domain interacts with Tim17p but not with other Tim23p molecules. *Mol Cell Biol* 18, 178-187.

Ryan, K.R., Menold, M.M., Garrett, S., and Jensen, R.E. (1994). SMS1, a high-copy suppressor of the yeast mas6 mutant, encodes an essential inner membrane protein required for mitochondrial protein import. *Mol Biol Cell* 5, 529-538.

Sambrook, J., F., E.F. and Maniatis, T. (1989). *Molecular cloning: A Laboratory Manual* 2edn (Cold Spring Harbor, NY, Cold Spring Laboratory Press).

Sanchez-Pulido, L., Devos, D., Genevrois, S., Vicente, M., and Valencia, A. (2003). POTRA: a conserved domain in the FtsQ family and a class of beta-barrel outer membrane proteins. *Trends Biochem Sci* 28, 523-526.

Sato, T., Esaki, M., Fernandez, J.M., and Endo, T. (2005). Comparison of the protein-unfolding pathways between mitochondrial protein import and atomic-force microscopy measurements. *Proc Natl Acad Sci U S A* 102, 17999-18004.

Schiller, D., Cheng, Y.C., Liu, Q., Walter, W., and Craig, E.A. (2008). Residues of Tim44 involved in both association with the translocon of the inner mitochondrial membrane and regulation of mitochondrial Hsp70 tethering. *Mol Cell Biol* 28, 4424-4433.

Schmid, D., Baici, A., Gehring, H., and Christen, P. (1994). Kinetics of molecular chaperone action. *Science* 263, 971-973.

Schmidt, S., Strub, A., Rottgers, K., Zufall, N., and Voos, W. (2001). The two mitochondrial heat shock proteins 70, Ssc1 and Ssq1, compete for the cochaperone Mge1. *J Mol Biol* 313, 13-26.

Schneider, H.C., Berthold, J., Bauer, M.F., Dietmeier, K., Guiard, B., Brunner, M., and Neupert, W. (1994). Mitochondrial Hsp70/MIM44 complex facilitates protein import. *Nature* 371, 768-774.

Schnell, D.J., and Hebert, D.N. (2003). Protein translocons: multifunctional mediators of protein translocation across membranes. *Cell* 112, 491-505.

Sherman, E.L., Go, N.E., and Nargang, F.E. (2005). Functions of the small proteins in the TOM complex of *Neurospora crassa*. *Mol Biol Cell* 16, 4172-4182.

Sichting, M., Mokranjac, D., Azem, A., Neupert, W., and Hell, K. (2005). Maintenance of structure and function of mitochondrial Hsp70 chaperones requires the chaperone Hsp70. *Embo J* 24, 1046-1056.

Sikorski, R.S., and Hieter, P. (1989). A system of shuttle vectors and yeast host strains designed for efficient manipulation of DNA in *Saccharomyces cerevisiae*. *Genetics* 122, 19-27.

Slutsky-Leiderman, O., Marom, M., Iosefson, O., Levy, R., Maoz, S., and Azem, A. (2007). The interplay between components of the mitochondrial protein translocation motor studied using purified components. *J Biol Chem* 282, 33935-33942.

Soll, J., and Schleiff, E. (2004). Protein import into chloroplasts. *Nat Rev Mol Cell Biol* 5, 198-208.

Stevens, S.Y., Cai, S., Pellicchia, M., and Zuiderweg, E.R. (2003). The solution structure of the bacterial HSP70 chaperone protein domain DnaK(393-507) in complex with the peptide NRRLLTG. *Protein Sci* 12, 2588-2596.

Stuart, R.A., Gruhler, A., van der Klei, I., Guiard, B., Koll, H., and Neupert, W. (1994). The requirement of matrix ATP for the import of precursor proteins into the mitochondrial matrix and intermembrane space. *Eur J Biochem* 220, 9-18.

Swain, J.F., Dinler, G., Sivendran, R., Montgomery, D.L., Stotz, M., and Gierasch, L.M. (2007). Hsp70 chaperone ligands control domain association via an allosteric mechanism mediated by the interdomain linker. *Mol Cell* 26, 27-39.

Szyrach, G., Ott, M., Bonnefoy, N., Neupert, W., and Herrmann, J.M. (2003). Ribosome binding to the Oxa1 complex facilitates co-translational protein insertion in mitochondria. *Embo J* 22, 6448-6457.

Tamura, Y., Harada, Y., Yamano, K., Watanabe, K., Ishikawa, D., Ohshima, C., Nishikawa, S., Yamamoto, H., and Endo, T. (2006). Identification of Tam41 maintaining integrity of the TIM23 protein translocator complex in mitochondria. *J Cell Biol* 174, 631-637.

Tanaka, N., Nakao, S., Chatellier, J., Tani, Y., Tada, T., and Kunugi, S. (2005). Effect of the polypeptide binding on the thermodynamic stability of the substrate binding domain of the DnaK chaperone. *Biochim Biophys Acta* 1748, 1-8.

Terziyska, N., Lutz, T., Kozany, C., Mokranjac, D., Mesecke, N., Neupert, W., Herrmann, J.M., and Hell, K. (2005). Mia40, a novel factor for protein import into the intermembrane space of mitochondria is able to bind metal ions. *FEBS Lett* 579, 179-184.

Truscott, K.N., Kovermann, P., Geissler, A., Merlin, A., Meijer, M., Driessen, A.J., Rassow, J., Pfanner, N., and Wagner, R. (2001). A presequence- and voltage-sensitive

channel of the mitochondrial preprotein translocase formed by Tim23. *Nat Struct Biol* 8, 1074-1082.

Truscott, K.N., Voos, W., Frazier, A.E., Lind, M., Li, Y., Geissler, A., Dudek, J., Muller, H., Sickmann, A., Meyer, H.E., *et al.* (2003). A J-protein is an essential subunit of the presequence translocase-associated protein import motor of mitochondria. *J Cell Biol* 163, 707-713.

Ungermann, C., Guiard, B., Neupert, W., and Cyr, D.M. (1996). The delta psi- and Hsp70/MIM44-dependent reaction cycle driving early steps of protein import into mitochondria. *Embo J* 15, 735-744.

Ungermann, C., Neupert, W., and Cyr, D.M. (1994). The role of Hsp70 in conferring unidirectionality on protein translocation into mitochondria. *Science* 266, 1250-1253.

van der Laan, M., Chacinska, A., Lind, M., Perschil, I., Sickmann, A., Meyer, H.E., Guiard, B., Meisinger, C., Pfanner, N., and Rehling, P. (2005). Pam17 is required for architecture and translocation activity of the mitochondrial protein import motor. *Mol Cell Biol* 25, 7449-7458.

van Wilpe, S., Ryan, M.T., Hill, K., Maarse, A.C., Meisinger, C., Brix, J., Dekker, P.J., Moczko, M., Wagner, R., Meijer, M., *et al.* (1999). Tom22 is a multifunctional organizer of the mitochondrial preprotein translocase. *Nature* 401, 485-489.

Vergnolle, M.A., Baud, C., Golovanov, A.P., Alcock, F., Luciano, P., Lian, L.Y., and Tokatlidis, K. (2005). Distinct domains of small Tims involved in subunit interaction and substrate recognition. *J Mol Biol* 351, 839-849.

Voisine, C., Craig, E.A., Zufall, N., von Ahsen, O., Pfanner, N., and Voos, W. (1999). The protein import motor of mitochondria: unfolding and trapping of preproteins are distinct and separable functions of matrix Hsp70. *Cell* 97, 565-574.

Voisine, C., Schilke, B., Ohlson, M., Beinert, H., Marszalek, J., and Craig, E.A. (2000). Role of the mitochondrial Hsp70s, Ssc1 and Ssq1, in the maturation of Yfh1. *Mol Cell Biol* 20, 3677-3684.

von Ahsen, O., Voos, W., Henninger, H., and Pfanner, N. (1995). The mitochondrial protein import machinery. Role of ATP in dissociation of the Hsp70.Mim44 complex. *J Biol Chem* 270, 29848-29853.

Voos, W., and Rottgers, K. (2002). Molecular chaperones as essential mediators of mitochondrial biogenesis. *Biochim Biophys Acta* 1592, 51-62.

Voos, W., von Ahsen, O., Muller, H., Guiard, B., Rassow, J., and Pfanner, N. (1996). Differential requirement for the mitochondrial Hsp70-Tim44 complex in unfolding and translocation of preproteins. *Embo J* 15, 2668-2677.

- Voulhoux, R., Bos, M.P., Geurtsen, J., Mols, M., and Tommassen, J. (2003). Role of a highly conserved bacterial protein in outer membrane protein assembly. *Science* *299*, 262-265.
- Wach, A., Brachat, A., Alberti-Segui, C., Rebischung, C., and Philippsen, P. (1997). Heterologous HIS3 marker and GFP reporter modules for PCR-targeting in *Saccharomyces cerevisiae*. *Yeast* *13*, 1065-1075.
- Wachter, C., Schatz, G., and Glick, B.S. (1994). Protein import into mitochondria: the requirement for external ATP is precursor-specific whereas intramitochondrial ATP is universally needed for translocation into the matrix. *Mol Biol Cell* *5*, 465-474.
- Waizenegger, T., Habib, S.J., Lech, M., Mokranjac, D., Paschen, S.A., Hell, K., Neupert, W., and Rapaport, D. (2004). Tob38, a novel essential component in the biogenesis of beta-barrel proteins of mitochondria. *EMBO Rep* *5*, 704-709.
- Waizenegger, T., Schmitt, S., Zivkovic, J., Neupert, W., and Rapaport, D. (2005). Mim1, a protein required for the assembly of the TOM complex of mitochondria. *EMBO Rep* *6*, 57-62.
- Webb, C.T., Gorman, M.A., Lazarou, M., Ryan, M.T., and Gulbis, J.M. (2006). Crystal structure of the mitochondrial chaperone TIM9.10 reveals a six-bladed alpha-propeller. *Mol Cell* *21*, 123-133.
- Weiss, C., Oppliger, W., Vergeres, G., Demel, R., Jenö, P., Horst, M., de Kruijff, B., Schatz, G., and Azem, A. (1999). Domain structure and lipid interaction of recombinant yeast Tim44. *Proc Natl Acad Sci U S A* *96*, 8890-8894.
- Westermann, B., and Neupert, W. (1997). Mdj2p, a novel DnaJ homolog in the mitochondrial inner membrane of the yeast *Saccharomyces cerevisiae*. *J Mol Biol* *272*, 477-483.
- Wiedemann, N., Kozjak, V., Chacinska, A., Schonfisch, B., Rospert, S., Ryan, M.T., Pfanner, N., and Meisinger, C. (2003). Machinery for protein sorting and assembly in the mitochondrial outer membrane. *Nature* *424*, 565-571.
- Wittung-Stafshede, P., Guidry, J., Horne, B.E., and Landry, S.J. (2003). The J-domain of Hsp40 couples ATP hydrolysis to substrate capture in Hsp70. *Biochemistry* *42*, 4937-4944.
- Wu, Y., and Sha, B. (2006). Crystal structure of yeast mitochondrial outer membrane translocon member Tom70p. *Nat Struct Mol Biol* *13*, 589-593.
- Yamamoto, H., Esaki, M., Kanamori, T., Tamura, Y., Nishikawa, S., and Endo, T. (2002). Tim50 is a subunit of the TIM23 complex that links protein translocation across the outer and inner mitochondrial membranes. *Cell* *111*, 519-528.

Young, J.C., Hoogenraad, N.J., and Hartl, F.U. (2003). Molecular chaperones Hsp90 and Hsp70 deliver preproteins to the mitochondrial import receptor Tom70. *Cell* 112, 41-50.

Zhu, X., Zhao, X., Burkholder, W.F., Gragerov, A., Ogata, C.M., Gottesman, M.E., and Hendrickson, W.A. (1996). Structural analysis of substrate binding by the molecular chaperone DnaK. *Science* 272, 1606-1614.

ABBREVIATIONS

α	anti-body
AAC	ADP/ATP carrier
Ab	antibody
ADP	adenosine diphosphate
Amp	ampicillin
APS	ammonium peroxodisulfate
ATP	adenosine triphosphate
ATPase	adenosine triphosphatase
BN-PAGE	blue native polyacrylamide gel electrophoresis
BSA	bovine serum albumin
C-	carboxy-
CBB	coomassie brilliant blue
cDNA	complementary DNA
CNBr	cyanogen bromide
CV	column volume
DHFR	dihydrofolate reductase
DMSO	dimethylsulfoxid
DNA	deoxyribonucleic acid
dNTP	deoxyribonucleoside triphosphate
DLD	D-lactate dehydrogenase
DSG	disuccinimidyl glutarate
DSS	disuccinimidyl suberate
DTT	dithiotreitol
$\Delta\Psi$	membrane potential
<i>E. coli</i>	<i>Escherichia coli</i>
EDTA	ethylendiamine tetraacetate
F1 β	F1 β subunit of the ATP synthase
FRET	Fluorescence Resonance Energy Transfer
gDNA	genomic DNA

HEPES	N-2 hydroxyl piperazine-N'-2-ethane sulphonic acid
His	histidine
Hsp	heat shock protein
IgG	immunoglobuline G
IM	inner membrane
Imp	inner membrane peptidase
IMS	intermembrane space
IPTG	isopropyl- β ,D-thiogalactopyranoside
KAN	kanamycin
kDa	kilodalton
LB	Luria Bertani
MBP	maltose binding protein
MOPS	N-morpholinopropane sulphonic acid
MPP	mitochondrial processing peptidase
MTS	matrix targeting signal
MTX	methotrexate
N-	amino-
<i>N. crassa</i>	<i>Neurospora crassa</i>
NADH	nicotine amide adenine dinucleotide
NADPH	nicotine amide adenine dinucleotide phosphate
Ni-NTA	nickel-nitrilo triacetic acid
NMR	nuclear magnetic resonance
OD _x	optical density at x nm
OM	outer membrane
Oxa	oxidase assembly
PAGE	polyacrylamide gel electrophoresis
PAS	protein A-Sepharose
PCR	polymerase chain reaction
PEG	polyethylene glycol
PI	preimmune serum
PIE	pulsed interleaved excitation

PK	proteinase K
PMSF	phenylmethylsulfonyl fluoride
Preprotein	precursor protein
ProtA	Protein A
PVDF	polyvinylidene difluoride
RNA	ribonucleic acid
RNasin	ribonuclease inhibitor
RT	room temperature
<i>S. cerevisiae</i>	<i>Saccharomyces cerevisiae</i>
SDS	sodium dodecyl sulfate
STD	mitochondria isolated under standard conditions
TBS	TRIS buffered saline
TCA	trichloroacetic acid
TEMED	N,N,N',N'-tetramethylene diamine
TIM	translocase of the inner mitochondrial membrane
TOB	translocase of outer membrane β -barrel proteins
TOM	translocase of the outer mitochondrial membrane
Tris	tris-(hydroxymethyl)-aminomethane
TX-100	Triton X-100
v/v	volume per volume
w/v	weight per volume
WT	wild type

Publications resulting from this thesis

Mapa K, Waegemann K, Neupert W and Mokranjac D.
Reconstitution of Tim44:Ssc1 interaction cycle of mitochondrial import motor in real-time.
(Manuscript in preparation).

Mapa K, Sikor M, Waegemann K, Neupert W, Lamb D and Mokranjac D.
Conformational dynamics of mitochondrial Hsp70 in its functional chaperone cycle.
(Manuscript in preparation).

Popov-Celeketić D, Mokranjac D, Waegemann K, **Mapa K** and Neupert W.
Molecular environment of individual components of mitochondrial TIM23 translocase in different sorting pathways.
(Manuscript in preparation).

Mokranjac D, Sichtung M, Popov-Celeketić D, **Mapa K**, Gevorkyan-Airapetov L, Zohary K, Hell K, Azem A, Neupert W.
Role of Tim50 in the Transfer of Precursor Proteins from the Outer to the Inner Membrane of Mitochondria.
Mol Biol Cell. 2009 Jan 14.

Gevorkyan-Airapetov L, Zohary K, Popov-Celeketić DA, **Mapa K**, Hell K, Neupert W, Azem A, Mokranjac D.
Interaction of tim23 with tim50 is essential for protein translocation by the mitochondrial tim23 complex.
J Biol Chem. 2008 Nov 18.

Popov-Celeketić D*, **Mapa K***, Neupert W, Mokranjac D.
Active remodelling of the TIM23 complex during translocation of preproteins into mitochondria.
EMBO J. 2008 May 21;27(10):1469-80.

(*Equally contributing first authors)

ACKNOWLEDGEMENTS

First and foremost I would like to thank Prof.Dr.Dr.Walter Neupert for giving me an opportunity to work in his group and to explore the mysteries in the field of mitochondrial protein transport. Though in the beginning it was scary but afterwards especially when I was playing around with the new 'Fluorimeter', it was always motivating and encouraging meeting him in the corridors and discussing new results. I have to thank heartily for his patience and faith in me to work with completely new techniques, so far unused by our lab.

I have to thank Dejana for many things starting from the first day when she taught me the very basics of yeast work to co-immunoprecipitations, till the late years when she was patient and enthusiastic to get the new results from fluorimeter and single molecule experiments. I have to thank her and Zdravko specially to convince Prof. Neupert to get a very expensive 'Fluorimeter' which made my life much easier instead of going to MPI with all reagents and pipettmans by bus.

I have to thank Prof. Don Lamb and Martin Sikor for the fruitful collaboration we had.

I have to thank Prof. Ullrich Hartl and Dr. Hans-Joerg Schäffer for giving me an opportunity to be a part of IMPRS and to have the excellent opportunity to take part in various IMPRS activities like seminars and workshops which were perfect in grooming-up. Special thanks goes to my TAC members Dr. Enrico Schleiff and Dr. Andreas Bracher who managed to give their precious times for reading my TAC report and giving feed-backs in meetings from their busy schedules. I would like to thank Dr. Manajit Hayer-Hartl and Dr. Alvaro Crevenna, of Max Planck Institute of Biochemistry, for letting me use the stopped-flow mixing apparatus for the fast mixing kinetics reported in this thesis. I am greatly indebted to Dr. Alex Hastie for editing the english of this thesis.

This thesis would have been much more boring if I hadn't worked with Dusan, my benchmate in the lab and the only fellow PhD student in our group. In the first two months he was the 'Friend, philosopher and guide' introducing me to all the little things I

needed to make simple buffers to perform complicated experiments. He was the one who made the lab really lively, which even I felt, being one of the most silent persons in the lab. The smiling presence of his family (Jelena and Relja) was also very refreshing in between work.

I have to thank other labmates like Nadia, Barbara, Jelena, Shukry, Silvia and lately Karin, Bernadette, Marta with whom I had spent nice times chatting science and non-science (sometimes non-sense like Indian marriages and hierarchy of Hindu Gods) which were perfect stress-releivers.

My heartiest thanks goes to our hard-working, efficient technicians Marica, Heiko, Petra Robisch who made it easier to do some real experiments by providing nice mitos, cell pellets after expressing proteins or ten thousand different reagents we always needed.

It was always easy to work in peace without thinking of running out of contract or visa having efficient secretaries like Frau Werner and Frau Hauck in the institute.

I have to thank the ordering persons like Anja, Nikola, Lisi, Martin for their help in getting all the reagents in time. Special thanks also goes to Stefan and Verena with whom I worked as the 'media in-charge' in the lab. My dearest gratitude goes to all other members of the Neupert lab both present and past.

Friends outside the lab like Sankarda and Shilpi, Shruti and Bhumi, Jyoti, Rashmi and Sathish, Swasti, Bharthi and Vasu and many others were always there to share the ups and downs of PhD life and to chat for hours to forget everything.

This was a long journey starting from a very small town in India to Munich to do my PhD in basic science after getting a Medical graduate degree. This would never have been possible without the support and patience of my parents and mother-in-law.

I would not have been in a position to write this acknowledgement without my dearest husband 'Kausik' whose scientific inquisitiveness inspired me to explore this field. It is difficult for me to express in words about his contributions behind this work, so I have to quote him only 'It will be a futile attempt to thank him enough for everything we shared.'

Curriculum Vitae

Koyeli Mapa

- 05.03.1977 Born in Chinsurah, West Bengal, India
- 1983-1986 Primary School, Chinsurah, West Bengal, India
- 1987-1993 Secondary School, West Bengal Board of Secondary Education
- 1993-1995 Higher Secondary School, with Mathematics, Physics, Chemistry and Biology as the majors
- 1995-1996 B.Sc. with Chemistry Honours, Burdwan University, discontinued after June, 1996
- 1996-2002 Bachelor of Medicine and Surgery (M.B.B.S.) with one year medical Internship at Calcutta Medical College, Calcutta University
- 2002-2004 Worked as a Junior Research Fellow, Department of Microbiology and Cell Biology, Indian Institute of Science, Bangalore
- 2004-2005 PhD thesis work, Technical University Dresden as a part of International Max-Planck Research School (IMPRS)
- 2005-present PhD thesis work, Ludwig Maximillian Universität as a part of International Max-Planck Research School (IMPRS) under the supervision of Prof. Dr.Dr. Walter Neupert